

2001

## Post-glacial sedimentation in a river -dominated epicontinental shelf: The Yellow Sea example

Jing-pu Liu

*College of William and Mary - Virginia Institute of Marine Science*

Follow this and additional works at: <https://scholarworks.wm.edu/etd>



Part of the [Geology Commons](#), and the [Oceanography Commons](#)

---

### Recommended Citation

Liu, Jing-pu, "Post-glacial sedimentation in a river -dominated epicontinental shelf: The Yellow Sea example" (2001). *Dissertations, Theses, and Masters Projects*. Paper 1539616747.

<https://dx.doi.org/doi:10.25773/v5-4384-vh22>

This Dissertation is brought to you for free and open access by the Theses, Dissertations, & Master Projects at W&M ScholarWorks. It has been accepted for inclusion in Dissertations, Theses, and Masters Projects by an authorized administrator of W&M ScholarWorks. For more information, please contact [scholarworks@wm.edu](mailto:scholarworks@wm.edu).



**POST-GLACIAL SEDIMENTATION IN A RIVER-DOMINATED  
EPICONTINENTAL SHELF: THE YELLOW SEA EXAMPLE**

---

A Dissertation

Present to

The Faculty of the School of Marine Science

The College of William & Mary in Virginia

In Partial Fulfillment

Of Requirement for the Degree of

Doctor of Philosophy

---

by

Jing-pu Liu

2001

UMI Number: 3029880

UMI<sup>®</sup>

---

UMI Microform 3029880

Copyright 2002 by Bell & Howell Information and Learning Company.

All rights reserved. This microform edition is protected against  
unauthorized copying under Title 17, United States Code.

---

Bell & Howell Information and Learning Company

300 North Zeeb Road

P.O. Box 1346

Ann Arbor, MI 48106-1346

APPROVAL SHEET

This dissertation is submitted in partial fulfillment of


The requirement for the degree of

Doctor of Philosophy

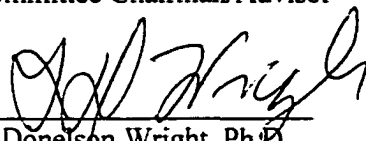


Jing-pu Liu

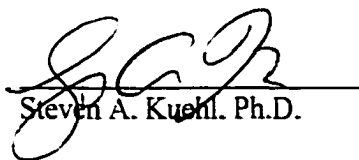
Approved. November 2001




John D. Milliman, Ph.D.  
Committee Chairman/Advisor



L. Donelson Wright, Ph.D.



Steven A. Kuehl, Ph.D.



James E. Perry, Ph.D.



Yoshiki Saito, Ph.D.

Coastal Environment Research Group  
Geological Survey of Japan, Tsukuba, Japan

## TABLE OF CONTENTS

	Page
ACKNOWLEDGEMENTS.....	v
LIST OF TABLES.....	vi
LIST OF FIGURES.....	vii
ABSTRACT.....	ix
INTRODUCTION.....	2
References.....	6
CHAPTER 1: Research Background.....	7
Overview Epicontinental Shelf Sediment Accumulation.....	7
Geologic and Physical Setting.....	12
Oceanographic Circulation in the East China Sea and Yellow Sea.....	17
Previous studies of the early Holocene and modern sediments.....	20
Holocene Sediment Depositional Patterns.....	20
Historical Changes of the Yellow River Sediment.....	24
The Problems and Questions.....	27
References.....	31
CHAPTER 2: The Shandong Mud Wedge and Post-glacial Sediment	
Accumulation in the Yellow Sea.....	39
Abstract.....	39
Introduction.....	40
Shandong Mud Wedge.....	42
Materials and Methods.....	43
Results.....	44
Discussion.....	45
Acknowledgements.....	49
References.....	50
CHAPTER 3: Post-Glacial Sea-Level Transgression in the East China and	
Yellow Seas: Significance of Periodic Rapid Flooding Events.....	59
Abstract.....	59

Sea Level History Derived from Coral Reefs.....	60
East China and Yellow Seas.....	63
Discussion.....	65
References and Notes.....	68
CHAPTER 4: Sedimentary Processes of the Yellow River's Subaqueous Delta	
in the North Yellow Sea .....	76
Abstract.....	76
Introduction.....	78
Study area.....	80
Methods.....	84
Results.....	86
Shallow Structure.....	86
Sediments and Recent Rates of Sediment Accumulation.....	88
Development of the Shandong Clinoform.....	89
Conclusions.....	94
References.....	97
CHAPTER 5: Late Quaternary sequence stratigraphy model in the	
epicontinental shelf – The Yellow Sea.....	123
The Post-glacial sea-level history and climatic changes.....	123
Evolution of the Yellow River and its deltaic depocenters on the shelf.....	125
Sequence stratigraphy model on the Yellow Sea epicontinental shelf .....	127
References.....	129
APPENDICES.....	134
VITA.....	151

## ACKNOWLEDGEMENTS

More people than I can mention here helped me reach this stage, but a number of them deserve special recognition.

First, many, many thanks to my major professor, Dr. John D. Milliman, for his advice and strong support, and his insight and foresight to question the conventional wisdom about how coral reefs responded to rapid sea-level rise. I would like to thank other members of my advisory committee for their support throughout my study and research. Dr. Wright and Dr. Kuehl have given their generous assistance to help me understand worldwide deltaic deposits and seismic applications. Dr. Saito hosted my visits and helped a lot to collect extensive references and sea-level data; he also gave me lots of critical suggestions and invaluable advice. Dr. Perry and Dr. Roth also gave their great help in forming the research topics. This research work would not have been possible without the support, encouragement, and advice of Peggy Schexnayder.

I would also like to thank Prof. Qin Yunshan, Yang Zuosheng, Gao Shu and Zhao Songling for their hosting and assistance with cruises and data acquisition. Many thanks to Mr. Cheng Peng, Prof. Guan Chengzhong, and Wang Shaozhi for their help in the seismic profiling and geological sampling.

Sincere thanks to Linda Meneghini for her invaluable help in sample analysis. Katie Farnsworth helped in so many ways, including GIS application, seismic profile processing, discussions, my English writing, etc. Help from the Graduate Office, School of Marine Science, Dr. Mike Newman, Sarah Hamrick, and Sue Presson, are invaluable. I am also grateful to Kevin Kiley and Gary Anderson for their IT assistance.

Finally, thanks to my parents, and whole family for their understanding, encouragement, and special thanks to Jing and David for their patience, support and love.



## LIST OF TABLES

	Page
CHAPTER ONE	
Table 1-1. Marginal seas and shelves in the west Asian-Pacific Ocean .....	10
CHAPTER TWO	
Table 1. Holocene sediment and accumulation in the Bohai and Yellow Sea..	54
Table 2. $^{14}\text{C}$ ages of the sedimentary fossils from the Yellow Sea.....	55
CHAPTER THREE	
Table 1. Time, rises and rates of the post-LGM sea-level.....	72

## LIST OF FIGURES

	Page
<b>CHAPTER ONE</b>	
Figure 1. The distribution of worldwide modern epicontinental shelves.....	8
Figure 2. Geographic map of Bohai, Yellow, and East China Seas.....	13
Figure 3. Surficial sediment distribution in the Yellow and East China Seas...	16
Figure 4. Major current systems in the Yellow and East China Seas .....	19
Figure 5. Erosion and transport of suspended sediment in the Yellow Sea ....	21
Figure 6. Fate of the Huanghe (Yellow River) sediment.....	22
Figure 7. Historical shifts of the Yellow River and its superlobes.....	25
 <b>CHAPTER TWO</b>	
Figure 1. Location map of the seismic lines and cores in the YS and BS.....	56
Figure 2. Main depocenters in the western Yellow Sea.....	57
Figure 3. Selected high-resolution seismic profiles from the Yellow Sea.....	58
 <b>CHAPTER THREE</b>	
Figure 1. Coral reef-derived sea-level curves from B-H-T.....	73
Figure 2. Newly proposed sea-level curve based on the ECS and YS data.....	74
Figure 3. Proposed sea-level, meltwater, climatic and oceanic events.....	75
 <b>CHAPTER FOUR</b>	
Figure 1. Location and bathymetric map of the BS, ECS, NYS. SYS.....	103
Figure 2. Seismic profile lines and sample site locations in the NYS.....	104
Figure 3. 3-D seafloor morphology of the NYS.....	105
Figure 4. Oceanographic observation stations in the NYS.....	106
Figure 5. Vertical profiles of Temperature and Salinity across the NYS.....	107
Figure 6. Vertical profiles of Temperature and Salinity around Shandong Pen	108
Figure 7. Vertical profiles of TSS distribution across the NYS.....	109
Figure 8. Profiles of temperature and current in the east tip of Shandong Pen.	110

Figure 9. GeoPulse records from 99-A and 83-a.....	111
Figure 10. High-resolution GeoPulse records of the westernmost of 99-A....	112
Figure 11. GeoPulse record of profile 99-B.....	113
Figure 12. GeoPulse profiles of 99-E and 99-F.....	114
Figure 13. GeoPulse record of profile 99-C and 99-D.....	115
Figure 14. GeoPulse record of profiles 98a and 98b.....	116
Figure 15. GeoPulse profile of 84-4.....	117
Figure 16. Grain-size and water content pattern in the surface sediment .....	118
Figure 17. Stratigraphic transect through the foreset to bottomset.....	119
Figure 18. Activity profile for excess $^{210}\text{Pb}$ of S44, S45, S46, S54.....	120
Figure 19. Total activity profile for $^{210}\text{Pb}$ of S49 from topset.....	121
Figure 20. Modern local sedimentary processes in the NYS.....	122

## CHAPTER FIVE

Figure 1. Proposed eustatic sea-level curve based on the ECS &YS data.....	131
Figure 2. Historical evolution of the Yellow River and its deltaic deposits....	132
Figure 3. Idealized depositional sequences on an epicontinental shelf.....	133

## ABSTRACT

The Yellow Sea, North Yellow Sea (NYS) and South Yellow Sea (SYS), stretching from the Gulf of Bohai in the north to the East China Sea (ECS) in the south, represents an end member of modern epicontinental seas. Because of its shallow depths (nowhere deeper than 80-90 m) the Yellow Sea was entirely exposed subaerially during the last glacial maximum (LGM). Moreover, due to its generally shallow gradient (often  $<1:1000$ ) and sediment input from two of the world's largest rivers, the Yangtze and Yellow rivers, the Yellow Sea has been more likely to preserve post-LGM events as sea-level transgressed and climate changed.

The new sea-level curve derived from an extensive local dataset shows that post-LGM sea level rose through a series of rapid flooding events (12-45 mm/y), separated by a series of slow rises (2-6 mm/y). By about 15 ka, sea level had reached about -100 m, and seawater began to enter the central SYS. A rapid rise during melt water pulse 1A (MWP-1A) occurred between 14.7 -14.1 ka, when sea level jumped from -98 m to -74 m (40 mm/yr). At the end of this flooding event, the sea water had reached the southern edge of the NYS, after which sea level rose again slowly (6 mm/yr) from -72 m to -60 m. Beginning about 11.7 ka, sea level again jumped, from -60 m to -42 m (MWP-1B), resulting in a rapid westward flooding of the NYS and initial entrance into the Bohai Sea. Sea-level rise then again stagnated (between -42m to -36 m) for about 1.8 ky. Starting about 9.8 ka, the sea-level advanced again from -36m to -16 m at 9.0 ka (MWP-1C), after which most of BS, YS, and ECS had been submerged. Then another slowdown occurred between 9.0-8.0 ka when sea-level rose from -16m to -10m. The last major transgression happened between 8.1 and 7.0 ka (MWP-D), and resulted in Holocene highstand of at least +2 to 4 m along most of Chinese and Korean coastlines. Sea level during these rapid rise intervals may have back-stepped by as much as 40-100 m/y, whereas during the long periods of stable or slowly rising sea level, shoreline regression may have been only a few m/y.

Sequence structures on this epicontinental shelf show strong landward horizontal changes, instead of the vertical changes. The first major deltaic system was developed in the NYS together with the decreased sea-level rise after MWP-1B event, and the intensified summer monsoon and subsequent increased river discharge at about 11 ka. At about 9.2 ka, the Yellow River shifted southward to the Jiangsu coast, and the second subaqueous delta was built in the SYS between 9-7 ka which during another slackened sea-level after MWP-C. The river north-shifted back to the BS at around 7 ka, then modern subaqueous and subaerial deltas in the west Bahai Gulf have been formed during the sea-level highstand after the last jump of MWP-1D.

POST-GLACIAL SEDIMENTATION IN A RIVER-DOMINATED  
EPICONTINENTAL SHELF: THE YELLOW SEA EXAMPLE

## INTRODUCTION

Epicontinental seas are wide shallow bodies of water that border continental margins or occupy the interior of a continent. They are defined as being broad ( $10^2$ - $10^3$  km), relatively shallow (generally less than 100 m), and often underlain by thick sedimentary sequences ( $10^2$ - $10^4$  m). Because of their shallow-water depositional environment, epicontinental sea sediments can reflect land-ocean and atmosphere-sea interactions, varying degrees of physical, chemical and biological processes, and fluctuations in sea level. The latter aspect is a critical controlling factor in sequence stratigraphy (Boyd et al., 1989). The response to relative sea-level fluctuations can be further complicated by intermittent opening and closing of seaways that can expose an epicontinental basin to varying degrees of oceanic influence.

The Yellow and East China seas, stretching from the Gulf of Bohai in the north to the Okinawa Trough in the south, represent an end member of modern epicontinental seas in terms of the very high terrigenous sediment loads they receive. The Yangtze (Changjiang) and Yellow River (Huanghe) rivers alone have been cited as discharging an average of  $1.6 \times 10^9$  t annually, about 10% of the annual global flux (Qian & Dai, 1980; Milliman & Meade, 1983). The Yellow Sea (Huanghai) is a semi-enclosed marginal sea north of latitude  $32^\circ\text{N}$  and has an area of  $380 \times 10^3$  km<sup>2</sup> and average depth of 44 m. The Yellow Sea, so named because of the vast amount of sediment discharged by the Yellow River, is characterized by a flat, broad, featureless sea floor with a maximum depth of 90 m. It is probably the only modern analogue to these ancient epicontinental environments to have

received large amounts of sediment during the late Quaternary (Milliman et al., 1989; Alexander et al., 1991).

The general objective of this dissertation is to reconstruct and explain the paleo-environmental changes and sedimentary processes in late Quaternary using seismic profiling, geo-technical methods, and geochronologies in an epicontinental setting. The nature of the sedimentary processes of the late Quaternary in the Yellow and East China Sea can be evaluated by studying of the sea-level history (regressive and transgressive processes), modern sediment distributions (Holocene mud isopachs), sedimentation rates (100-y and 1000-y timescales), and river sediment discharge variations. The specific objectives of this study are:

- a) *What is the nature of the Last Glacial Maximum (LGM) sediments; are they aeolian rather than fluvial? If so, what does this tell us about the glacial climate in this area?*
- b) *How much and where has the Yellow River discharged since the LGM*
- c) *What are the nature and timing of the transgressive facies in the North and South Yellow Sea? If the LGM sedimentation was largely aeolian, when did the Yellow River again begin discharging to the Yellow Sea?*
- d) *How much of the Yellow River sediment load has been transported into the Bohai Sea and North Yellow Sea during Holocene, and does the North Yellow Sea serve as a conduit for transport to the South Yellow Sea?*
- e) *What are the relationships among relative sea-level changes and the formations of subaqueous deltas in the North and South Yellow Sea shelves?*
- f) *What was the sedimentological impact of the north-south shift of Yellow River discharge from the north (Gulf of Bohai) to the south (South Yellow Sea) in the post-LGM.*

Answers to these questions can help us to understand the dynamic and interactive sea-level changes and fluvial sediment discharge and distribution processes in this epicontinental environment.

**Chapter 1** – reviews studies of the epicontinental shelves globally; outlines the geological features and physical settings of the epicontinental shelves in the Bohai, Yellow, and East China Seas; and summarizes the previous studies of the Yellow River deltaic deposits;

**Chapter 2** – reviews and re-defines the Holocene accumulation of Yellow River-derived sediments. Two well-defined deltaic sequences in the Bohai Sea and in the South Yellow Sea are discussed first. Another prominent depocenter, Shandong mud wedge, wrapping around the eastern end of the Shandong Peninsula has also been quantitatively defined using the high-resolution seismic profiles and radiocarbon dating. *(This chapter was written in the format for Geo-Marine Letters)*

**Chapter 3** – reviews the well-accepted sea-level curve derived from the coral reefs and other shallow marine sediments, and then reconstructs the late Quaternary Sea-level history in the Yellow Sea and East China Sea using the more than 200 available cores with radiocarbon dates. The proposed sea level shows a step-like post-glacial transgression marked by 5 short periods of rapid rise (11-45 mm/yr), some of which corresponds with periods of rapid climatic change. *(This chapter was written in the format for Science Report)*

**Chapter 4** – discusses the high-resolution seismic profiles from the North Yellow Sea and the sedimentary processes of the Yellow River's subaqueous delta formed around the eastern end of the Shandong Peninsula since. The complex sigmoidal-oblique clinoform



overlies prominent transgressive surfaces and has been deposited the Yellow River's sediment proximally and distally since early Holocene. Basin-wide circulation, along-shore transport, and upwelling rework the modern and relict sediment, and help maintain the morphology of the clinoform mud wedge. *(This chapter was written in the format for Marine Geology)*

**Chapter 5**– The paleo-environment and paleo-coast lines are reconstructed based on the sea-level history and climate studies. The sedimentary processes of land-ocean interaction during post-glacial transgression have been discussed in this chapter. A new sequence stratigraphy conceptual model, which might reflect the sea-level fluctuation, climatic changes, and large river sediment input on a modern, shallow, and broad epicontinental shelf, is established and discussed.

## References

- Alexander C.R., DeMaster D.J., and Nittrouer C.A., 1991. Sediment accumulation in a modern epicontinental-shelf setting: The Yellow Sea. *Marine Geology*, 98: p51-72.
- Boyd. R., Suter, J., and Penland, S., 1989. Relation of sequence stratigraphy to modern sedimentary environments. *Geology*, Vol. 17, no. 10, pp. 926-929
- Milliman, J.D., and Meade, R.H., 1983. World-wide delivery of river sediment to the oceans. *Journal of Geology*, Vol. 91, No.1, p1-21.
- Milliman. J.D., Qin. Y.S., and Park. Y., 1989. Sediment and sedimentary processes in the Yellow and East China Seas. *Sedimentary Facies in the Active Plate Margin*, edited by A. Taira and F. Masuda. p 233-249.
- Qian. N., and Dai. D.Z., 1980. The problems of river sedimentation and present status of its research in China: Chinese Hydraul. Eng., Proc. Int. Symp. River Sedimentation, v.1, p.1-39.

## Chapter One

### RESEARCH BACKGROUND

#### Overview Epicontinental Shelf Sediment Accumulation

Nearshore environments and continental shelves have played major roles through time in the storage, passage, and redistribution of land-derived sediment to the deeper ocean. About 80 percent of all sediments of the earth are trapped on certain continental margins. A vast amount of terrigenous sediment (about  $13\text{-}20 \times 10^9$  tons annually) is delivered to the marine environment (Milliman and Meade, 1983; Milliman and Syvitski, 1992). Continental shelves off the mouths of large to moderate-size rivers, like the Amazon, Ganges-Brahmaputra, Mississippi, Nile and Indus, are commonly the sites of accumulation of thick deposits of fine-grained terrigenous sediments.

An epicontinental sea is an ocean on the continental lithosphere. At sea-level high stand, marine waters can flood large portions of the underlying continent, creating an epicontinental sea. Hence, epicontinental shelf seas have been important sites for the accumulation of sediment and formation of sedimentary rocks (Fig. 1). Because some of these ancient sediments are economically important, their conditions of deposition need to be understood (Niino and Emery, 1961). In order to interpret better the stratigraphic record of such deposits, an increased understanding of the variability in sedimentary processes and products must be derived from modern epicontinental environments (Alexander et al., 1991).

**Figure 1.** The distribution of worldwide modern epicontinental shelves. Six shallow, modern, and epicontinental seas located at high and low latitude represent six different types sedimentary processes and environmental changes in late Quaternary. (Detailed info regarding a vast of broad and shallow shelf seas in the Western Pacific have been listed in Table 1-1)

1) Barents Sea—Deep, high-latitude coastlines, dominated by cryological processes and glacial marine sedimentation (Saettem et al., 1992; Polyak et al., 1994; Kleiber et al., 2000).

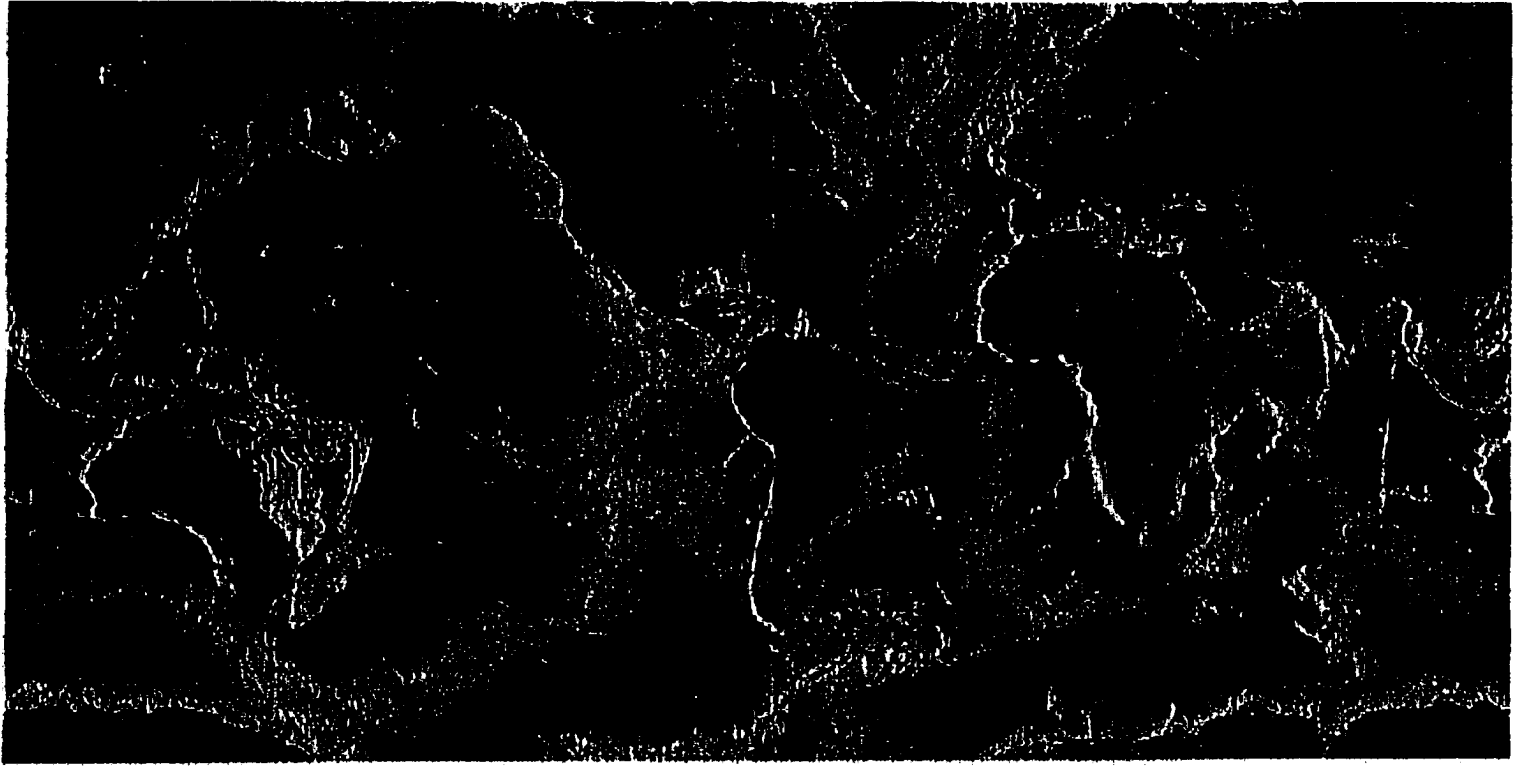
2) North Sea and English Channel -- rapid terrigenous accumulation during the last ice age (Auffret et al., 1996);

3) Persian Gulf and Adriatic Sea-- high-frequency and high-amplitude eustatic changes with the strong aeolian input (Trincardi et al., 1994);

4) Java Sea and Gulf of Capentaria -- subaerial paleosol during sea-level lowstand (Torgersen, et al., 1985; Deckker, et al., 1991).

5) Alaska shelf and Bering Sea—Pacific –Arctic –Atlantic gateway, (Nelson, et al., 1979; Takahashi, 1999);

6) Yellow Sea and East China Sea—Flat, shallow and broad, large fluvial sediment input (Milliman, et al., 1989 Alexander, et al., 1991).



1. Barents Sea
2. North Sea, English Channel
3. Persian Gulf, Adriatic Sea
4. Java, Gulf of Carpentaria
5. Alaska, Bering Sea
6. Yellow and East China seas

**TABLE 1-1**

Areas and mean depths of important marginal seas and shelves in the west Asian-Pacific Ocean.

<b>Name</b>	<b>Area (10<sup>3</sup> km<sup>2</sup>)</b>	<b>Average Depth (m)</b>
Bering Sea	2270	1440
Bering shelf	1120	50% < 50
Sea of Okhotsk	1530	840
Okhotsk-Sakhalin shelf	715	50-100
Sea of Japan / East Sea	978	1750
Yellow Sea	417	40
East China Sea	752	350
YS & ECS shelves	915	Mostly <100
South China Sea	3685	1060
Tonkin(North Bay) Shelf	435	Mostly<100
Sulu Sea	420	1139
Java Sea	433	46
Sunda (Borneo-Java) Shelf	1850	50-100
NW Australian Shelf (including Sahul Shelf)	590	50-100
Gulf of Thailand	320	45
Arafura Sea (including G. of Carpentaria)	1037	200
Arafura Shelf	930	50-100
Coral Sea	4791	2400
South Australian Shelf	320	50-100
Queensland Shelf	190	Mostly < 100

(From Lyman, 1961, Fairbridge, 1968, and Britannica, 2001)

Previous research in Quaternary epicontinental seas has looked at a variety of geologic and climatic settings (Fig.1). For example, effects of high-frequency and high-amplitude eustatic changes have been documented in the Adriatic basin (Trincardi et al., 1994); In contrast, studies off French Guiana have shown a dominant influence from late Quaternary sea-level fluctuations (Pujos and Odin, 1986); Cores from the Celtic Margin of the North Sea show high terrigenous accumulation rates during the last ice age (Auffret et al., 1996). The most outstanding features of the Gulf of Carpentaria, a shallow, flat-floored epicontinental sea that lies on the Australian plate between northern Australia and New Guinea, are the buried channels and flat paleosol surfaces, having been formed under subaerial conditions following rapid regressions over large areas and largely preserved by late Quaternary low-energy transgressions (Deckker, et al., 1991; Torgersen, et al., 1985). The adjacent shallow epicontinental shelf, Gulf of Papua, is covered with a clinoform sequence of Holocene sediment with thickness as locally greater than 40 m near the coast, due to input from several rivers (Milliman et al., 1999).

Shallow epicontinental, or shelf seas, also play important roles in the present and past global climate systems. Their Quaternary sedimentary records may represent an important and hitherto neglected archive of environmental change. In particular, the western Pacific accounts for more than half of the present-day shelf sea area (Table 1-1). Because of their unique locations and morphology, they can provide a detailed record of sea-level fluctuations and adjacent continental and marine climatic change. Therefore, analysis of the sedimentary record on epicontinental shelves can contribute significantly to the understanding of modern and palaeo-sedimentary processes. In addition, such sediments may also yield important clues to the history of delivery of sediment from the catchments

of the river systems and thereby facilitate a better understanding of the changing nature and rates of soil erosion over time.

The Yellow and East China seas, stretching from the Gulf of Bohai in the north to the Okinawa Trough in the south, represent an end member of modern epicontinental seas in terms of the very high terrigenous sediment loads they receive. In their west, the Yangtze (Changjiang) and Yellow River (Huanghe) rivers alone discharge an average of  $1.6 \times 10^9$  t annually, about 10% of the annual global flux (Milliman & Meade, 1983).

### **Geologic and Physical Setting**

The seas which border the southeastern Asian mainland on the east-southeast, consist of four parts. the South China Sea (Nan Hai), the East China Sea (Dong Hai), the Southern and Northern round of the Yellow Sea (Huang Hai), and Northern Gulf (Bo Hai) to the west). In this paper we will only focus on the north parts, i.e. the East China Sea (ECS), South Yellow Sea (SYS), North Yellow Sea (NYS) and Bohai Sea (BS) (Fig 2).

### **East China Sea**

The East China Sea extends northeastward from the South China Sea and is bounded on the west by the China mainland and on the east by the Ryukyu Islands chain, Japan's southernmost main island of Kyushu, and Cheju Island, off South Korea (Guan, 1984, 1994; Su and Wang, 1994). An imaginary east-west line connecting Cheju Island with the Yangtze River mouth on the mainland of China separates the East China Sea from the Yellow Sea to its north (Qin et al., 1987) (Fig. 2). The East China Sea, which has an area of 752,000 km<sup>2</sup>, has an average depth of only 350 m, and almost three-fourths of the area less than 200 m. The deeper part of the ECS is the Okinawa Trough, extending alongside the Ryukyu Islands, with a large area deeper than 1,100 m. A large number of islands and



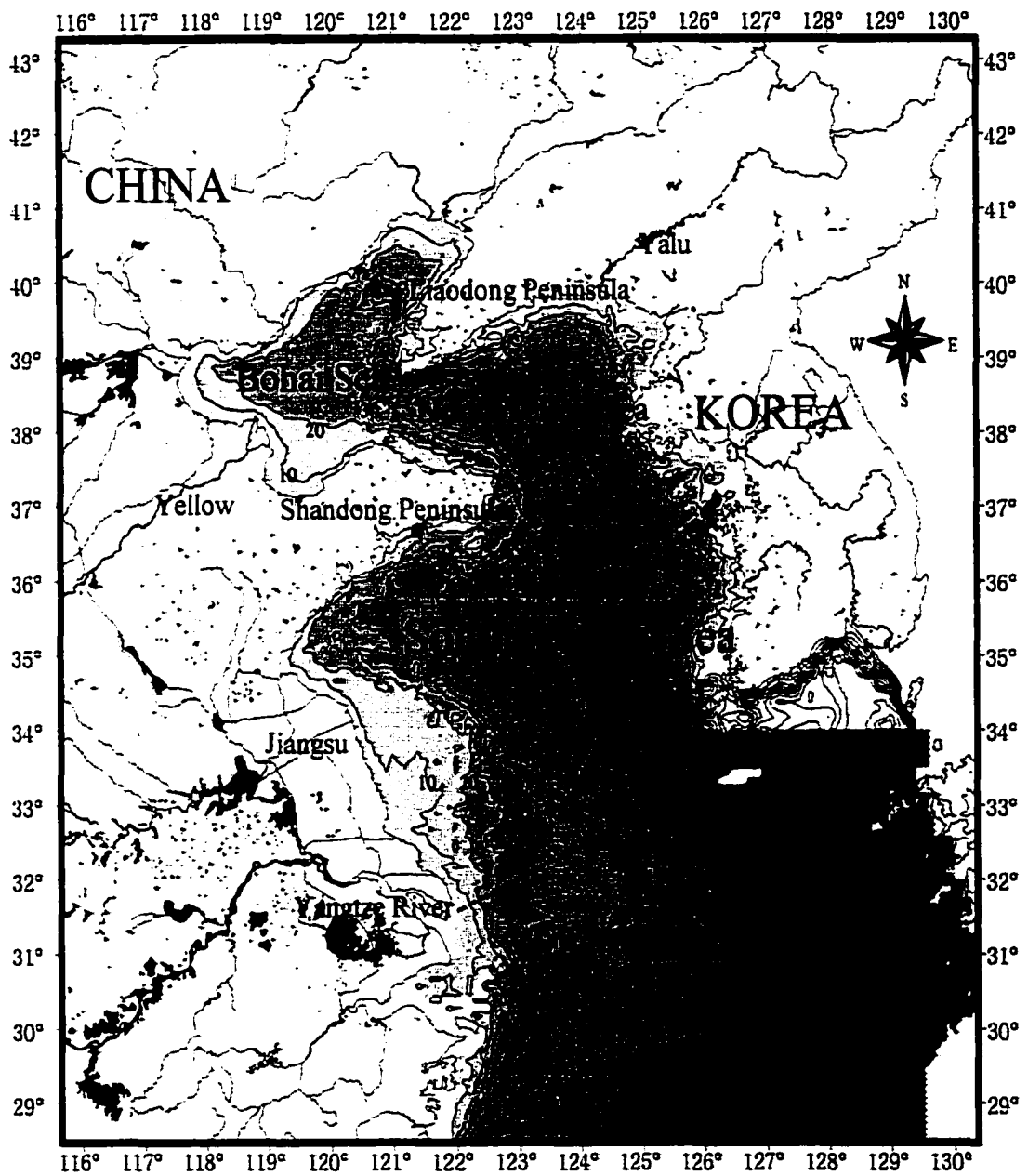


Fig. 2 – Bathymetric map showing the geographic locations of Bohai Sea, Yellow Sea, and East China Sea. Note that the modern Huanghe(Yellow River) enters the Bohai Sea basin and the Changjiang(Yangtze River) enters East China Sea.

shoals dot the eastern boundary as well as the area near the Chinese mainland.

The shallow shelf areas are covered with fine-grained terrigenous sediments derived mainly from the Yangtze River (Chang Jiang) from the west and (to a lesser extent) the Yellow River which has alternatively debauched into the BS and YS from the north. Coarser sediments of relict sand occur farther out, and rocks, muds, and oozes are also found in scattered areas (Niino and Emery, 1961), primarily transgressive and regressive relict sediments deposited during the last regression and low-stand of sea level (Saito et al., 1998). Seismic profiling indicates that the geologic structure beneath the ocean floor consists of nearly parallel folded Mesozoic or Paleozoic strata, with rock ridges near the northern limits of the East China Sea, near the edge of the continental shelf, and along the Ryukyus (Wageman, et al., 1970; Li, 1984).

### **The Yellow Sea**

The Yellow Sea is a large inlet of the western Pacific Ocean lying between the Chinese mainland to the west and north and the Korean Peninsula to the east. Situated to the north of the East China Sea, it forms a partly enclosed, flat, and shallow marine embayment (Fig. 2). It measures about 960 km from north to south and about 700 km from east to west. In the northwest part of the sea, the Bohai Sea lies in northwest of the demarcated line between the Liaodong Peninsula to the north and the Shantung Peninsula to the south. The area of the Yellow Sea proper (excluding the Bohai) is about 417,000 km<sup>2</sup>, its mean depth is 40 m, and its maximum depth is 103 m. The western side of the South Yellow Sea is delineated the low-lying Jiangsu coast into which flow the Yellow and Yangtze rivers, and the northern side by the Shandong Peninsula (Milliman et al., 1983; 1985; 1986; 1987; 1989; Qin, et al., 1986, 1989). Its eastern side is fringed by numerous rocky islands,

lowlands of river mouths, and macrotidal flats along the western Korean coast (Wells and Huh, 1984).

The floor of the Yellow Sea is a geologically unique, the shallow portion of the continental shelf that was submerged only after the last Ice Age (i.e., within the past 10,000 years). It probably represents the only modern analogue to those ancient epicontinental shelf seas which have received large amounts of sediment during late Quaternary. The seafloor slopes gently from the Chinese mainland and more rapidly from the Korean Peninsula to a north-south-trending seafloor valley with its axis close to the Korea side. Many researchers thought this axis represents the path of the meandering Huang He (Yellow River) when it flowed across the exposed shelf during times of lowered sea levels and emptied sediments into the Okinawa Trough (Li, 1998). The Yellow Sea derives its name from the color of the silt-laden water discharged from the major Chinese rivers emptying into it. The sea annually receives an immense quantity of sediments, mostly from the Huang He and Yangtze River, both of which have formed large deltas. Relict sandy sediments occupy the northern part of the Yellow Sea, the nearshore northern Bohai Sea, and the offshore old Huang He delta, and the central part of the south Yellow Sea (Fig. 3). The sandy layer is covered with silty and muddy sediments derived from the large rivers of China and Korea since the last glacial period. The dividing line between silt derived from China and sand derived from Korea nearly coincides with the seafloor valley.

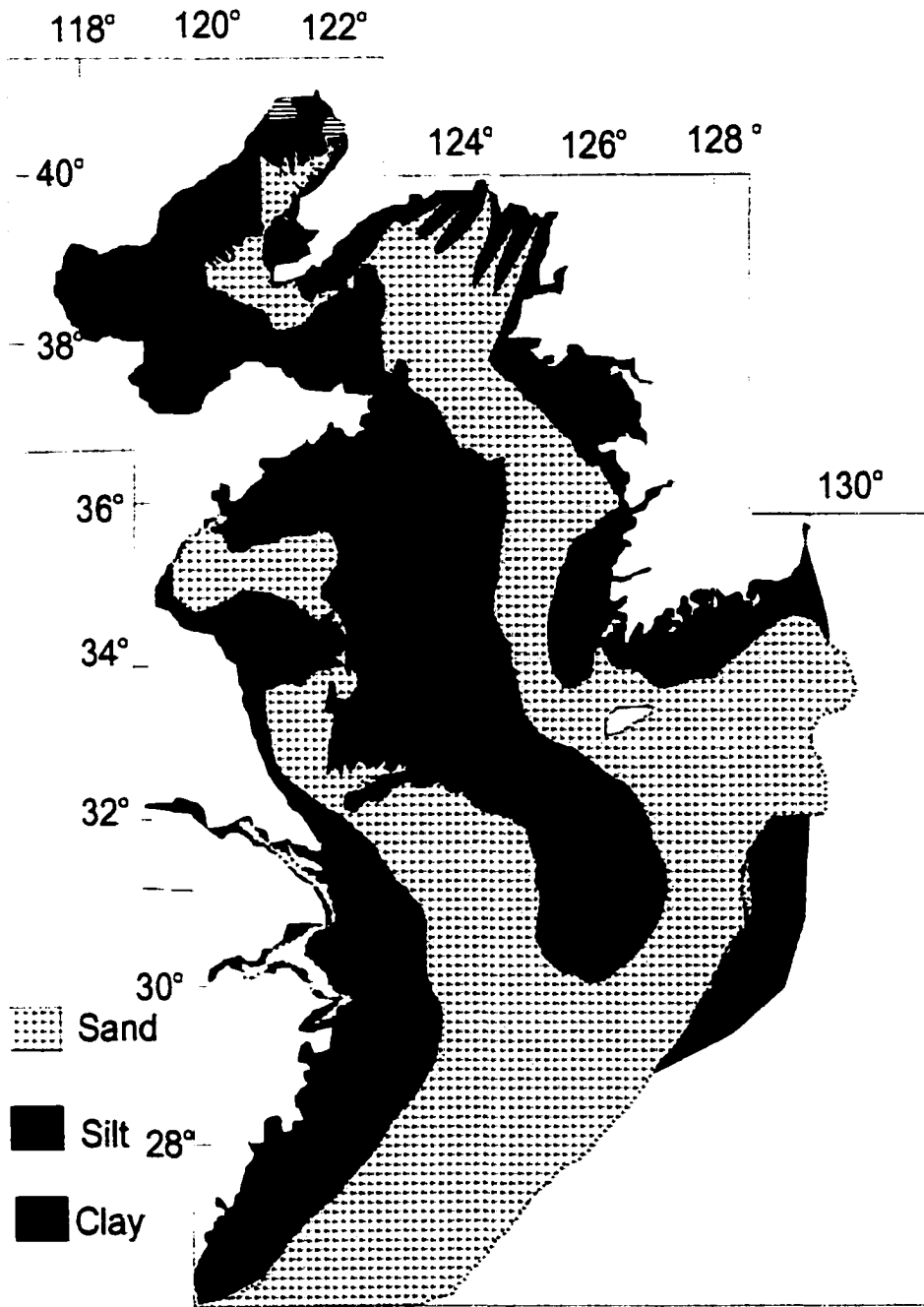


**Fig. 3 – Map of surficial sediment distribution in the Yellow and East China Seas. Relict coarse, and sandy deposits directly spread on seafloor of the most East China Sea, West and central South Yellow Sea, East part of the North Yellow Sea and Bohai Strait. Huge Huanghe-related fine sediments distribute in the Bohai, South Yellow Sea. Most of the Changjiang's input was shifted southward along the Zhejiang coast. (Redrwan from Milliman et al., 1989; Saito and Yang, 1994)**

## **The Bohai Sea**

The Bohai Sea, also called Gulf of Bohai, is a shallow northwestern arm of the Yellow Sea. It is a shallow, semiclosed marginal sea enclosed by the Liaodong Peninsula (northeast) and the Shandong Peninsula (south), and frequently describe in the literature as a Gulf (Fig. 2). The broad Gulf of Liaodong on the northeast, the Gulf of Bohai on the west, and the Gulf of Laizhou on the South are generally considered parts of the Bohai Sea. Within these limits, the gulf's maximum dimensions are 480 km from northeast to southwest and 306 km east-west. The strait leading to the gulf is about 105 km in width. The Huang He (Yellow River), China's second longest river, discharges into the gulf with one billion tons of sediment annually.

## **Oceanographic Circulation in the East China Sea and Yellow Sea**

The western boundary Kuroshio Current is dominant current system off eastern Asia. It flows towards the north along the eastern offshore area of Taiwan, then enters the East China Sea (Fig.4) The current is swift at 80 cm/s in the west and 45 cm/s on the east side (Qin et al., 1987). It plays a very important role in the transport of sediment and heat.

The general circulation in the Yellow Sea is characterized by a counterclockwise gyre, with northward flow in the Yellow Sea trough, in which has generally been referred to as the Yellow Sea Warm Current (YSWC) along the eastern and northern margin of the basin (Fig.4). Uda (1934) was the first to recognize this current and to suggest that it was a branch of the eastward flowing Kuroshio current or Taiwan Warm Current (TWC) along the continental shelf of the East Chin Sea. During the winter, due to the strong northwesterly winds drive surface and nearshore transport southward, demanding a northward return flow at depth, the

Yellow Sea Warm Current can reach its strongest, about 5 cm/s (Yuan and Su, 1984), and produces a warm tongue of water that follows a path along the deepest axis in the eastern Yellow Sea basin (Zheng and Klemas, 1982). The YSWC also penetrates into the Gulf of Bohai from the north channel of the Bohai Strait, and helps to form the sand ridges in the east Bohai Gulf and disperse the fine sediments into the west side of the Gulf (Liu et al., 1998). The nearshore Cold Coastal Current, also known as the YSCC, flows eastward from the Gulf of Bohai along the Shandong Peninsula and western margin (Fig.4), with strongest flow in winter due to Arctic outbreaks of cold air. During the summer, the dense YSCW dominates the central Yellow Sea, resulting in a basin-scale low pressure system and cyclonic circulation. Wind forcing during this period is significantly reduced and in the opposite direction relative to the winter, resulting in an interruption of the northward flow associated with TWC. Under this scenario, coastal currents would be directed northward along Korea and southward along the China (Naimie, et al., 2001). The basin-wide cyclonic gyre system is considered to play a great role in trapping the fine sediments on the Yellow Sea shelf (Hu, 1984).



Fig. 4 – Schematic diagram of the major current systems in the Yellow and East China sea. Note that the Yellow Sea Warm Current (YSWC) intrudes the Yellow Sea only in winter time. (Redrawn from Niino and Emery, 1961; Beardsley et al., 1985)

### **Previous studies of the early Holocene and modern sediments**

The Gulf of Bohai and South Yellow Sea have been extensively studied since the 1980s (Qin et al., 1985, Milliman et al., 1985, 1987, 1989; Qin and Li, 1986; Wright, et al., 1986, 1988; Geng et al., 1987; Liu et al., 1987; Yang, et al., 1989; Alexander et al., 1991; Saito and Yang, 1994; Saito et al., 2000). Prior studies indicated that both Gulf of Bohai and South Yellow Sea received a huge amount of sediments via the Yellow River discharge. And the North Yellow Sea has been assumed to be an escape pathway by which Yellow River sediments reach the South Yellow Sea from the Gulf of Bohai (Fig. 5) (Milliman et al., 1986, Wiseman et al., 1986; Alexander et al., 1991; Liu et al., 1999).

### **Holocene Sediment Depositional Patterns**

The most conspicuous and unique geological feature in this region is the huge amount of terrigenous sediments has been discharged to the Bohai and Yellow Seas from the Yellow River. During the Holocene, sediment input from the Yellow River directly into the Yellow Sea and adjacent areas has amounted to about 3000km<sup>3</sup> (Bornhold et al., 1986; Milliman, et al., 1987), about 90 percent of which has remained within the deltaic system (Fig 6) (Wright et al., 1986, 1988, 1990; Martin et al., 1993). Previous studies show that the sediments deposited in the Gulf of Bohai could be resuspended and transported down to the South Yellow Sea via the North Yellow Sea (Alexander et al., 1991; Milliman et al., 1985, 1989) (Fig.5). In terms of the sediment inputs, the Yellow River is clearly the largest, but there are several other small rivers directly input to the Yellow Sea from both Korea and China sides. Of these, Yalu River, is the largest, being 800 km long and within a drainage area of 61,000 km<sup>2</sup> (Schubel et al., 1984), with a maximum 4.8×10<sup>6</sup> tons/yr, and average 1.13×10<sup>6</sup> tons/yr (Qin et al., 1989)





Fig. 5 Conceptualized erosion and transport of suspended sediment in the Yellow Sea during winter (red arrows) and summer (blue arrows). Hatched Yellow areas were those containing more than 5 m thickness of Holocene sediments from Milliman et al.(1986).

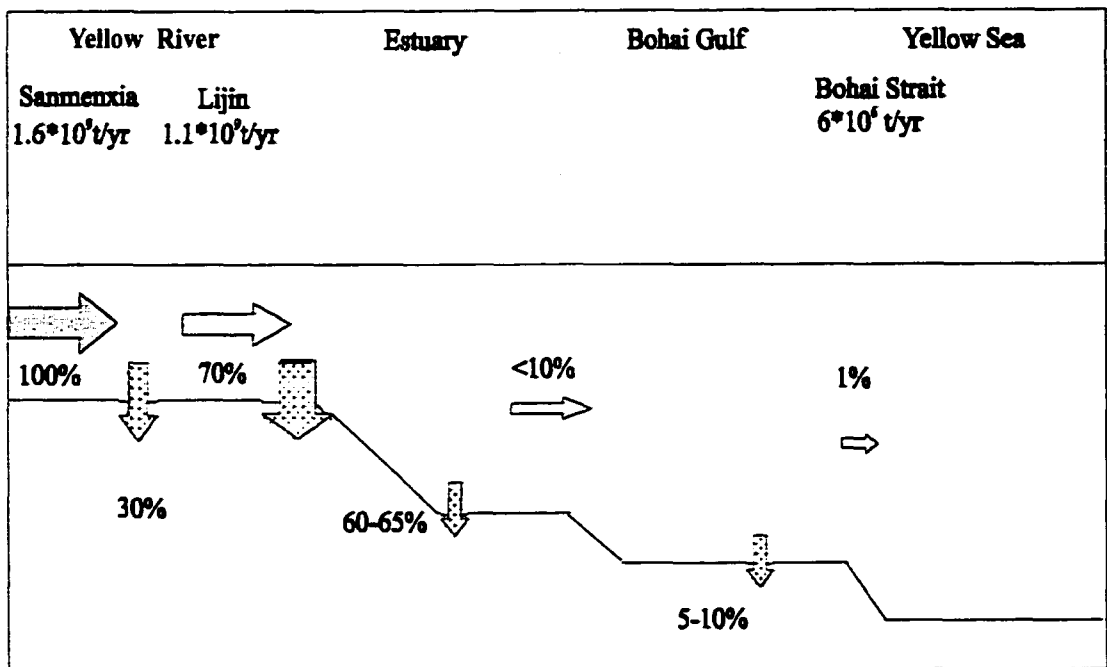


Fig. 6 Fate of the Huanghe (Yellow River) sediment. Note that more than 90-95% of the sediment load transport to the lower part of the river is deposited within the river course and shallow-water area, only <5-10% entering the central Bohai. The suspended-sediment transport to the North Yellow Sea is very limited, ~1% of the Huanghe sediment load (Redrawn from Martin et al., 1993)

During the last sea-level lowstand about 15~18 ka B.P., sea-level fell about -130 m, and the entire Yellow Sea basin and most of East China Sea was subaerially exposed (Emery et al., 1971; Zhu et al., 1979; Geng, 1982). Previous studies assumed that during the LGM sea-level lowstand, the Yellow River might extend to the paleo-coastline located south of Cheju Island, incised many old river channels into the pre-existing strata, and deposited huge amount of fluvial sediment on the subaerially exposed North and South Yellow Sea (Milliman et al., 1985, 1989; Qin and Li, 1986).

Later, the sea-level rose and reached the central part of the Yellow Sea by around 15.09 ka B.P. (Kim and Kucera, 2000). With the onset of the rapid the Holocene transgression as early as 12.9 ka B.P. (Kim and Kennett, 1998), sea level advanced rapidly across the exposed shelf at a horizontal rate approaching 80 m/yr, due to the very shallow gradient in the Yellow Sea basin (<1m/km) (Milliman et al., 1987). Sea level reached the deepest parts of the North Yellow Sea approximately 12,000 yrs BP, and seawater completely covered most of the North Yellow Sea around 9,000 yrs BP (Geng, 1982).

During the early stage of the marine transgression (~13 to 7.5 ka), the low  $\delta^{18}\text{O}$  values and the benthic foraminiferal assemblages indicate low paleosalinities (~24.8‰) in the central Yellow Sea due to strong fresh water runoff. The low  $\delta^{13}\text{C}$  values also suggest significant terrestrial organic carbon influences resulting from higher continental runoff (Kim and Kennett, 1998). The stable isotope, carbon and sulfur elemental analysis show that sedimentation in the central yellow Sea basin took place 3 times higher in a lower salinity environment in the early to mid -Holocene transgression than at present of the high sea-level and high salinity environment (Kim et al., 1999).

Between 8.47 and 6.63 ka B.P., there was a major faunal transition with a clear increase in bottom-water salinity, and may indicate the modern-type circulation in the Yellow Sea had begun to be established (Kim and Kucera, 2000). After the sea reached its present level during the mid-Holocene, it has remained relatively stable in the Bohai Sea and Yellow Sea.

Over the past 5,000 years, sediment input from the Yellow River to the Yellow Sea and adjacent areas has amounted to about 3000 km<sup>3</sup>, most of which has accumulated only over the past 2-3 thousand years due to the poor soil conservation in the Loess Plateau (Milliman et al., 1987).

An extensive and thick (up to 40m) Cliniform mud layer (Subaqueous delta) extends southward around the eastern end of the Shandong Peninsula into the South Yellow Sea; Milliman et al. (1989) suggested that this layer is Holocene in age. However <sup>210</sup>Pb and <sup>14</sup>C dating of surface sediments (Alexander et al., 1991) and depositional sequences in the seismic profiling (Liu et al. 2001) call into question rather the sediment is late Holocene or was deposited during the early Holocene transgression.

### **Historical Changes of Yellow River (Huanghe) Sediment**

During the Holocene, the Yellow River has changed its course frequently, both regionally (flowing into the Bohai Sea or South Yellow Sea) and locally (e.g., northwestern or southwestern Bohai Sea) (Fig. 7). Moreover, the Yellow River's load has increased by as much as an order of magnitude because of human disturbance of the river's watershed (Milliman et al. 1987), and recently the river's load has decreased

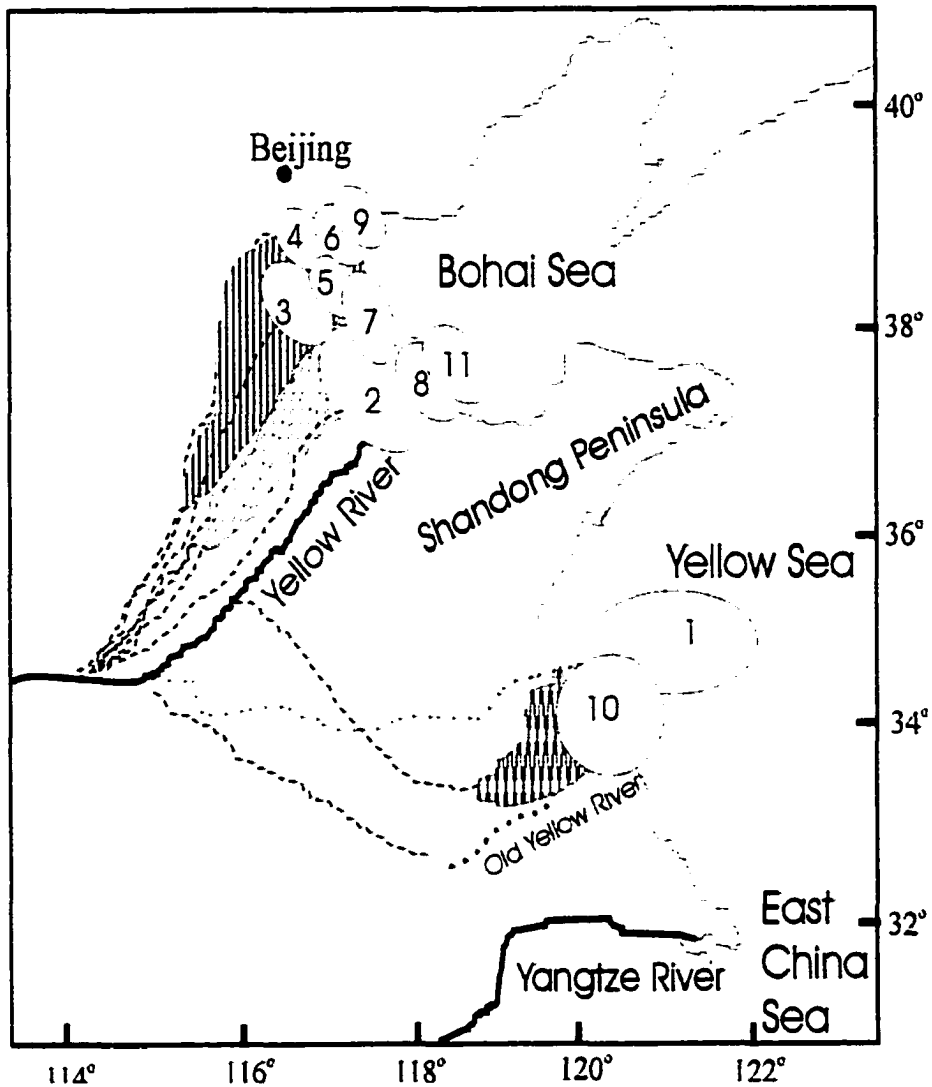


Fig. 7 Historical course shifts of the Yellow River lower reaches and the distribution of the superlobes.

- (1) 9000-7000 a B.P.; (2) 7000-5000 a B.P.; (3) 5000-4500 a B.P.;  
 (4) 4500-3400 a B.P.; (5) 3400-3000 a B.P.; (6) 3000 a B.P. -602 BC;  
 (7) 602 BC--11 AD; (8) 11 AD-1048 AD; (9) 1048 AD-1128AD;  
 (10) 1128 AD-1855AD; (11) 1855 AD - Present

((1) from Milliman *et al.*, 1989; (2) ~ (9) modified from Xue, 1993. Saito *et al.*, 1994)

substantially in response to increased aridity and a corresponding divergence of water for societal consumption (Yang et al. 1998; Galler 1999). There have been eleven documented shifts in the Yellow River's path over the past 8500 years, and nearly 500 km<sup>3</sup> of sediment have been deposited in the South Yellow Sea (SYS) and about 600 km<sup>3</sup> in the Bohai Sea (Liu et al., 2001)(Fig. 7).

To understand the history of Yellow-River-derived sedimentation in the study area, we must keep in mind the extensive and active shifting of the river's path throughout the Holocene. Seismic reflection studies in the South Yellow Sea indicate a major submarine delta offshore from Jiangsu Province, locally thicker than 20 m (Fig. 7 lobe-1) (Milliman et al. 1989). Preliminary data suggest that this offshore delta accumulated during the latter stages of eustatic sea-level rise, approximately 7-8.5 ka (Milliman et al. 1989); accumulation ceased when the river shifted back to the north of Shandong Peninsula. Total sediment volume in this subaqueous deltaic sequence is 200 km<sup>3</sup>; assuming a sediment density of 1200 kg/m<sup>3</sup>, this would be  $240 \times 10^9$  tons. Assuming that this sequence represents 1500 years deltaic sedimentation from the Yellow River, this would equate to an annual sedimentation rate of  $0.16 \times 10^9$  t/yr, which agrees quite closely with inferred Yellow River sediment fluxes prior to agricultural activity in the loess plateau of northern China (Milliman et al., 1987; Saito and Yang, 1994).

The next major shift of the Yellow River was northward into the Bohai Sea around 7000 yrs BP, where the river discharged until 1128 AD and at least formed 8 superlobes in the west of the Bohai Sea (Fig. 7, lobe 2~9) (Xue, 1993). The total sediment volume of the eight Bohai deltas that formed during this 6000-year period is 500 km<sup>3</sup> or  $600 \times 10^9$  tons,

which would equate to an annual accumulation rate of  $0.1 \times 10^9$  t/yr . This estimate, however, should be considered a minimum, since some sediment almost certainly escaped the deltaic system. Assuming a trapping efficiency of 70-80%, the total Yellow River sediment flux during this period would have been about  $0.12$  to  $0.14 \times 10^9$  t/yr.

From 1128 to 1855 AD, the Yellow River again flowed south, discharging on the Jiangsu coast (Fig. 7, lobe 10). In this 700+ year interval, approximately  $250 \text{ km}^3$  of sediment was added along the Jiangsu coast, which equates to an annual sediment load of  $0.43 \times 10^9$  t/yr, reflecting the increased erosion from increased agricultural activity in the loess hills of northern China. Nearly 700 years without the Huanghe emptying into the Gulf of Bohai and North Yellow Sea must have had a major effect on the sedimentological regime, but how much, is still unclear.

The final shift of the Yellow River to the north occurred in 1855 AD (Fig. 7, lobe-11), and in the intervening 145 years, the Bohai Delta has accumulated an estimated  $108 \text{ km}^3$ , which equates to  $130 \times 10^9$  tons, giving an annual sediment load of the river of  $0.9 \times 10^9$  t/yr.

## **The Problems and Questions**

### **1) Last Glacial Maximum (Stage 2) period**

Previous studies assumed that during the last sea-level lowstand the paleo-Yellow River extended to coastline, incised many paleo-river channels into the pre-existing strata, and deposited huge amount of fluvial sediment on the subaerially exposed North and South Yellow Sea (Milliman et al., 1985, 1989; Qin and Li, 1986). However, recent coastal paleo-environmental studies show that all of northern China had a very cold and arid

climate resulting from the intensified winter-monsoon system from the northwest during the last glacial maximum (LGM) (An et al., 1991; Zhao, 1991). Through the studies of cores in from the Gulf of Bohai and Yellow Sea, Liu and Zhao (1995) identified pre-Holocene deposits as mainly aeolian loess sediments accumulated during sea level lowstands.

In term of the late stage-2 sediment, I identify the following questions:

- a) *How did the Yellow River flow during the last sea-level regression and low stand? Did it prograde the paleo-coastline or did it retreat in response to an arid climate*
- b) *What is the nature of the LGM (stage 2) sediments; are they aeolian rather than fluvial?*

## **2) Late Pleistocene-Holocene Transgression**

With the onset of the Holocene transgression, sea level advanced rapidly across the exposed shelf, and reached the deepest parts of the North Yellow Sea approximately 12,000 yrs BP. By 9,000 a BP the seawater completely covered most of this area. The coarse-grained sands in the eastern third of the South Yellow Sea are usually transgressive and relict (Emery et al., 1971). In contrast, in the western two-thirds of the Yellow Sea is covered dominantly with fine-grained sediment that reflects the Yellow River inputs (Qin and Li, 1986).

Several questions still remain concerning the last transgressive period, specifically,

- What are the nature and timing of the transgressive facies in the North Yellow Sea?*
- With the sea level rising, when did the Yellow River begin to discharge again into this area?*



### **3) Holocene High-stand**

After the sea reached its present level during the mid-Holocene around 6,000 years, it has remained relatively stable in the Gulf of Bohai and Yellow Sea. The Yellow River has meandered greatly throughout the Holocene period. It has had more than 4 north-south shifts since early Holocene from the Bohai Sea to the South Yellow Sea, and built 3 major deltaic systems distributed respectively around the west of Bohai Sea, north and south side of Shandong Peninsula, and east of the Jiangsu coast in the west of South Yellow Sea (Milliman, 1989, Liu et al 2001).

This raises two key questions:

- a) How much of the Yellow River sediment load is transported into the North and South Yellow Sea in Holocene time, and does the North Yellow Sea serve as a conduit for transport to the South Yellow Sea?*
- b) What is relationship of the relative sea-level changes and the formation of the subaqueous deltas in the North and South Yellow Sea shelf respectively?*
- c) What was the sedimentological impact of the shifts of Yellow River discharge from the north (Gulf of Bohai) to the south (South Yellow Sea during the Holocene?*

### **4) Land-Ocean Interaction**

The Yellow and East China Seas represent an end member of modern epicontinental seas in term of the very high terrigenous sediment loads they received. The relative flat and very shallow gradient in the Yellow Sea basin (<1m/ km) makes sea-level advance or retreat very rapidly during the last transgression and regression. At same time, the large rivers in the west, i.e. Huanghe and Changjiang, and many small rivers in the east, i.e.

Yulu, Han and Keum etc, began to flow to the shelf, in the middle to meet the sea. The shallow, flat epicontinental sea contains significant information regarding the past land-ocean interaction. for instance, the transgressive process vs. the deltaic progradation. One interesting question is:

*How did the land-ocean interaction processes come across this broad shallow epicontinental shelf with the Holocene transgressive and large rivers sediment input?*

Once again, the East China Sea and Yellow Sea represent an end member of modern epicontinental seas. It contains substantial geological info regarding lowstand terrestrial deposits, subtle sea-level variations, large river sediment inputs, land-ocean interaction, highstand proximal and distal deltaic deposits, etc. It is a very unique and ideal place to trace the above information in this single shelf sea.

## **References**

- Alexander C.R., DeMaster D.J., and Nittrouer C.A., 1991. Sediment accumulation in a modern epicontinental-shelf setting: The Yellow Sea. *Marine Geology*, 98: p51-72.
- An, Z., Kukla, G.J., Porter, S.C., and Xiao J., 1991. Magnetic susceptibility evidence of monsoon variation on the Loess Plateau of central China during the last 130,000 years, *Quaternary Research*, Vol. 36 P.29-36.
- Auffret, G.A., Pujol, C., Baltzer, A., Bourillet, J.F., Mueller, C., Tisot, J.P., 1996. Quaternary sedimentary regime on the Berthois Spir (Bay of Biscay). *Geo-Marine Letter*, Vol. 16, No.2. p76-84.
- Beardsley, R.C., Limeburner, R., Yu, and H., and Cannon, G.A. 1985. Discharge of the Cahngjiang (Yangtze River) into the East China Sea. *Cont. Shelf Res.*, 4: 57-76.
- Bornhold, B.D., Yang Z.S., Keller, G.H., Prior, D.B., Wiseman, W.J., Wang, Q., Wright, L.D., Xu, W.D., and Zhuang Z.Y., 1986. Sedimentary framework of the modern Huanghe (Yellow River) Delta. *Geo-Marine Letter*, 6. p77-83.
- Boyd, R., Suter, J., and Penland, S., 1989. Relation of sequence stratigraphy to modern sedimentary environments. *Geology*, Vol. 17, no. 10, pp. 926-929.
- Britannica. 2001. Web edition: <http://www.Britannica.com/>.
- Deckker, P. de., Correge, T., and Head, J. 1991. Late Pleistocene record of cyclic eolian activity from tropical Australia suggesting the Younger Dryas is not an unusual climatic event. *Geology*, 19(6): 602-605.
- Emery K.O., Niino H., and Sullivan B., 1971. Post-Pleistocene levels of the East China Sea. In: *The late Cenozoic glacial ages*, K.K. Turekian, editor, Yale University Press.381-390.

- Fairbridge, R.W., 1968. Continental Shelf, Encyclopedia of Geomorphology. Reinhold Book Corporation, New York, Amsterdam, London.
- Galler, J.J., 1999. Medium and long-term changes in fluvial discharge to the sea: The Yellow River case study. Master of Science Thesis. College of William & Mary, 78 pp
- Geng, X., 1982. Marine transgressions and regressions in East China since the late Pleistocene Epoch. *Collection of Oceanic Works*. 5: 100-123.
- Geng X., Wang, Y., and Fu, M. 1987. Holocene sea level oscillations around Shandong Peninsula. In: Qin, Y., and Zhao S., (Eds), *Late Quaternary Sea-level Changes*. Beijing: China Ocean Press. p81-96.
- Guan, B. X., 1984. Major features of the shallow water hydrography in the East China Sea and Huanghai Sea. in *Ocean Hydrodynamics of the Japan and East China Seas*, ed., T. Ichiye. Elsevier. 1-13.
- Guan B.-X., 1994. Patterns and structures of the currents in Bohai, Huanhai and east China Seas. in *Oceanology of China Seas*, eds., Zhou and Tseng, 17-26.
- Hu D.X., 1984. Upwelling and sedimentation dynamics, *Chin. J. Oceanol. Limnol.*, 2(1): 12-19.
- Kim Jung-Moo and Kennett James P., 1998. Paleoenvironmental changes associated with the Holocene marine transgression, Yellow Sea (Hwanghae). *Marine Micropaleontology* 34: 71-89.
- Kim Jung-Moo and Kucera Michal. 2000. Benthic foraminifer record of environmental changes in the Yellow Sea (Hwanghae) during the last 15,000 years. *Quaternary Science Reviews*, 19: 1067-1085.

- Kim, Y.H., Lee, H.J., Chun, S.S., Han, S.J., and Chough, S.K. 1999. Holocene transgressive stratigraphy of a macrotidal flat in the southeastern Yellow Sea: Gomso Bay, Korea. *Journal of Sedimentary Research Section B: Stratigraphy and Global Studies*, vol. 69, no. 2, pp. 328-337.
- Kleiber, H.P., Knies, J., and Niessen, F., 2000. The Late Weichselian glaciation of the Franz Victoria Trough, northern Barents Sea: ice sheet extent and timing. *Marine Geology*, vol. 168, no. 1-4, pp 25-44.
- Li, D.S., 1984. Geologic Evolution of Petroliferous Basins on Continental Shelf of China. *Am. Ass. Petr. Geo. Bul.* 68 (8): 993-1003.
- Li Fan, Zhang Xiurong, Li Yongzhi, and Li Benzhaoh. 1998. Buried paleo-delta in the South Yellow Sea. *Acta Geographica Sinica*. Vol. 52, No.3 238-244.
- Liu, J.P., and S.L. Zhao. 1995. Origin of the buried loess in the Bohai Sea bottom and the exposed loess along the coastal zone. *Oceanologia et Limnologia Sinica*, 26, 4: 363-368.
- Liu, J.P., Milliman, J.D., and Gao S., 2001. The Shandong mud wedge and Holocene sediment accumulation in the Yellow Sea. *Geo-Marine Letter*, (in press).
- Liu Z.X., Xia D.X., Berne S., Wang, K.Y., Marsset T., Tang Y.X., and Bourillet J.F., 1998. Total deposition systems of China's continental shelf, with special reference to the eastern Bohai Sea. *Marine Geology*, 145, p225-253.
- Lyman, J., 1961. "Oceans and Sea", in "Encyclopedia of Science and Technology", New York, McGrawHill Book Co.
- Martin, J.M., Zhang, J., Shi, M.C. and Zhou Q. 1993, Actual flux of the Huanghe (Yellow River) sediment to the western Pacific Ocean. *Netherlands Journal of Sea Research*. 31(3):243-254.

- Milliman, J.D., and Meade, R.H., 1983. World-wide delivery of river sediment to the oceans. *Journal of Geology*, Vol. 91, No.1, p1-21.
- Milliman, J.D., Xie, Q.-c. and Yang, Z.-s., 1984. Transfer of particular organic carbon and nitrogen from the Yangtze River to the ocean. *Amer. J. Sci.*, 284:824-834.
- Milliman, J.D., Beardsley, R.C., Yang, Z.S., and Limeburner, R., 1985. Modern Huanghe-derived muds on the outer shelf of the East China Sea: identification and potential transport mechanisms. *Continental Shelf Research*, 4:p175-188.
- Milliman J.D., Li, F., Zhao, Y.Y., Zheng, T.M., and Limeburner R., 1986. Suspended matter regime in the Yellow Sea. *Prog. Oceanog.*, Vol. 17, p215-227.
- Milliman, J.D., Qin Y.S., Ren M.E. and Saito Y., 1987. Man's influence on the erosion and transport of sediment by Asian rivers: the Yellow River (Huanghe) example. *J. Geology*, V. 95, p751-762
- Milliman, J.D., Qin, Y.S., and Park, Y., 1989. Sediment and sedimentary processes in the Yellow and East China Seas. *Sedimentary Facies in the Active Plate Margin*, edited by A. Taira and F. Masuda, p 233-249
- Milliman, J.D., and Syvitski J.P.M., 1992. Geomorphic/Tectonic Control of Sediment Discharge to the Ocean: The Importance of Small Mountainous Rivers., *Journal of Geology*, Vol. 100, p525-544.
- Naimie, C.E., Blain C.A., Lynch D.R., 2001. Seasonal mean circulation in the Yellow Sea – a model-generated climatology. *Continental Shelf Research* 21: 667-695.
- Nelson, H., Thor, D.R., and Sandstrom, M.W. 1979. Modern Biogenic Gas-Generated Craters (Seafloor ' Pockmarks') on Bering Shelf, Alaska. *Environmental Assessment of the*

- Alaskan Continental Shelf. Annual Reports of Principal Investigators for year ending March 1979. Vol X, Hazards, Data Management, p 110-131, October 1979.
- Niino H., and Emery K.O., 1961. Sediments of shallow portions of East China Sea and South China Sea. *Geological Society of America Bulletin*, 72, 731-762.
- Polyak, L. and Solheim, A. 1994. Late- and postglacial environments in the northern Barents Sea west of Franz Josef Land. *Polar Research*. 12, 197-207.
- Pujos. M., and Odin G.S.. 1986. Late Quaternary sedimentation on the shelf off French Guiana. *Oceanologica ACTA*. Vol. 9, No. 4, p363-382.
- Qian, N., and Dai, D.Z.. 1980. The problems of river sedimentation and present status of its research in China: Chinese Hydraul. Eng.. Proc. Int. Symp. River Sedimentation, v.1, p.1-39.
- Qin, Y.S. and Li F.. 1986. Study of the influence of sediment loads discharged from Huanghe river on sedimentation in the Bohai and Yellow Seas. *Oceanologia et Limnologia Sinica*, No. 27, p125-135.
- Qin, Y.S. and Zhao S.L.. (ed.) 1986 Late Quaternary Sea-level Changes, China Ocean Press. pp1-251.
- Qin Y.S., Zhao, Y.Y., Chen L.R., Zhao, S.L., 1987. *Geology of the East China Sea*. China Science Press, Beijing.
- Qin Y.S., Zhao, Y.Y., Chen L.R., Zhao, S.L., 1989. *Geology of the Yellow Sea*. China Ocean Press, Beijing.
- Saettem, J., Poole, D.A.R., Ellingsen, L., and Sejrup, H.P., 1992. Glacial geology of outer Bjoernoyrenna, southwestern Barents Sea. *Marine Geology*, 103(1-3): 15-31.

- Saito, Y., and Yang Z.S., 1994. The Huanghe River: its water discharge, sediment discharge, and sediment budget, *J. Sed. Soc. Japan*, No. 40, p7-17.
- Saito, Y. and Yang, Z.S., 1995. Historical change of the Huanghe (Yellow River) and its impact on the sediment budget of the East China Sea. *Global Fluxes of Carbon and Its Related Substances in the Coastal Sea-Ocean-Atmosphere System*, Editors: S. Tsunogai, K. Iseki, I. Koike and T. Oba, M&J International, Yokohama, pp. 7-12.
- Saito, Y., Katayama, H., Ikehara, K., Kato, Y., Matsumoto, E., Oguri, K., Oda M., Yumoto, M., 1998. Transgressive and highstand systems tracts and post-glacial transgression, the East China Sea. *Sedimentary Geology*. 122, 217-232.
- Saito, Y., Wei, h., Zhou, Y., Nishimura, A., Sato, Y. and Yokota S., 2000. Delta progradation and chenier formation in the Huanghe (Yellow River), delta China. *Journal of Asian Earth Sciences*, v.18: 489-497.
- Saito, Y. Yang, Z.S., Hori, K., 2001. The Huanghe (Yellow River) and Changjiang (Yangtze River) deltas: a review on their characteristics, evolution and sediment discharge during the Holocene. *Geomorphology* 41, 219-231.
- Schubel J.R., Shen H.T., and Park, M.J., 1984. A comparison of some characteristic sedimentation processes of estuaries entering the Yellow Sea. In *Proc. Korea-US. Seminar and Workshop: Marine Geology and Physical Processes of the Yellow Sea*. P286-308.
- Takahashi K., 1999. The Okhotsk and Bering Seas: critical marginal seas for the land-ocean linkage. *Land-Sea Link in Asia: Proceedings of an international workshop on sediment transport and storage in coastal sea-ocean system*, Japan. 341-353.



- Trincardi, F., Correggiari, A., and Roveri, M., 1994. Late Quaternary transgressive erosion and deposition in a modern epicontinental shelf: the Ariatic Semienclosed Basin. *Geo-Marine Letters*, 14: 41-51.
- Torgersen, T., Jones, M.R., Stephens, A.W., Searle, D.E. & Ullman, W.J. 1985 Late Quaternary hydrological changes in the Gulf of Carpentaria. *Nature*. 313, 785-787.
- Wageman, J.M., T.W., Hilde, and Emery, K.O., 1970. Structural framework of East China Sea and Yellow Sea. *American Association of Petroleum Geologists Bulletin*, v.54, no.9, 1611-1643.
- Wang, P. & Sun, X., 1994. Late glacial maximum in China: comparison between land and sea. *Catena*, 23, 341-353.
- Wells, J.T., Huh, O.K., 1984. Fall-season patterns of turbidity and sediment transport in the Korea Strait and southeastern Yellow Sea. In: Ichiye, T. (Ed), *Ocean Hydrodynamics of the Japan and East China*. Elsevier, Amsterdam, pp387-397.
- Wiseman, W.J., Fan Y.B., Bornhold B.D., Keller, G.H., Su, Z.Q., Prior D.B., Yu, Z.X., Wright, L.D., Wang F.Q. and Qian, Q.Y., 1986. Suspended sediments advection by tidal currents off the Huanghe (Yellow River) delta. *Geo-Marine Letter*, 9: 107-113.
- Wright L.D., Yang Z.S., Bornhold B.D., Keller, G.H., Prior D.B., Wiseman, W.J., 1986. Hyperpycnal plumes and plume fronts over the Huanghe (Yellow River) delta front. *Geo-Marine Letter*, 6: 97-105.
- Wright L.D., Wiseman, W.J., Bornhold B.D., Prior D.B., Suhayda J.N., Keller, G.H., Yang Z.S., and Fan Y.B., 1988. Marine dispersal and deposition of Yellow River silts by gravity-driven underflows. *Nature*, Vol, 332, 14: p629-632.

- Wright L.D., Wiseman, W.J., Yang Z.S., Bornhold B.D., Keller, G.H., Prior D.B., Suhayda J.N., 1990. Processes of marine dispersal and deposition of suspended silts off the modern mouth of the Huanghe (Yellow River). *Continental Shelf Research*. 10, 1-40.
- Uda, M., 1934. The results of simultaneous oceanographical investigations in the Japan Sea and its adjacent waters in May and June, 1932, Japan Imperial Fish. Exped. Station, 5: 57-190.
- Xia, D.X., Wang W.H., Wu G.Q., Cui, J.R., and Li F.L., 1993 Coastal Erosion in China. *Acta Geographica Sinica*. 48: 468-476.
- Yang, Z.-S., Milliman, J.D., Galler, J., Liu, J.P. and Sun, X.G., 1998. Yellow River's Water and Sediment Discharge Decreasing Steadily. *EOS*, v.79, 48:589-592.
- Yuan, Y. and SU, J., 1984. Numerical modelling of the circulation in the East China Sea, In *Ocean Hydrodynamics of Japan and East China Sea*. Elsevier Oceanography Series. 39. Ichiye, T., ed. Elsevier, New York, 167-186.
- Zhao, S.L., 1991. China shelf sea desertization and its derived deposits during the last stage of Late Pleistocene. *Oceanologia et Limnologia Sinica*, Vol. 22, No. 3, p285-293.
- Zheng, Q.A., and Klemas V., 1982. Determination of Winter Temperature Patterns, Fronts, and Surface Currents in the Yellow Sea and East China Sea from Satellite Imagery. *Remote Sensing of Environment*, 12, 201-218.
- Zhu Yongqi, Li Chengyi, Zeng Chengkai and Li Bogen, 1979. Lowest sea-level of the continent of the East China Sea in the late-Pleistocene. *Chinese Science Bulletin*, Vol.24, No.7: 317-320.

## Chapter Two

### The Shandong mud wedge and post-glacial sediment accumulation in the Yellow Sea\*

J.P. Liu, J.D. Milliman and S. Gao<sup>#</sup>

School of Marine Science, College of William and Mary, Gloucester Point, VA 23062, USA

<sup>#</sup> Institute of Oceanology, Chinese Academy of Sciences, Qingdao 266071, China

#### Abstract

Two well-defined deltaic sequences in the Bohai Sea and in the South Yellow Sea represent post-glacial accumulation of Yellow River-derived sediments. Another prominent depocenter on this epicontinental shelf, a pronounced clinoform in the North Yellow Sea, wraps around the northeastern and southeastern end of the Shandong Peninsula, extending into the South Yellow Sea. This Shandong mud wedge is 20 to 40 m thick and contains an estimated 300 km<sup>3</sup> of sediment. Radiocarbon dating, shallow seismic profiles, and regional sea-level history suggest that the mud wedge formed when the rate of post-glacial sea-level rise slackened and the summer monsoon intensified, about 11 ka. Geomorphic configuration and mineralogical data indicate that present-day sediment deposited on Shandong mud wedge comes not only from the Yellow River but also from coastal erosion and local rivers. Basin-wide circulation in the North Yellow Sea may transport and redistribute fine sediments into and out of the mud wedge.

---

\* Submitted to *Geo-Marine Letters* (in press)

## Introduction

The Yellow Sea and adjacent East China Sea form a broad, tectonically stable shelf that represents one of the few modern examples of an epicontinental sea (Fig. 1). Throughout the 20th century the Yellow and East China seas have received about 10% of the total fluvial sediment flux to the global ocean, the Yellow River (Huang He) and the Yangtze River (Chang Jiang) discharging about 0.9 and  $0.5 \times 10^9$  t/year, respectively (Milliman and Meade 1983; Galler 1999). Most of the Yangtze's sediment is dispersed southwards into the East China Sea (e.g., Milliman et al. 1984), whereas the Yellow River has discharged most of its sediment into the western Yellow Sea. During the Holocene, however, the Yellow River has changed its course frequently, both regionally (flowing into the Bohai Sea or South Yellow Sea) and locally (e.g., northwestern or southwestern Bohai Sea) (Fig. 2a). Moreover, the Yellow River's load increased by as much as an order of magnitude in response to human disturbance of the river's watershed (Milliman et al. 1987). Recently the river's load has decreased substantially because of increased aridity and the divergence of water for human consumption (Yang et al. 1998; Galler 1999). Eleven documented shifts in the Yellow River's path have been documented over the past 9 ky (Milliman et al. 1987, Xue, 1993, Saito et al. 2000), such that nearly  $500 \text{ km}^3$  of sediment have been deposited in the South Yellow Sea and about  $600 \text{ km}^3$  in the Bohai Sea (Fig. 2a, Table 1).

To understand the history of Yellow River-derived sedimentation in the study area, we must keep in mind three things: 1) post-glacial sea-level transgression across the low-gradient Yellow Sea shelf; 2) intensification of the SE monsoon about 11 ka, thereby increasing precipitation and runoff within the Yellow River's drainage basin; and 3) the extensive and active north-south shifting of the Yellow River's path throughout the

Holocene. Seismic reflection studies in the South Yellow Sea (Fig. 1) indicate a major submarine delta offshore from Jiangsu Province (Fig. 2a, lobe 1), locally thicker than 20 m (Yang 1985; Shi et al. 1986; Milliman et al. 1987, 1989). Previous data have suggested that this offshore delta accumulated during the latter stages of eustatic sea-level rise, approximately 9-7.5 ka. (Yang 1985; Shi et al. 1986; Milliman et al. 1987, 1989). Accumulation ceased when the river shifted back into the Bohai Sea north of the Shandong Peninsula. Based on the above seismic data, total sediment volume calculated for the Jiangsu offshore delta is  $200 \text{ km}^3$ . Assuming a sediment density of  $1200 \text{ kg/m}^3$ , this would be  $240 \times 10^9 \text{ t}$ . Assuming that this sequence represents 1.5 ky of deltaic sedimentation from the Yellow River, this would equate to an annual mass accumulation rate of  $0.16 \times 10^9 \text{ t/y}$ , which agrees quite closely with inferred Yellow River sediment fluxes prior to agricultural activity on the loess plateau of northern China (Milliman et al. 1987; Saito and Yang 1994).

Following its northward shift around 7-7.5 ka, Yellow River continued to discharge into the Bohai Sea until 1128 AD. During this approximately 6-ky interval, it formed at least eight superlobes (Fig. 2a, lobes 2-9) (Xue, 1993), accounting for a total sediment volume/mass of  $500 \text{ km}^3/600 \times 10^9 \text{ t}$ , which would equate to an annual accumulation rate of  $0.1 \times 10^9 \text{ t/y}$  (Table 1). This estimate, however, should be considered as a minimum, since some sediment almost certainly escaped the deltaic system. If the trapping efficiency in the modern delta is about 90% (Bornhold et al. 1986), the annual Yellow River sediment flux during this period would have been about  $0.11 \times 10^9 \text{ t/y}$ .

From 1128 to 1855 A.D., the Yellow River again flowed south, discharging onto the Jiangsu coast (Fig. 2a, lobe 10). In this 700+-y interval, approximately  $250 \text{ km}^3$  of

sediment were deposited along the Jiangsu coast, which equates to a mean annual sediment load of  $0.43 \times 10^9$  t/y, reflecting enhanced erosion from increased agricultural activity in the loess hills of northern China (Milliman et al., 1987). The last shift of the Yellow River to the north occurred in 1855 A.D. (Fig. 2a, lobe 11), assuming an annual riverine sediment load of  $0.9 \times 10^9$  t/y (Milliman and Meade 1983; Galler 1999), in the intervening 145 years an estimated  $130 \times 10^9$  t (or  $108 \text{ km}^3$ ) (Table 1) of sediment passed Lijin Hydrographic Station (150 km inland from the river mouth) (Fig. 2b), of which about  $78 \text{ km}^3$  accumulated on the prograding delta (Qian 1993; Y. Saito's written communication). This would infer a 72% trapping efficiency on the subaerial delta, the remainder being deposited either above the delta or offshore, mostly within 30 km of the delta front, being transported by gravity-driven underflow (Wright et al. 1988). Less than 1% of the Lijin load is assumed to be transported out of the Bohai and into the North Yellow Sea (Martin et al. 1993).

### **Shandong Mud Wedge**

A third depocenter was identified in the mid-1980s by high-resolution seismic profiling and sediment coring, extending south from the eastern tip of the Shandong Peninsula into the South Yellow Sea. Based on a few seismic profiles and oceanographic measurements, Milliman et al. (1987, 1989) suggested that this mud wedge represents an escape route for Yellow River sediment from the Bohai Sea to the South Yellow Sea. Alexander et al. (1991) called this feature the Shandong Subaqueous Delta, inferring its similarity to an Amazon-like subaqueous delta system. Based on  $^{210}\text{Pb}$  profiles, these

authors reported present-day sedimentation rates of 1 mm/year or less in the topset and bottomset beds, and up to 8 mm/year in the foreset beds.

Because of the lack of data in the North Yellow Sea, however, important questions remained unanswered, foremost amongst them was the geographic extent of the mud wedge within the North Yellow Sea. Did the wedge extend north of the Shandong Peninsula, and if so, did it connect with the Yellow River delta in the Gulf of Bohai? Other questions concerned the possible dispersal of Yellow-River sediment from the Bohai Sea to the South Yellow Sea, how this dispersal has been affected by north-south shifts in the Yellow River's course throughout the Holocene, and the possible sedimentary influence of local rivers draining the Shandong Peninsula.

### **Materials and Methods**

To delineate sediment dispersal from the Yellow River's mouth to the South Yellow Sea, two geophysical and geological cruises were carried out in the Bohai and North Yellow seas in 1998 and 1999 aboard the RV Gold Star II from the Institute of Oceanology, Chinese Academy of Sciences, during which we collected approximately 1200 km of high-resolution seismic profiles (Fig.1), 10 gravity cores, 4 box cores, and 70 surface sediment samples. Seismic data were obtained with a 450-kJ ORE GeoPulse boomer system fired at 0.5 sec intervals; records were filtered between 500 and 3000 Hz. These complemented seismic profiles taken in the South Yellow Sea (Fig.1) in the 1980s, which permit us to delineate the Holocene sediment thickness and thereby sediment volume (Milliman et al. 1987, 1989).

Well-documented peat deposits that underlie the mud wedge in the North Yellow Sea were sampled in the gravity cores (NYS-3 and NYS-5) (Fig. 2c, 3). AMS  $^{14}\text{C}$  dating of two peat samples was done at the Woods Hole Oceanographic Institution's NOSAMS lab. Radiocarbon ages were calculated using a 5568-y half-life. They are reported in calendar years using the newly updated CALIB4.3 (Stuvier et al. 1998); other published dates from this region also were converted to calendar years (Table 2).

## Results

Seismic profiles show a prominent subsurface reflector in the North Yellow Sea, overlain by a thick clinoform that thickens towards the Shandong Peninsula (Fig. 3). Although we could not profile in water depths shallower than about 10 m, some profiles did cover both the foreset and topset beds of the clinoform. Foreset gradients were somewhat less than 2/1000, whereas topset gradients were less than 1/1000.

Based on previous experience in the South Yellow Sea (Milliman et al. 1987, 1989) we interpret the prominent subsurface reflector to be the base of the post-glacial transgressive sequence. Cores penetrating this reflector at the base of the foreset or bottomset sequences sampled peat deposits 11-12 ka in age (Table 2). Although biogenic gas obscured the nearshore portions of our records, the soft bottom and the strong acoustic return of the transgressive reflector allowed us to calculate the thickness of the mud wedge in waters far shallower than the depth of the first multiple (Profile 99-D, Fig. 3). Accordingly, we can delineate the overlying Holocene clinoform as being at least 40 m thick north of the Peninsula, extending at least 150 km east to  $123^{\circ} 30'E$  (Figs. 2, 3). The wedge thins offshore, and most of the northern half of the NYS appears to be covered by no more than



1 m of Holocene sediment. Based on the seismic profiles (Fig. 3) and thickness of the Holocene sediment (Fig. 2b, c), total sediment volume of this mud wedge is calculated to be about 300 km<sup>3</sup> (Table 1). Seismic profiling at offshore of the modern delta (Bornhold et al. 1986), our profiles (Fig.1) and borehole data (Qin et al. 1983) within the Bohai Sea indicate that the wedge in the eastern part of the Bohai thins to less than 10 m (Fig. 2c), suggesting that there is no present connection between the Shandong mud wedge and the Yellow River delta.

## **Discussion**

Total sediment volume within the three major depocenters in the Yellow Sea (Bohai delta, Jiangsu delta, and Shandong mud wedge) is more than 1300 km<sup>3</sup>, nearly all of it apparently derived from the Yellow River (Qin and Li, 1986; Milliman et al. 1989) – but perhaps not all, as will be discussed below. Moreover, we suspect that much of this sediment was deposited during the early Holocene during a period of slow sea-level rise. Several lines of evidence allow us to reach this conclusion.

First, in contrast to Alexander et al.'s (1991) descriptions and definitions, the Shandong mud wedge appears to be a complex system that differs from modern and relict subaqueous deltas (e.g., Amazon clinoform; Jiangsu delta), in that it essentially drapes off the Shandong coast normal to the direction of ultimate sediment transport (Fig. 2b). Moreover, as mentioned above, the mud wedge is not directly connected to the modern Yellow River delta. Analysis of extensive sediments cores (Qin et al. 1983) and geophysical data show generally less than 10 m of Holocene sediment along the southern Bohai Sea. Based on field observations, Martin et al. (1993) calculated that only about

$6 \times 10^6$  t/year sediment is transported eastwards through the Bohai Strait, similar to the estimate of  $5\text{-}10 \times 10^6$  t/year by Qin and Li (1986). This represents 0.5 – 1% of the Yellow River's annual sediment load. If correct, these calculations give further evidence for a different time and mode of formation of the mud wedge, although it may presently still accept limited input from the river via the seasonal sediment flux.

Unfortunately, sedimentation rates determined from the short-term dating ( $^{210}\text{Pb}$ ) using the shallow box cores (< 1 m) (Alexander et al. 1991) cannot delineate the entire history of a mud wedge that locally exceeds 40 m in thickness. In spite of the lack of deep cores, however, we find it interesting that the transgressive surface appears to lie at present-day water depths of 50-60 m (Fig. 3) and that the mud wedge lies just seaward of the 40-m paleo-bathymetric contour (Fig. 2c), when sea level rose quickly from -60 to -42 m during Melt-Water Pulse (MWP)-1B, 11.8-11.4 ka cal BP (Fig. 2d) (Fairbanks, 1989; Liu and Milliman, 2001). Dates for peat samples recovered in cores NYS-3 and NYS-5 (12.8 and 11.8 ka, respectively) would support this assumption (Table-2). According to this scenario, during MWP-1B sea level rose at an average of 45 mm/year and advanced horizontally at least 200 m/year. By the end of MWP-1B, most of the North Yellow Sea had been flooded, after which sea level stabilized at -40 m at the mouth of the Bohai Sea for about 1.8 k years (Fig. 2c, 2d). The Asian Summer Monsoon intensified also during this same period, reaching its maximum after MWP-1B (Wang et al. 1999), resulting in increased fluvial runoff from most south Asian rivers (Wang et al. 1999; Prins and Postma, 2000). The more gradual rate of sea-level rise combined with increased runoff from the Yellow River meant rapid delivery of sediment and its accumulation in the North Yellow Sea (Fig. 2c).

Recent studies indicate that several extreme flooding events occurred along the middle reaches of the Yellow River at calendar years of 9.2, 8.17 and 6.95 ka and 1843 AD (Yang et al. 2000), with peak discharges greater than 30,000 m<sup>3</sup>/s, 2-3 times larger than the mean recurrence interval of once every 10 years. If the 1843's flooding event (15 m higher than the present-day mean high-water level) contributed to the northward-shift of the river into Bohai Sea in 1855 AD, the extreme flood at 9.2 ka B.P. might have initiated a southward-shift of the river to Jiangsu Province, and formed the lobe-1 in the South Yellow Sea (Fig. 2a). Similarly, after 2 ky it might have shifted back north during the 6.95 ka event. This time span, in fact, agrees roughly with the presumed age of the Jiangsu subaqueous delta (Milliman et al., 1989).

Second, the Yellow River may not be the sole source of sediment in the Shandong mud wedge. Mineralogical data indicate a somewhat different character from sediments presently discharged for the Yellow River (Liu et al. 1987; Qin et al. 1989). For instance, quartz and orthoclase represent 59 and 24%, respectively, in the Shandong mud wedge fine-sand fraction, compared to 31% and 7% in Bohai delta sediments (Qin et al. 1989). In addition, epidote content in the Shandong mud wedge is as high as 35, compared to 16.5% at the Yellow River mouth (Liu et al. 1987). Observed erosion rates of the loess deposits along the west coast of Shandong Peninsula are high, averaging 2 m/year (maximum ~10 m/year) (Xia et al. 1993), which could transport significant amounts of sediment to the mud wedge.

Basin-wide circulation patterns in the North Yellow Sea can also transport, redistribute, and trap fine-grained sediment in the mud wedge (Hu 1984), particularly relict loess which was deposited during the Last Glacial Maximum and is now undergoing local erosion (Liu

and Zhao 1995; Liu et al. 1999). High concentrations of suspended particulate matter in the water column in this region (Milliman et al. 1985, 1986, 1989) may indicate local resuspension, rather than large-scale west-east and north-south transport of Yellow River-derived sediment to the South Yellow Sea.

Although we still consider our data and interpretations preliminary, our data suggest that much of the Shandong mud wedge was deposited in the early Holocene, during a relatively slow rise of sea level and the onset of the Asian summer monsoon. The subsequent rapid jump sea level (-36 to -16 m) during MWP-1C (Fig. 2d) (Liu and Milliman 2001) and extreme flooding events in the Yellow River 9.0-7.5 ka (Yang et al. 2000), which may have shifted its mouth south of the Shandong Peninsula (Milliman et al. 1989), meaning that the sediment supply to North Yellow Sea was effectively cut between 9.0 and 7.5 ka, during which time sea level transgressed well into the Bohai Sea. (This post-7.5 ka period corresponds with the worldwide initiation of Holocene marine deltas in response to the decelerated sea-level rise; Stanley and Warne, 1994.) The disconnect between the post-7.5 ka Yellow River and the Shandong mud wedge means that local streams and coastal erosion, as well as basin-wide circulation, may account for an appreciable amount of sediment presently deposited on the upper parts of the mud wedge.

## **Acknowledgements**

We thank the crews of the RV Goldstar II and our Chinese and American colleagues for their help in obtaining and processing the geophysical and geological data. Prof. Guan Chenzhong's help in sediment sampling and Mr. Wang Shaozhi's help seismic profiling during our two cruises are particularly appreciated. We also thank Yoshiki Saito and Clark Alexander's valuable suggestions and reviews. Financial support for this program came from Natural Science Foundation of China (Grant Number 498), the U.S. Office of Naval Research and National Science Foundation. This is contribution No. 2425 from Virginia Institute of Marine Science, College of William and Mary.

## References

- Alexander CR, DeMaster DJ, Nittrouer CA (1991) Sediment accumulation in a modern epicontinental-shelf setting: The Yellow Sea. *Marine Geology* 98: 51-72
- Bornhold BD, Yang ZS, Keller GH, Prior DB, Wiseman WJ, Wang Q, Wright LD, Xu WD, Zhuang ZY (1986) Sedimentary framework of the modern Huanghe (Yellow River) Delta. *Geo-Marine Letter* 6: 77-83
- Fairbanks RG (1989) A 17,000-year glacio-eustatic sea level record: influence of glacial melting rates on the Younger Dryas event and deep ocean circulation. *Nature* 342: 637-642
- Galler JJ (1999) Medium and long-term changes in fluvial discharge to the sea: The Yellow River case study. Master of Science Thesis, College of William & Mary, 78 pp
- Hu DX (1984) Upwelling and sedimentation dynamics I. The role of upwelling in sedimentation in the Yellow Sea and East China Sea. *Chin. J. Oceanol. Limnol.*, 2(1): 12-19
- Liu MH, Wu SY, Wang YJ (1987) Late Quaternary deposits of the Yellow Sea (in Chinese). China Ocean Press, Beijing, 433 pp
- Liu JP, Zhao SL (1995) Origin of the buried loess in the Bohai Sea bottom and the exposed loess along the coastal zone (in Chinese with English abstract). *Oceanologia et Limnologia Sinica* 26: 363-368
- Liu JP, Cheng P, Gao S, Farnsworth K, Milliman JD (1999) A preliminary report about the recent cruise in the north Yellow Sea and Bohai Strait. Land-sea link in Asia. Proceedings of the international workshop Sediment Transport and Storage in Coastal Sea-Ocean Systems, Japan (1999). 44-48

- Liu JP, Milliman JD (2001) Post-glacial sea-level transgression in the East China and Yellow seas: Significance of periodic rapid flooding events. *Science* (in review)
- Kim DS, Park BK, Shin IC (1999). Paleoenvironmental changes of the Yellow Sea during the Late Quaternary. *Geo-Marine Letters* 18: 189-194
- Martin JM, Zhang J, Shi MC, Zhou Q (1993) Actual flux of the Huanghe (Yellow River) sediment to the western Pacific Ocean. *Netherlands Journal of Sea Research* 31:243-254
- Milliman JD, Meade RH (1983) World-wide delivery of river sediment to the oceans. *Journal of Geology* 91: 1-21
- Milliman JD, Xie QC, Yang ZS (1984) Transfer of particulate organic carbon and nitrogen from the Yangtze River to the ocean. *Amer. J. Sci.* 284:824-834
- Milliman JD, Beardsley RC, Yang ZS, Limeburner R (1985) Modern Huanghe-derived muds on the outer shelf of the East China Sea: identification and potential transport mechanisms. *Continental Shelf Research* 4:175-188
- Milliman JD, Li F, Zhao YY, Zheng TM, Limeburner R (1986) Suspended matter regime in the Yellow Sea. *Prog. Oceanogr.* 17: 215-227
- Milliman JD, Qin YS, Ren ME, Saito Y (1987) Man's influence on the erosion and transport of sediment by Asian rivers: the Yellow River (Huanghe) example. *J. Geology* 95: 751-762
- Milliman JD, Qin YS, Park Y (1989) Sediment and sedimentary processes in the Yellow and East China Seas. In: Taira A, Masuda F (eds) *Sedimentary Facies in the Active Plate Margin*. Terra Scientific Publishing Company, Tokyo, 233-249
- Prins MA, Postma G (2000) Effects of climate, sea level, and tectonics unraveled for last deglaciation turbidite records of the Arabian Sea. *Geology*, 28: 375-378

- Qian YY, Ye QC, Zhou WH (1993) Variation of water discharge and evolution of river bed of the main channel of the Huanghe (in Chinese). Publishing House of China Construction Material Industry, Beijing, 230pp
- Qin YS, Xu SM, Li F, Zhao SJ (1983) Study on geotechnical properties of sediment cores in Western Bohai Sea (in Chinese with English abstract). *Oceanologia et Limnologia Sinica* 14: 305-324
- Qin YS, Li F (1986) Study of the influence of sediment loads discharged from Huanghe River on sedimentation in the Bohai and Yellow Seas (in Chinese with English abstract). *Oceanologia et Limnologia Sinica* 27: 125-135
- Qin YS, Zhao YY, Chen LR, Zhao SL (1989) *Geology of the Yellow Sea* (in Chinese). China Ocean Press, Beijing, 289 pp
- Saito Y, Yang ZS (1994) The Huanghe River: its water discharge, sediment discharge, and sediment budget. *J. Sed. Soc. Japan* 40: 7-17
- Saito Y, Wei H, Zhou Y, Nishimura A, Sato Y, Yokota S (2000) Delta progradation and chenier formation in the Huanghe (Yellow River), delta China. *Journal of Asian Earth Sciences* 18: 489-497
- Shi WB, Li DP, Wang XC, Zhang ZX (1986) Shallow seismic surveying in south Huanghai Sea and its geological significance (in Chinese with English abstract). *Marine Geology & Quaternary Geology*, 6: 87-104
- Stanley DJ, Warne AG (1994) Worldwide initiation of Holocene marine deltas by deceleration of sea-level rise. *Science* 265: 228-231



- Stuiver M, Reimer PJ, Bard E, Beck JW, Burr GS, Hughen KA, Kromer B, McCormac FG, v. d. Plicht J, Spurk M (1998) INTCAL98 Radiocarbon age calibration 24,000 - 0 cal BP. *Radiocarbon* 40:1041-1083
- Wang L, Sarnthein M, Erlenkeuser H, Grimalt J, Grootes P, Heilig S, Ivanova E, Kienast M, Pelejero C, Pflaumann U (1999) East Asian monsoon climate during the Late Pleistocene : high-resolution sediment records from the South China Sea. *Marine Geology*. 156, 245-248
- Wright LD, Wiseman WJ, Bornhold BD, Prior DB, Suhayda JN, Keller GH, Yang ZS, Fan YB (1988) Marine dispersal and deposition of Yellow River silts by gravity-driven underflows. *Nature* 332(14): 629-632
- Xia DX, Wang WH, Wu GQ, Cui JR, Li FL (1993) Coastal Erosion in China (in Chinese with English abstract). *Acta Geographica Sinica* 48: 468-476
- Xue CT (1993) Historical changes in the Yellow River delta, China. *Marine Geology* 113, 321-329
- Yang DY, Yu G, Xie YB, Zhan DJ, Li ZJ (2000) Sedimentary records of large Holocene floods from the middle reaches of the Yellow River, China. *Geomorphology* 33: 73-88
- Yang ZG (1985) Sedimentary and environment in south Huanghai Sea since late Pleistocene (in Chinese with English abstract). *Marine Geology & Quaternary Geology* 5: 1-19
- Yang ZS, Milliman JD, Galler J, Liu JP, Sun XG (1998a) Yellow River's Water and Sediment Discharge Decreasing Steadily. *EOS* 79(48): 589-592

**Table 1. Holocene sediment and accumulation in the western Bohai and Yellow seas (see Fig. 2 for locations)**

	11 - 4 k cal yr B.P.	9 - 7.5 k cal yr B.P.	7 - 1 k cal yr B.P.	1128 -1855 A.D.	1855 A.D. - Present
	N. & S. Yellow seas (Shandong Mud Wedge)	South Yellow Sea (Lobe 1)	Bohai Sea (Lobe 2-9)	South Yellow Sea (Lobe 10)	Bohai Sea (Lobe 11)
<b>Volume (km<sup>3</sup>)</b>	300	200	500	250	108
<b>Mass (t)</b>	360×10 <sup>9</sup>	240×10 <sup>9</sup>	600×10 <sup>9</sup>	300×10 <sup>9</sup>	130×10 <sup>9</sup>
<b>Accumulation rate: (t/year)</b>	0.05×10 <sup>9</sup>	0.16×10 <sup>9</sup>	0.1×10 <sup>9</sup>	0.43×10 <sup>9</sup>	0.9×10 <sup>9</sup>

**Table 2.** Radiocarbon ages of sedimentary fossils from the North and South Yellow seas (locations in Fig. 2c)

Cores	Water and (Sampling) Depth (m)	Materials (facies)	<sup>14</sup> C Age ± error (yr)	δ <sup>13</sup> C (‰)	Conventional <sup>14</sup> C Age (yr)	Cal. Age (yr) #	Ref.
NYS-3	-50.0 (-0.7)	Peat (fresh water)	10700 ± 55	-25	10700 ± 55	12839	this study
NYS-5	-57.3 (-1.6)	Peat (fresh water)	10200 ± 60	-25	10200 ± 55	11804	this study
H80-23	-55.0 (-1.7)	<i>Peat</i> (fresh water)	11690 ± 300	-25	11690 ± 300	13680	Liu et al., 1987
H80-18	-72.0 (0)	<i>Ostrea gigas</i> (brackish)	10390 ± 100	-1	10790 ± 100	12105	Liu et al., 1987
CC02	-77.5 (-0.2)	Foraminifera (open marine)			2200 ± 100	1806	Kim et al., 1999
CC02	-77.5 (-0.95)	Foraminifera (open marine)			5370 ± 60	5722	Kim et al., 1999
CC02	-77.5 (-1.8)	Foraminifera (shallow maine)			9840 ± 200	10599	Kim et al., 1999
CC02	-77.5 (-2.75)	Foraminifera (coastal marine)			11340 ± 80	12903	Kim et al., 1999
YK07	-30 ? (-2.5)	Organic carbon (marine)	6448* ± 147	-1	6848 ± 147	7370	Alexander et al., 1991
PK48	-70 ? (-2.0)	Organic carbon (marine)	9047* ± 144	-1	9447 ± 144	10261	Alexander et al., 1991

# Calibration have been made using the latest program of CALIB4.3 ( Stuiver et al. 1998)

\* The 5730 half life <sup>14</sup>C age have been corrected by multiplying 1.029 (=5730/5568).

? Water depth are obtained from the bathymetric map.

**Figure 1:** Location map of the Yellow Sea and Bohai Sea, showing seismic lines and cores used to calculate Holocene sediment thickness. Highlighted seismic lines are shown in Figs. 2C and 3. Water depths in meters.

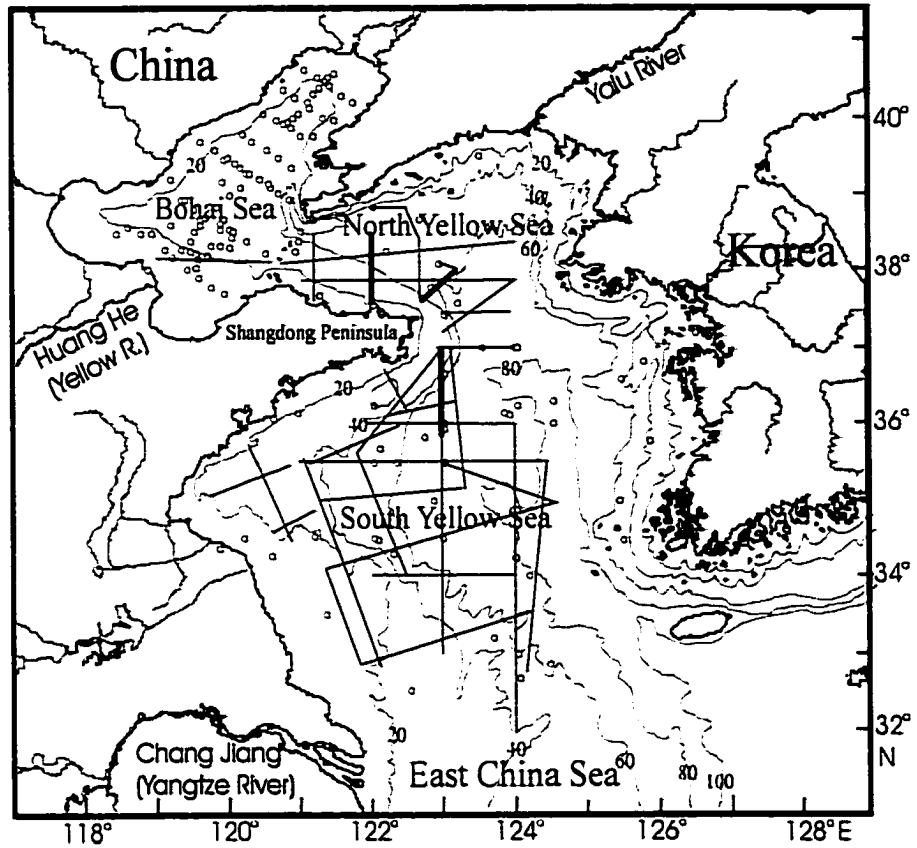


Figure 1.

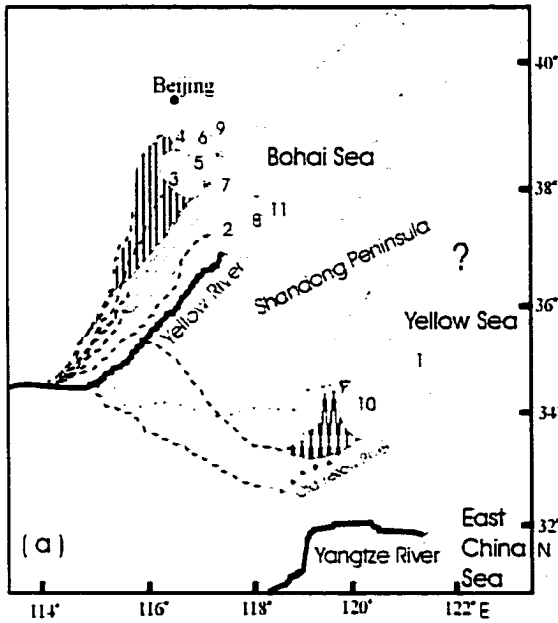
**Figure 2: Main depocenters in the western Yellow Sea.**

(a). Historic N-S shifts of the Yellow River's course, and corresponding ages of superlobes/deltas (after Milliman et al. 1987, 1989; Xie 1993). Question mark (?) represents the Shandong mud wedge.

(b). Holocene sediment thickness (m) in the western Yellow Sea (modified from Milliman et al. (1989), together with data shown in Fig. 2c.

(c). Shandong Peninsula clinoform mud wedge, and location of the seismic profiles shown in Fig. 3. Black line represents the paleo-coastline of -40 m at around 11-10 ka. Black points show locations of cores listed in Table 2.

(d). Post-glacial sea-level curve of the Yellow and East China seas (after Liu and Milliman 2001).



- Superlobe age:
- (1) 9.0 - 7.5 ka B.P.
  - (2) 7.0 - 5.0 ka B.P.
  - (3) 5.0 - 4.5 ka B.P.
  - (4) 4.5 - 3.4 ka B.P.
  - (5) 3.4 - 3.0 ka B.P.
  - (6) 3.0 - 2.5 ka B.P.
  - (7) 602 B.C. - 11 A.D.
  - (8) 11 A.D. - 1048 A.D.
  - (9) 1048 A.D. - 1128 A.D.
  - (10) 1128 A.D. - 1855 A.D.
  - (11) 1855 A.D. - Present

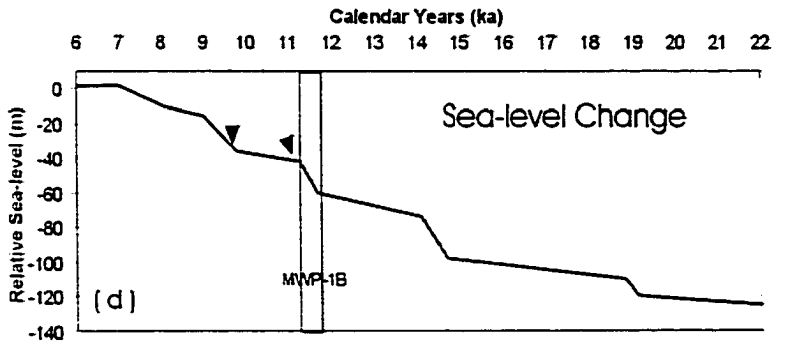
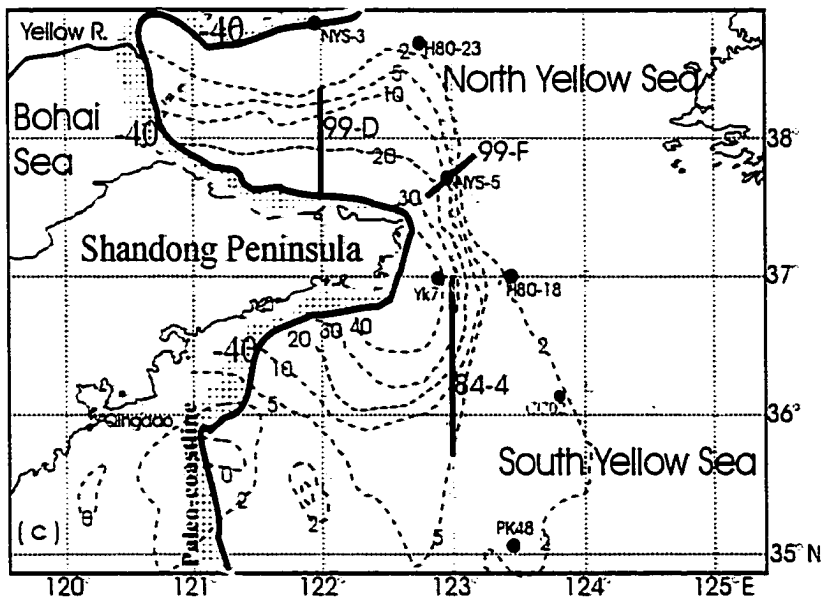
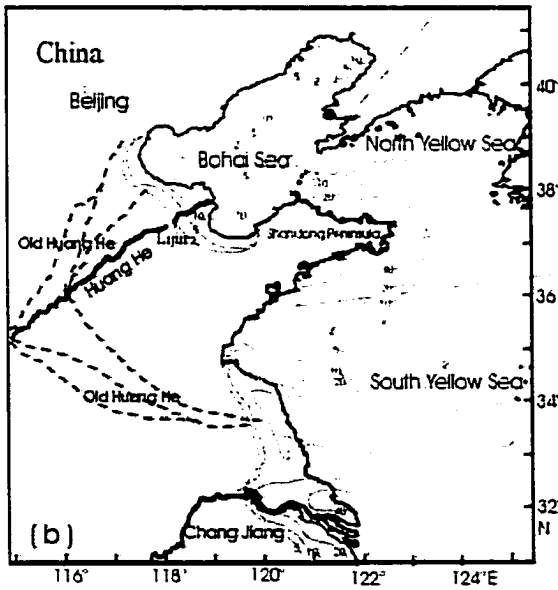


Figure 2.

**Figure 3:** Selected high-resolution seismic profiles from the North and South Yellow seas showing the clinoform morphology of the Shandong mud wedge, which overlies a well developed reflector. Biogenic gas obscures the internal reflector in the thicker portion of the mud wedge (see locations in Fig. 2c). Vertical scale: 10 ms two-way travel time = 8.0 m). Core NYS-5 at the toe of the bottomset strata in profile 99-F shows mud overlying a peat layer whose age is 11.8 ka (Table 2).



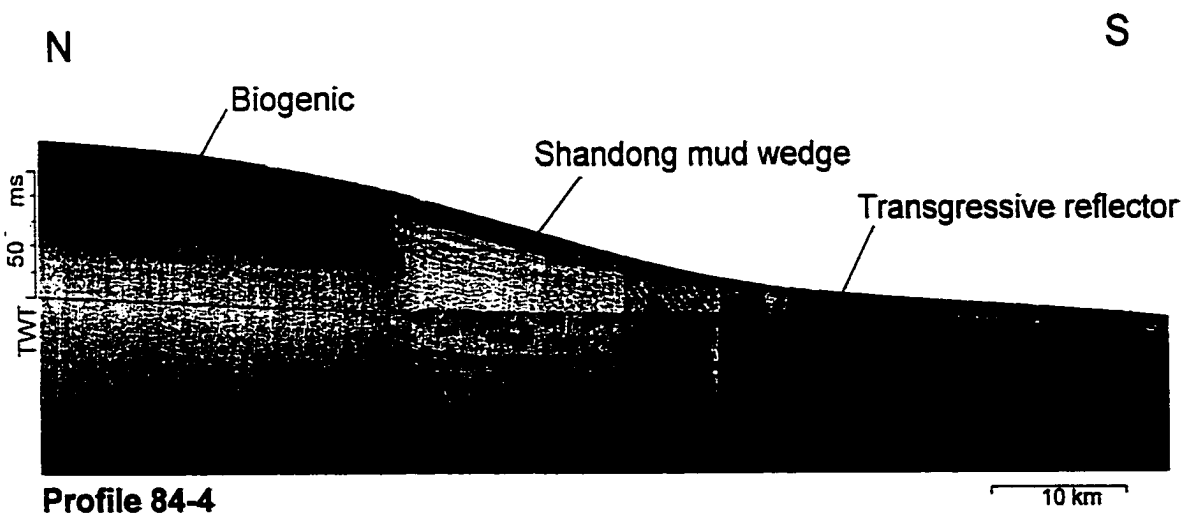
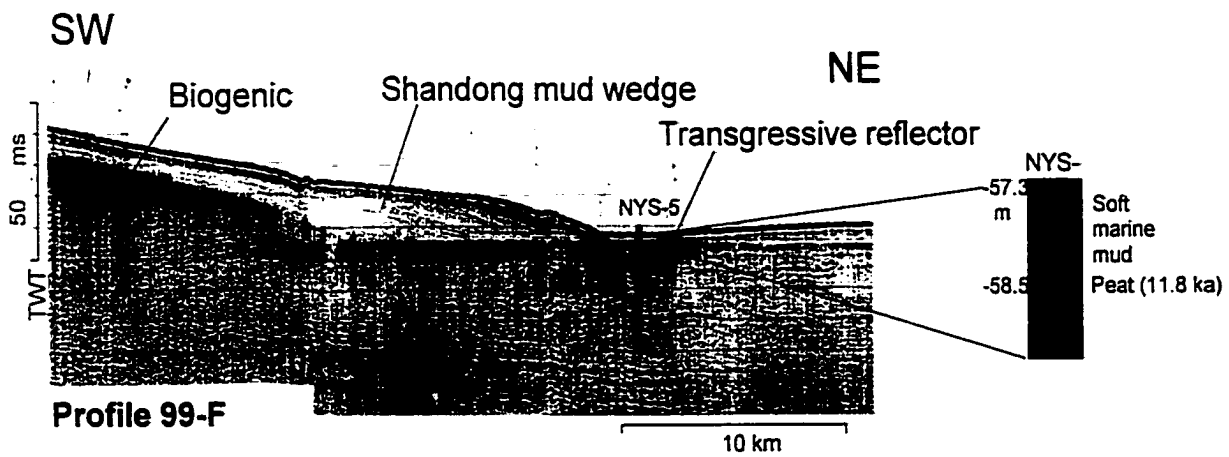
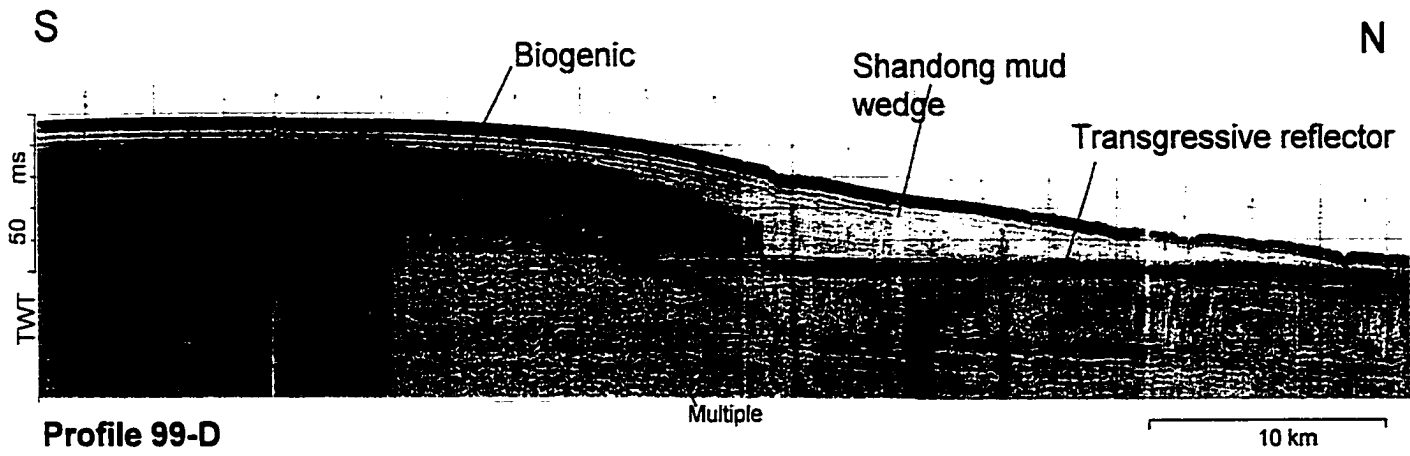


Figure 3.

## **Chapter Three**

### **Post-Glacial Sea-Level Transgression in the East China and Yellow Seas: Significance of Periodic Rapid Flooding Events\***

Paul J. Liu and John D. Milliman

School of Marine Science, College of William & Mary, Gloucester Point, VA, 23062, USA.

#### **Abstract**

Coral reefs generally cannot accrete vertically faster than 10-15 mm/yr, thereby causing reef-based sea-level curves to under-estimate rapid flooding events and over-estimate intervening slow rates of transgression. Integrating coral-reef dates with other published dates, primarily from the East China and Yellow seas, shows a step-like post-glacial transgression of sea level marked by 5 short periods of rapid rise (11-45 mm/yr), at least some of which correspond with periods of rapid climatic change.

---

\*Submitted to **Science REPORT**

## Sea Level History Derived from Coral Reefs

Delineating global sea-level rise since the Last Glacial Maximum (LGM) has proved a difficult task [Pirazzoli, 1991] <sup>(1)</sup> because of the dearth of reliable sea-level indicators [van de Plasche, 1986] <sup>(2)</sup>, possible post-mortem transport of indicators via currents or down-slope movement [Macintyre et al., 1978] <sup>(3)</sup>, local and regional tectonic movement [Lambeck and Chappel, 2001] <sup>(4)</sup>, and the large sample size needed for <sup>14</sup>C dating. The latter problem was solved by the increased use of Accelerator Mass Spectrometry (AMS), which requires three orders of magnitude less sample for <sup>14</sup>C analysis. The first two problems were mitigated by dating coral-reef material obtained from a series of borings in drowned coral reefs off Barbados, which resulted in a 22,000-yr record sea-level record [Fairbanks, 1989; Bard et al., 1990] <sup>(5, 6)</sup>. An additional advantage of reef corals is that U/Th dating of their aragonitic skeletons yields absolute ages, commonly termed calendar years [Bard et al., 1990; Stuvier et al. 1998] <sup>(6, 7)</sup>. In this paper we report dates in calendar years.

The Barbados sea-level curve showed that the post-LGM sea level rose approximately 100 m between 22 and 8.5 ka (an average rise of 7.4 mm/yr), punctuated by two intervals of rapid rise, 14.2-13.8 and 11.5-11.1 ka [Bard et al., 1990] <sup>(6)</sup>, which Fairbanks termed melt water pulses (MWP) 1A and 1B [Fairbanks, 1989] <sup>(5)</sup>(Fig. 1A). The Barbados curve was supported by subsequent borings on an elevated reef on the Huon Peninsula, Papua New Guinea [Chappell and Polach, 1991; Edwards et al., 1993] <sup>(8, 9)</sup> and on a barrier reef off Tahiti [Bard et al., 1996] <sup>(10)</sup>. Neither drilling penetrated material older than 13.8 ka, thus missing the MWP-1A event, and neither registered as abrupt an MWP-1B flooding event noted at Barbados (Fig. 1A). Another rapid-rise event was noted at 7.6-7 ka in

Caribbean coral reefs [Blanchon and Shaw, 1995] <sup>(11)</sup>, and recent dating of mangrove peat and other sea-level indicators from the Sunda Shelf [Hanebuth et al., 2000] <sup>(12)</sup> and the Bonaparte Gulf north of Australia [Yokoyama et al., 2000] <sup>(13)</sup> identified a possible early flooding event at 19 ka [see reference note (14)] <sup>(14)</sup>, which, in keeping with Fairbanks's original terms, we call MWP-1.

This is not to say that coral reef-derived sea-level curves are not without problems. First, framework-building corals may not be uniformly accurate sea-level indicators: in clear waters, for instance, they can grow at depths as great as 5-10 m and occasionally deeper [Goreau and Wells, 1967; Lighty et al, 1982] <sup>(15, 16)</sup>. Second, all three sites display long-term vertical uplift (Barbados and Huon) or subsidence (Tahiti), which were corrected by calculating short-term movement from long-term rates. A non-constant rate of tectonic movement, however, could lead to some error, particularly at Huon, where mean annual uplift rate is 1.9 mm [Chappell and Polach, 1991] <sup>(8)</sup>. The most critical problem in using coral-reef data, however, is that reef corals generally can accrete vertically no faster than 10-15 mm/yr [Buddemeier and Smith, 1988; Chappell and Polach, 1991; Collins et al., 1993] <sup>(8, 17, 18)</sup>, which means, to use the words of Neumann and Macintyre (1985) <sup>(19)</sup>, that a reef can *keep-up* only with relatively slow rates of sea-level rise. If the rate of transgression exceeds 15-20 mm/yr, corals cannot keep pace; they either must try to *catch-up* with higher sea level or, if the rise is too fast or for too long, *give-up* once water depths exceed 10-20 m. The end result of giving up is a drowned reef, of which there are many examples throughout the Caribbean [Macintyre, 1972] <sup>(20)</sup>. It was on such give-up reefs, in fact, that the Barbados drillings were made.

These problems become more obvious when one looks carefully at the apparently close fit between the Barbados, Huon and Tahiti (B-H-T) curves (Fig. 1B). Between 18.9 and 14.6 ka, core RGF-9 from Barbados defined a flooding event at 19 ka, which was short-lived and resulted in a fairly small rise in sea level; the presence of “sand or gravel” at about 18.95 ka (Fig. 1B), however, suggests a possible temporary reef die-off of the Barbados reef. Between 18.9 and 14.6 ka, sea level rose slowly and the Barbados reef corals accreted vertically an average of 3.5 mm/yr. The subsequent rapid transgression during MWP-1A, however, was sufficiently fast and long to drown RGF-9. After MWP-1A, when the rate of sea-level rise had slackened, a new reef (RGF-12) was established at a shallower site 13.8 ka (Fig. 1B). RGF-12, in turn, gave up during MWP-1B, after which reefs at site RGF-7 accreted an average of 8.8 mm/yr until 11.1 ka. At Tahiti (site P7) a *Porites*-dominated framework grew at an average rate of 13.8 mm/yr between 13.5 and 12.0 ka, which was sufficient for it to catch-up to sea-level; it was replaced at 12.0 ka BP by a reef-edge *Acropora-Hydrolithon* assemblage in a keep-up growth mode [Montaggioni et al. 1997]<sup>(21)</sup>. The rapid flooding of MWP-1B again put the Huon and Tahiti reefs into catch-up mode: at 11 ka they may have been as much as 10 m deeper than the newly established corals at Barbados, but by 8.5 ka BP they had effectively caught up with RGF-7 (Fig.1B). The Huon reefs may have survived MWP-1B because the reef facies changed to a deeper water *Porites* assemblage, but the effect of sea-level flooding also may have been offset partly by tectonic uplift [Chappell and Polach, 1991]<sup>(8)</sup>.

While the drilling and dating of corals reefs have contributed greatly to our understanding of post-LGM sea-level rise, particularly in identifying periods of rapid transgression, the keep-up, catch-up, give-up problem may prevent us from delineating

post-LGM sea-level history more accurately. Using reef corals to chart sea-level rise tends to minimize the timing and rate of rapid flooding events (as the reefs fall behind sea-level rise) and over-estimate the slower transgressions (as the reefs struggle to catch-up). The Tahiti corals, for example, seemed to grow more or less uniformly from 13.8 to 8.5 ka, generally between 10 and 13 mm/yr (Table 1).

### **East China and Yellow Seas**

To help solve the coral-reef conundrum, we have utilized dates of marine and terrestrial indicators to "fine-tune" the B-H-T sea-level curve. We chose the East China Sea (ECS) and Yellow Sea (YS) for several reasons: 1) its depth range (0-130 m) matches closely the depth range of the post-LGM transgression; 2) it is tectonically stable [Emery and Aubrey, 1991] <sup>(22)</sup> and lies far from the North American-European glacial epicenter [Lambeck and Chappel, 2001] <sup>(4)</sup>; 3) because of its low morphologic gradient, locally less than 1m/km, and because nearly all samples came from sediment cores, the possibility of post-mortem transport seems minimal; 4) Shallow gradients plus large sediment inputs from the Yangtze and Yellow rivers resulted in extensive shoreline transgression and sediment accumulation, thus improving the likelihood of preserving small-scale changes in sea level; 5) there are more than 250 published dates of samples taken from cores around ECS and YS, of which we have used 169 [see web map/table] <sup>(23)</sup>. Many of the dates come from a number of facies (e.g., terrestrial, intertidal, and marine) within a single core, thereby allowing us to define local timing of post-LGM sea-level change (Fig. 2C).

Dated materials include shells of ostracods, mollusks, and foraminifera, peat, and wood. All radiocarbon dates used in this paper have been calibrated to calendar ages using the

newly updated program of CALIB4.3 by correcting for  $\delta^{13}\text{C}$  fractionation and reservoir effects<sup>(24)</sup>. To define the land-ocean interface, we classified the samples as marine (formed at or beneath sea level), intertidal-brackish (formed at or near sea level), terrestrial (formed subaerially), and peat<sup>(25)</sup> (which may have formed in salt- or fresh-water). Sea level should fall above the dates and depths of the marine samples, close to or just above the intertidal-brackish samples, and below terrestrial dates. Most of the peat samples, in fact, appear to have been deposited in fresh-water conditions (Fig. 2A).

Combining ECS/YS data with those from the Sunda Shelf and Bonaparte Gulf results in a sea-level curve that at first glance falls close to the B-H-T curve (Fig. 2A): relative sea level was 125 m lower than present 22 ka and rising to about +4 m 6.7 ka, in accordance with a high-stand seen at other Australasian margins [Pirazzoli, 1991; Lambeck and Chappel, 2001]<sup>(1,4)</sup>. Closer inspection of Fig. 2A, however, shows significant differences between the ECS/YS data and the coral-reef-driven curve. ECS/YS data, combined with Sunda Shelf data, for instance, indicate that MWP-1A was somewhat earlier (14.7-14.1 ka) and greater (24 m) than defined by the Barbados curve (14.3-13.8 ka; 20 m). For the 1 ky after MWP-1A (just before the Younger Dryas), our data suggest that sea level rose slightly, if at all; the possibility of a slight regression also could be inferred from presence of sand and gravel at 12.89 ka in the Barbados curve (Fig. 1B). After about 12.3 ka, the rate of transgression increased until MWP-1B, which a cluster of five intertidal dates suggest occurred at 11.7-11.3 ka (in contrast to 11.5-11.0 ka driven the Barbados curve (Fig. 2B); the mean annual rate of sea-level rise during MWP-B was 45 mm/yr. After 11.3 ka, sea level again rose gradually to about 10 ka, during which the B-H-T reefs were

apparently in a catch-up phase, giving a more rapid apparent “sea-level rise” (9-13 mm/yr) than the 4 mm/yr derived from our data.

Six tightly clustered intertidal and peat dates define a flooding event at 9.8-9.0 ka, previously identified on the Great Barrier Reef [Larcombe and Carter, 1998; Harris, 1999] <sup>(26, 27)</sup>, which we term MWP-1C. After this event sea-level rise again slackened for about 1 ky before again accelerating. Several intertidal and terrestrial dates between 8.1 and 7 ka suggest the flooding event noted by Blanchon and Shaw <sup>(11)</sup>, which we term MWP-1D (Table-1); the rate of transgression (11 mm/yr), however, was considerably more gradual than noted for the other four melt-water events (Table 1).

## Discussion

Integrating ECS/YS data with coral reef and other published dates shows a step-like post-LGM sea-level rise, reaching a +4 m about 6.5 ka, in accordance with other Australasian sites. The five flooding events noted in our curve required only 3-ky to account for a cumulative 86 m vertical rise, the three main events (MWP-1A, 1B and 1C) averaging more than 35 mm/yr (Table 1, Fig. 3). In contrast, sea-level rise during the remaining time span between 22 and 6.5 ka was about 41 m, a mean annual rise of 3.3 mm/yr

Paleoenvironmental indicators provide added evidence for the timing and cause of at least some of these events. The new dates for MWP-1A and 1B, for instance, correspond well to the sharp increases in atmospheric temperature and methane at 14.7 and 11.6 ka BP in ice cores GRIP and GISP-2 [Johnsen et al. 1992, Grootes et al, 1993] <sup>(28, 29)</sup>. MWP-1A, in fact, coincides exactly with the Bølling-Allerød event as well as with rising sea-surface



temperatures recorded by planktonic foraminifera in the North Atlantic Ocean [Bard et al., 1987; Waelbroeck et al., 2001] <sup>(30, 31)</sup> and South China Sea [Kienast et al., 2001] <sup>(32)</sup> (Fig. 3). The slow transgression following MWP-1A (or perhaps, even a slight drop in sea level between 13 and 12 ka) corresponds to the first cold reversal of the Bølling-Allerød (14.1-13.8 ka BP) and the subsequent Younger Dryas (12.6-11.9 ka).

The high rates of meltwater discharge to the oceans during MWP-1A and 1B,  $14.5$  and  $16 \times 10^3$  km<sup>3</sup>/yr, respectively, are equivalent to about 30-40% of the present-day freshwater runoff to the global ocean [Korzoun et al., 1977] <sup>(33)</sup>. Presumably much of this runoff came from North American and European glaciers draining into the North Atlantic. Fluvial discharge into the North Atlantic presently is less than  $4 \times 10^3$  km<sup>3</sup>/yr [Milliman and Farnsworth, in press] <sup>(34)</sup>, which means that during MWP 1A and 1B average freshwater discharge into the North Atlantic periodically must have increased many-fold. Recent post-LGM runoff models [Marshall and Clarke, 1999; Clark et al., 2001] <sup>(35, 36)</sup> show that discharge from both the Mississippi and St. Lawrence may have reached  $12 \times 10^3$  km<sup>3</sup>/yr during MWP-1A. Such large freshwater fluxes to the North Atlantic could have provided the mechanism for the cooling responsible for the reduced sea-level rise [Broecker et al. 1989; Clark et al., 2001] <sup>(36, 37)</sup>. Runoff models, however, do not show a major meltwater discharge during MWP-1B, but rather large St. Lawrence runoff during the pre-Boreal interval (coincident with SST increases in the South China Sea and North Atlantic). Arctic meltwater discharge may account for part of the sea-level rise noted in MWP-1C, and Hudson Strait discharge coincides with MWP-1D (Fig. 3 D). The small and short 8.2 ka cold event [Alley et al, 1997, Barber et al., 1999] <sup>(38, 39)</sup> appears to have occurred just before MWP-1D, analogous to the Younger-Dryas cooling event prior to

MWP-1B (Fig 3B). While our sea-level curve seems to coincide with (and perhaps be defined by) environmental events, other connections (e.g., modeled flooding of the St. Lawrence River about 10 ka, when sea level was rising slowly) still need further clarification.

Recognizing a stepwise transgression in post-LGM sea level allows marine geologists an opportunity to view the deposition of shelf and inner shelf deposits in a new light. Rapid sea-level rise during melt-water pulses back-stepped the shoreline, thereby increasing the accommodation space to be filled during the subsequent slow transgression. Combined with climatic change (e.g., increased SW monsoon about 11 ka BP), post-LGM continental margin sedimentation history may have been more episodic than previously believed.

## References and Notes

1. P.A. Pirazzoli, *World Atlas of Holocene Sea-level Changes* (Elsevier Oceanography Series. 58. Amsterdam-London-New York-Tokyo, 1991), p.300.
2. Van de Plassche, *Sea-level Research*. (Geo Books Norwich, 1986), p.618.
3. I.G. Macintyre, O.H. Polkey, R. Stuckenrath. *Geol. Soc. Am. Bull.* **89**, 277 (1978).
4. K. Lambeck, J. Chappell. *Science* **292**, 679 (2001).
5. R.G. Fairbanks. *Nature* **342**. 637 (1989).
6. E. Bard, B. Hamelin, R.G. Fairbanks, A. Zindler, *Nature* **345**, 405 (1990a).
7. M. Stuiver et al., *Radiocarbon* **40**. 1041 (1998).
8. J. Chappell. H.A. Polach. *Nature* **349**, 147 (1991).
9. R. Edwards. et al., *Science* **260**, No.14: 962 (1993).
10. E. Bard et al., *Nature* **382**. 241 (1996).
11. P. Blanchon, J. Shaw, *Geology* **23**, No.1, 4 (1995).
12. T. Hanebuth, K. Stattegger, P.M. Grootes. *Science* **288**, 1033 (2000).
13. Y. Yokoyama, K. Lambeck, P. De Deckker, P. Hohnston, L. K. Fifield, *Nature* **406**, 713-716 (2000).
14. Sunda shelf data show that sea level rose slowly between 21.0 and 19.0 cal. ka BP at a rate of 0.14 m per 100 years. After the 19.0 cal ka BP flooding event, sea- level transgressed at a rate of 4.1 mm/yr until 14.6 ka BP (Hanebuth et al., 2000). Sea-level data from Bonaparte Gulf suggest a rapid decrease in ice volume by about 10% within a few hundred years terminated the LGM at  $19.0 \pm .25$  ka BP (Yokoyama et al., 2000).
15. T.F. Goreau, J.W. Wells. *Bulletin of Marine Science* **17** 442, (1967).

16. R.G. Lighty, I.G. Macintyre, Stuckenrath, *Coral Reefs* **1**, 125 (1982)
17. R.W. Buddemeier, S.V. Smith, *Coral Reefs* **7**, 51-56 (1988).
18. L.B. Collins et al., *Marine Geology* **115**, 29-46 (1993).
19. A.C. Neumann, I.G. Macintyre, in *Proc. 5<sup>th</sup> International Coral Reef Congress, Tahiti*, **3**, 105 (1985) Also See in detail from [www.nmnh.si.edu/paleo/macintyre/](http://www.nmnh.si.edu/paleo/macintyre/)
20. I.G. Macintyre, *Am. Ass. Petrol. Geol. Bull.* **56**, 720-738 (1972).
21. L.F. Montaggioni et al., *Geology* **25**, 6, 555-558 (1997).
22. K.O. Emery, D. G. Aubrey, Ed. *Sea levels, land levels, and tide gauges*, (New York: Springer-Verlag, 1991) p237.
23. Supplementary table and map are available in Appendices with the detailed information about cores and sea-level data from ECS and YS.
24. For most non-marine radiocarbon samples (terrestrial and peat), the 1998 International <sup>14</sup>C atmospheric decadal curve (Dataset A) was used. For marine samples such as shells, fossils, the 1998 International <sup>14</sup>C marine decadal dataset C (24,000 to 0 BP) was used. The marine calibration incorporates a time-dependent global ocean reservoir correction of about 400 years. Detailed info about the <sup>14</sup>C dates calibrating procedures is available at <http://www.calib.org/>
25. Based on the East China /Yellow Sea biosedimentological sequences, we determined the brackish-water or intertidal-flat indicators that could constrict sea-level position around  $\pm 3$  m. "Brackish-water" or "intertidal-flat facies" in ECS and YS was identified by the euryhaline foraminifers *Ammonia beccarii*, *Ammonia annectensi*, *Ammonia confertitesta*, *Elphidium incertum*, *Pseudonionlla varibilis*, etc; and accompanied by the salt- to fresh-water mollusks *Ostrea sp.*, *Ostrea gigas*.

*Ostrea rivularis*, *Corbicula fluminea*, *Corbicula japonica*, etc. "Margin marine facies" ( $\approx -5$  m) was identified by the benthic marine ostracods *Anadara subcrenata*, *Maetra chinensis*, *Mercenaria stimpsoni*, and benthic foraminifera *Ammonia confertitesta*, *Cribrononion subincertum*. "Shallow Marine facies" ( $\approx -10$  m) was distinguished by the well-preserved foraminifera *Ammonia tepida*, *Cribrononion incertum*, *Elphidium sp.*, *Elphidium asiaticum*, *Nonion sp.*, *Quinqueloculina sp.*, *Rosalina sp.*, *Schackoinella globosa*, *Spiroloculina laevigata.*, *Stomoloculina sp.*

26. P. Lecombe, R.M. Carter. *Sedimentary Geology*, **117**: 97 (1998).
27. P.T. Harris. *Sedimentary Geology*, **125**: 235 (1999).
28. S.J. Johnsen et al. *Nature* **359**, 311 (1992).
29. P.M. Grootes, M. Stuvier, J.W.C. White, S. Johnsen, J. Jouzel, *Nature* **366**, 552 (1993).
30. E. Bard et al., *Nature* **328**, 791(1987)
31. C. Waelbroeck et al., *Nature* **412**, 724 (2001).
32. M. Kienast, S. Steinke, K. Statterger, S.E. Calvert, *Science* **291**, 2132 (2001).
33. V.I. Korzoun et al, Atlas of World Water Balance. Gidrometeoizdat, Leningrad/The UNESCO Press, Paris. 35 p plus 65 maps (1977).
34. Milliman, J.D. and Farnsworth, K.L., River Runoff, Erosion and Delivery to the Coastal Ocean: A Global Analysis. Oxford University Press. In press.
35. S.J. Marshall, G.K.C. Clarke, *Quaternary Research* **52**, 300 (1999).
36. P.U. Clark et al., *Science* **293**, 283 (2001).
37. W.S. Broecker et al., *Nature* **341**, 318 (1989).

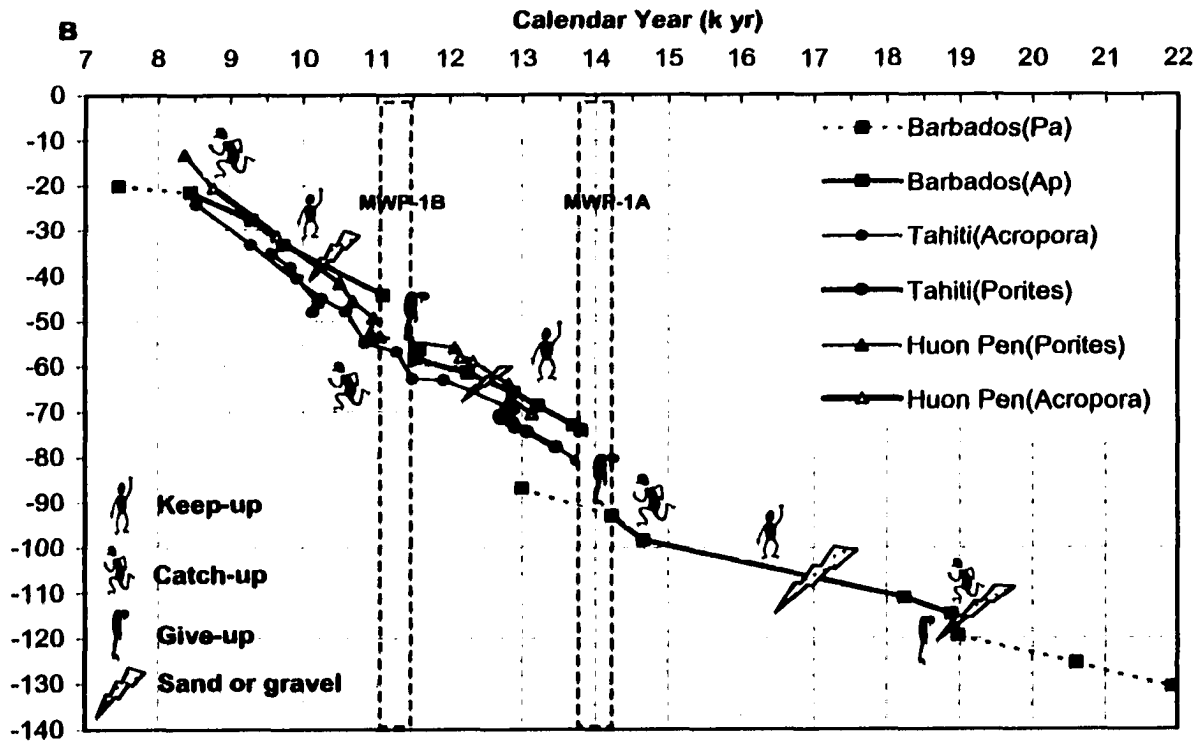
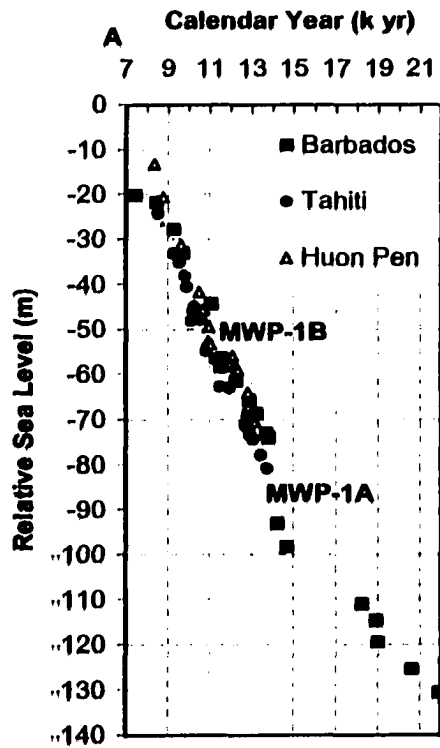
38. R.B. Alley et al. *Geology* 25, 483 (1997).
39. D.C. Barber et al. *Nature* 400, 344 (1999).
40. T. Blunier et al., *Nature* 394, 739 (1998).
41. We thank Edouard Bard, Yoshiki Saito, Lloyd Keigwin, and Neal Driscoll of their helpful comments on an earlier version of this paper. Peggy Schexnayder was particularly helpful during various phases of our ECS/YS research, for which we are most appreciative. This research was supported with funding from the Office of Naval Research and the National Science Foundation. This is Contribution XXXX from the Virginia Institute of Marine Science.

Table 1 Timing, rises and rates of various phases of post LGM sea-level compared with coral-reef derived rates.

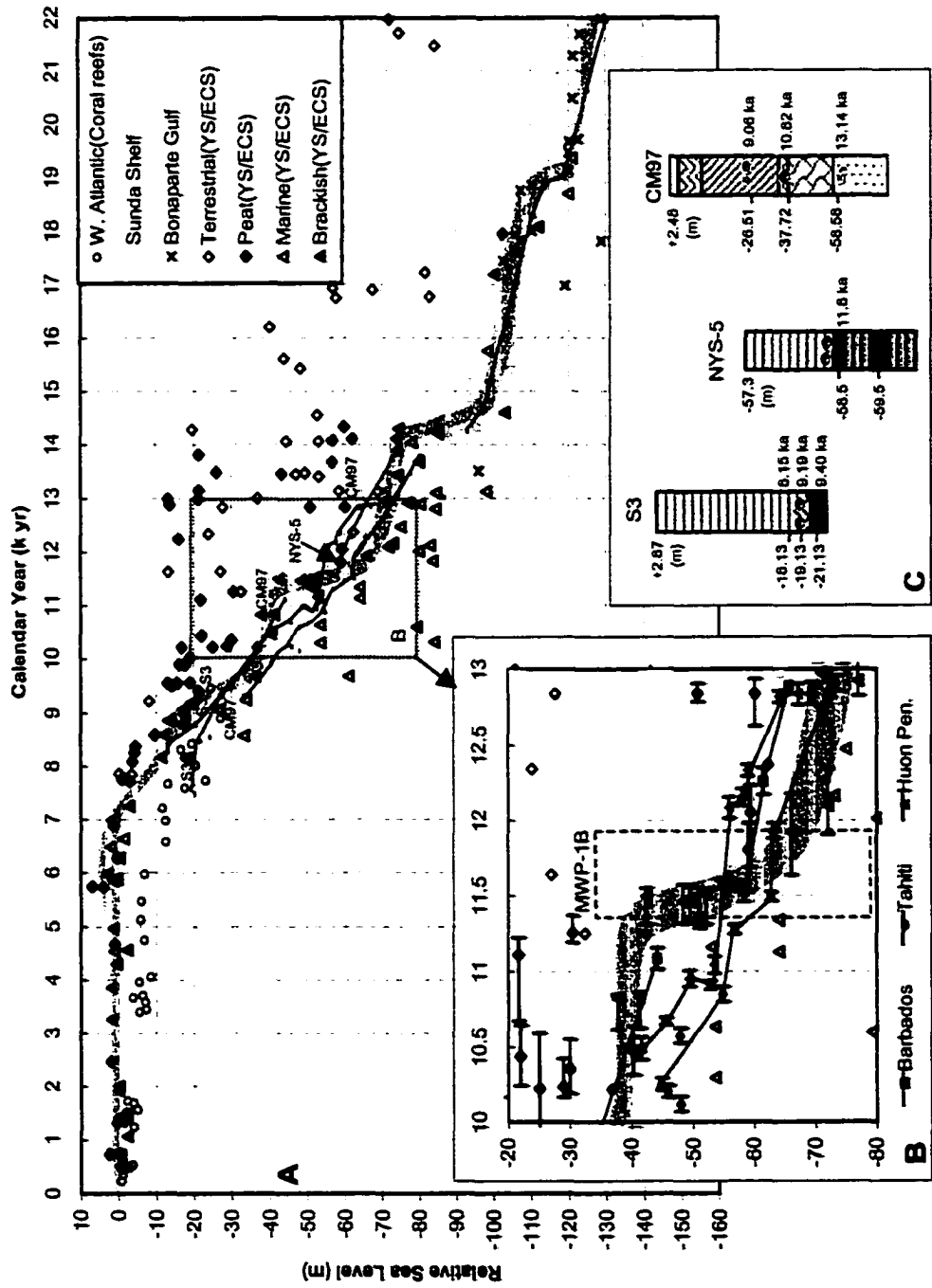
Flooding Event	Years ( $\pm$ ) (ka)	Sea-level Rises ( $\pm$ ) (m)	Rising Rate ( $\pm$ ) (mm/yr)	Coral-Reef Derived Rates (mm/yr)		
				Barbados	Huon	Tahiti
MWP-10	8.1 ( $\pm 0.1$ )	-10 ( $\pm 1$ )	11	X	X	X
	7.0 ( $\pm 0.1$ )	+2 ( $\pm 1$ )	( $\pm 1$ )			
	9.0 ( $\pm 0.1$ ) ~ 8.1 ( $\pm 0.1$ )	-16 ( $\pm 1$ ) ~ -10 ( $\pm 1$ )	6.4 ( $\pm 1$ )	X	X	X
MWP-9	11.3 ( $\pm 0.1$ )	-42 ( $\pm 2$ )	4	9	12	13
	~ 9.8 ( $\pm 0.1$ )	~ -36 ( $\pm 1$ )	( $\pm 1.5$ )			
MWP-10B	11.7 ( $\pm 0.1$ )	-60 ( $\pm 2$ )	4.5	35	22	18
	~ 11.3 ( $\pm 0.1$ )	~ -42 ( $\pm 2$ )	( $\pm 2$ )			
	14.1 ( $\pm 0.1$ ) ~ 11.7 ( $\pm 0.1$ )	-74 ( $\pm 2$ ) ~ -60 ( $\pm 2$ )	5.8 ( $\pm 0.1$ )	8	13	10
MWP-11	18.8 ( $\pm 0.2$ )	-110 ( $\pm 3$ )	3	3.5	X	X
	~ 14.7 ( $\pm 0.1$ )	~ -98 ( $\pm 2$ )	( $\pm 0.7$ )			
MWP-1	19.1 ( $\pm 0.2$ )	-120 ( $\pm 1$ )	3.3	X	X	X
	~ 18.8 ( $\pm 0.2$ )	~ -110 ( $\pm 3$ )	( $\pm 1.0$ )			
	22.0 ( $\pm 0.2$ ) ~ 19.1 ( $\pm 0.2$ )	-125 ( $\pm 3$ ) ~ -120 ( $\pm 1$ )	1.7 ( $\pm 1$ )	X	X	X

**Figure 1.** The Barbados, Huon Peninsula and Tahiti coral-reef-derived sea-level curves as commonly plotted (**A**) minimize their vertical and horizontal differences, which become obvious when the time axis is expanded (**B**). Based on their positions relative to one another as well as relative to our proposed curve (Fig. 2), we can assume that for much of their histories these reefs were in catch-up or give-up phases of growth. Lightning bolts represent breaks in the Barbados cores as indicated by sand or gravel deposits [Fairbanks, 1989]<sup>(5)</sup>. Vertical dashed blue lines represent the temporal limits of MWP 1A and 1B as defined by Barbados curve [Fairbanks, 1989; Bard et al, 1990]<sup>(5,6)</sup>. Sticklike *keep-up*, *catch-up*, and *give-up* figures are drawn in the spirit of Neumann and Macintyre<sup>19</sup>



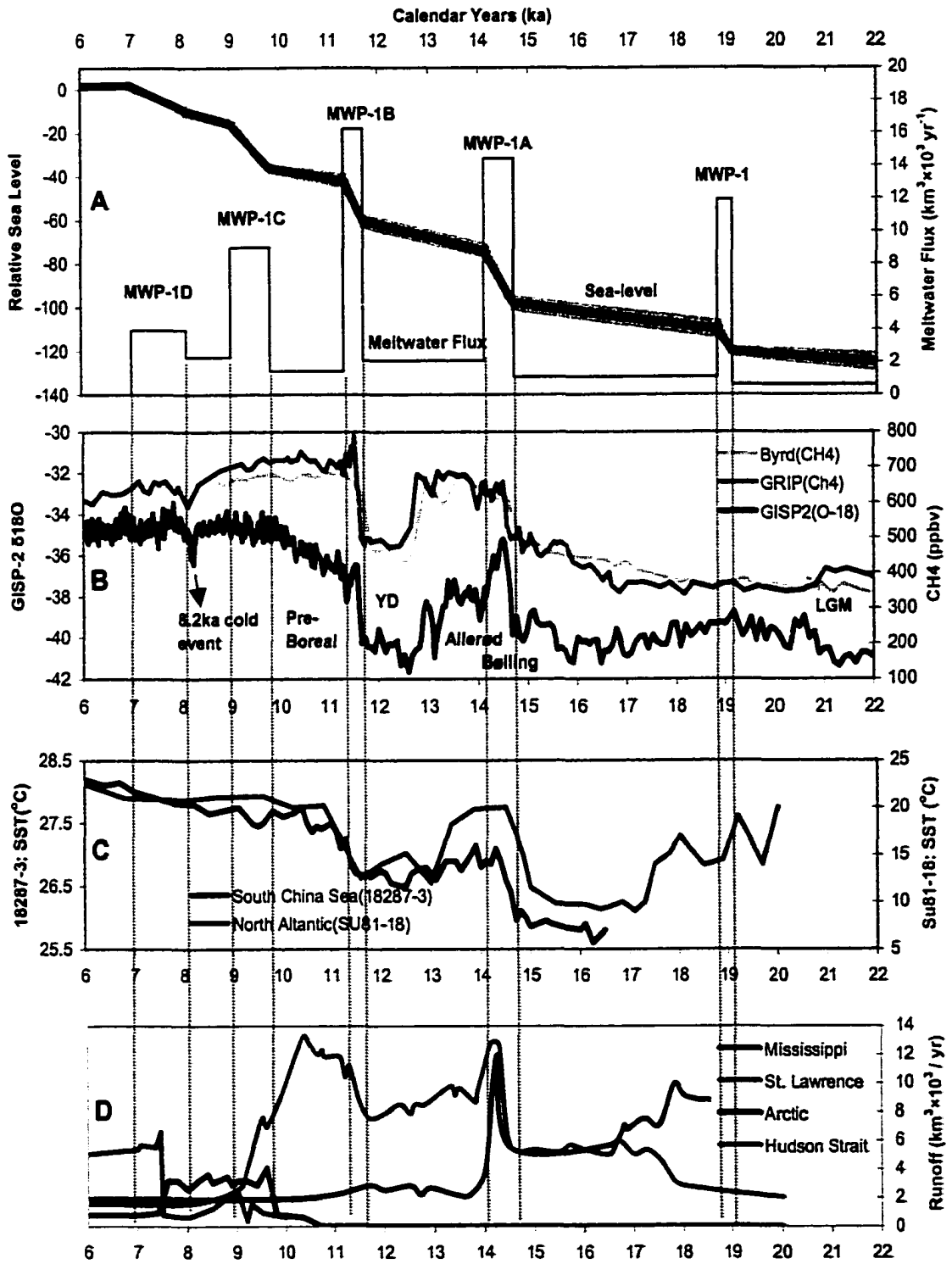


**Figure 2.** Proposed eustatic sea-level curve based on the East China Sea and Yellow Sea data together with data from the Sunda shelf [Hanebuth et al., 2000] <sup>(12)</sup>, and Bonaparte Gulf [Yokoyama et al., 2000] <sup>(13)</sup> as well as with the B-H-T coral reef data (thin lines) from Fig. 1B; dates from western Atlantic coral reefs [Lighty et al. 1982] <sup>(16)</sup> also are shown (A). We present our sea-level curve as a 2-3 m shading, reflecting uncertainties regarding both ages and water depths. An expanded 13-10 ka BP interval (B), including age ranges for intertidal-brackish, peat, and coral-reef data, shows in greater detail the difference between various data sets before, during and after MWP-1B. Core logs for sediment cores taken near Shanghai (CM97: 31°37'N, 121°23'E), in the North Yellow Sea (NYS-5: 37°47'N, 122°50'E), and on the Yellow River Delta (S3: 38°01'N, 118°51'E) (C) show dates of various depositional facies. Pale yellow – terrestrial; black/gray – peat; blue – marine (see detailed description in web table) <sup>(23)</sup>.



Reproduced with permission of the copyright owner. Further reproduction prohibited without permission.

**Figure 3.** The proposed sea-level curve and rapid melt-water events, with corresponding melt-water flux (A).  $\delta^{18}\text{O}$  from ice core of GISP2 in Greenland [Grootes et al, 1993] <sup>(29)</sup> and  $\text{CH}_4$  concentration from ice-cores Bryd in Antarctic and GRIP in Greenland [T. Blunier et al 1998] <sup>(40)</sup>. (B);  $U_{37}^k$  SST estimates of deep sea core of SU81-18 in North Atlantic [Bard et al., 1987; Waelbroeck et al., 2001] <sup>(30,31)</sup> and core 18287-3 from South China Sea [Kienast et al., 2001] <sup>(32)</sup> (C); The Model results of river basin runoff during LGM deglaciation (CCC/GRIP model) [Marshall and Clarke, 1999] <sup>(35)</sup> (D).



Reproduced with permission of the copyright owner. Further reproduction prohibited without permission.

## Chapter Four

### Sedimentary Processes of the Yellow River's subaqueous delta in the North Yellow Sea

J. Paul Liu, John D. Milliman, Shu Gao <sup>\*</sup>, Peng Cheng <sup>#</sup>

*School of Marine Science, College of William & Mary, VA, 23062, USA*

*<sup>\*</sup> Dept. of Geo-Ocean Science, Nanjing University, Nanjing, 210093, China*

*<sup>#</sup> Marine Sciences Research Center, Stony Brook University, NY 11794, USA*

#### Abstract

High-resolution seismic profiles from the North Yellow Sea reveal a 20-40 m-thick subaqueous clinoform delta that wraps around the eastern end of the Shandong Peninsula, extending into the South Yellow Sea. This complex sigmoidal-oblique clinoform, containing an estimated 300 km<sup>3</sup> of sediment, overlies prominent relict ravinement and transgressive surfaces. The nearshore topset of the clinoform, < 30 m water depth, has a << 1:1000 gradient; foreset beds (30 - 50 m) dip seaward at a steeper gradient (2:1000) and sedimentation rates (<sup>210</sup>Pb) ~ 3 mm/y; bottomset strata, in water depths > 50 m, contain less than 1 m of Holocene sediment. In contrast to other clinoforms, the Shandong clinoform appears to be a compound subaqueous deltaic system. The first (proximal) phase had been formed mostly by Yellow River sediment input between about 11 and 9.2 ka, in response to a temporary decrease in the rate of post-glacial sea-level rise and increased discharge from the Yellow River, due to intensification of the summer monsoon. Since 9.2 ka, the second (distal) phase has begun to form overlies the proximal phase, contributions from the Yellow River have been relatively small to the clinoform (because of shifting river path and sea-level rise), along with inputs from coastal erosion and small local

streams. Basin-wide circulation, along-shore transport, and upwelling rework the modern and relict sediment, and help maintain the morphology of the clinoform mud wedge. <sup>1</sup>

***Keywords:*** epicontinental sea; Yellow Sea; Yellow River; Subaqueous delta; seismic profiles; sea-level;

---

<sup>1</sup> Manuscript for Marine Geology

## 1. Introduction

Rivers and their deltas serve as the primary pathway for the transport of fresh water and terrigenous sediment to the coastal ocean (Milliman and Meade, 1983). The morphology of deltas, which constitute an important component within stratigraphic sequences in both modern and ancient continental margins (Morgan, 1970), is controlled largely by the fluvial, tidal, and wave regime (Wright and Coleman, 1973). Equally prominent off many large river mouths, however, are subaqueous delta clinoforms, meters in height and tens of kilometers in horizontal extent, characterized by relatively flat topset beds, steeper foresets, and gradual bottom sets. Modern examples include clinoforms off the Amazon (Nittrouer et al., 1986), the Huanghe (Alexander et al., 1991), the Ganges-Brahmaputra (G-B) (Kuehl et al., 1997), and the Yangtze (Chen et al., 2000) rivers.

As with other sedimentary features, clinoform development and resultant geometry are dictated by the complex interplay of sediment supply, depositional environment, and the extent and rate of the rise/fall of relative sea level. Kuehl et al. (1986) attributed the low accumulation rates ( $< 1$  mm/year) on the Amazon clinoform topset ( $< 20$  m water depth) to energetic physical conditions. Decreased wave and tidal energy on the thick foreset beds at 30-60 m water depth results in much higher rates of sediment accumulation, as much as 100 mm/year. Accumulation in bottom-set ( $> 70$  m water depth) strata decreases in response to reduced sediment supply. High-resolution seismic profiles on the Bengal shelf show the sediment accumulation rates also are highest ( $\geq 50$  mm/year) in the forest region of the G-B subaqueous delta (30-60 m water depth) and lower ( $< 3$  mm/year) in the bottomset (60-80 m water depth) (Kuehl et al., 1997). A similar stratigraphy also has been described for the Yangtze subaqueous delta (Chen et al., 2000).



Another common feature of subaqueous clinoforms is that they overlie a transgressive layer, often in water depths 60 to 70 m or greater. The seaward limit of the Yangtze subaqueous bottomset, for example, lies at 60 to 70 m, where sediments are composed of grayish yellow, well sorted fine to medium-fine sands containing shallow-water shells (Chen et al., 2000), representing transgressive and regressive relict sediments deposited during the last regression and low-stand of sea level (Saito et al., 1998). Thus, understanding of the geometry and formation of subaqueous clinoforms requires not only a knowledge of present-day environmental conditions, but also of sea-level change.

The modern Yellow River, which presently discharges into the west Bohai Sea, is widely recognized (along with the Amazon and Ganges-Brahmaputra) as having the highest sediment load on earth, about  $10^9$  t/y (Qian and Dai, 1980; Milliman and Syvitski, 1992). The highly turbid gravity flows transport some sediment off the modern delta (Wright et al., 1988, 1990), but most fluviially derived sediment (>90%) appears to remain trapped within the modern deltaic system (Bornhold et al., 1986, Martin et al., 1993, Wright et al., 2001). In the 1980s a prominent mud wedge was noted extending southward from the eastern tip of the Shandong Peninsula (Milliman et al., 1987). Named the Shandong Subaqueous Delta, Alexander et al. (1991) suggested that this extensive clinoform represented a direct escape route of Yellow River sediment into the South Yellow Sea. More recent work has shown that this clinoform also extends westward along the northern side of the Shandong Peninsula in the North Yellow Sea (Liu et al., 2002) (Fig. 1). In contrast to Alexander et al. (1991), however, Liu et al. (2002) suggested that this thick mud wedge is probably relict, having been formed during the early Holocene. In this paper we provide detailed interpretations of the high-resolution seismic structure and

sedimentary facies, and also discuss them relative to other sedimentological and oceanographic data that allow us to synthesize the history of this prominent clinoform.

## 2. Study Area

### 2.1 Bathymetry

The Yellow Sea is a shallow, relatively flat, semi-closed epicontinental sea bordered by China and the Korean peninsula. To the northwest is the very shallow Bohai Sea, with water depths generally less than 40 m; to the south is the East China Sea (Fig.1), which borders the Okinawa Trough to the south. A NW-SE trough, defined by the 80-m isobath (Fig. 1), transects the eastern part of the Yellow Sea; everywhere else water depths are shallower. The Shandong Peninsula separates the South from the North Yellow Sea. The latter, the subject of this paper, has an average water depth of 38 m; water depths exceed 60 m only in the southeast (Figs 1, 2).

The North Yellow Sea is defined largely by the 40- and 60-m isobaths. Most of the central portion of the basin is deeper than 50 m and characterized by a relatively flat bottom (Figs. 2, 3). East of about 123°30'E, however, large size, symmetrical bed forms occur north of about 38°N. The apparent symmetrical configuration of these mega-dunes suggests that they are heavily influenced by tidal oscillations within the NYS (Qin et al., 1989). Greatest depths in the NYS occur between the Shandong Peninsula and Korea, where depths locally exceed 70 m (Qin et al, 1989).

The 3-dimension bathymetric morphology (Fig. 3) shows a prominent terrace that wraps around the eastern Shandong Peninsula; it is this feature that we term the Shandong clinoform, the subject of this paper. Gradients in water depths shallower than about 20-25

m are  $\ll 1:1000$ , whereas on the clinoform's foresets gradients are somewhat steeper –  $2/1000$  m. There are, however, several subtle breaks in clinoform topography (Fig. 3). A 5-10 m linear depression is seen in water depths shallower than about 25-40 m (e.g. Profile 99-E in Fig. 12), landward of which the bottom shoals towards the peninsula. As will be discussed later, we suspect that this shallow trough may reflect erosion and eastward transport of clinoform sediment. The other morphologic break occurs at about 45 m in profiles 99-E and 99-F (Fig. 12) and represents what we term the toe of the clinoform (see below).

## 2.2 Regional Oceanography

The general circulation in the North Yellow Sea is characterized by a counterclockwise gyre, with northwestward inflow of Yellow Sea Warm Current (YSWC) in the winter along the eastern and northern sides of the basin and a cold, coastal current (known as the Yellow Sea Cold Coastal Current – YSCCC) flowing eastward from the Gulf of Bohai along the Shandong Peninsula into South Yellow Sea (Fig. 1). During the winter, strong northwesterly winds drive surface and nearshore transport southward, demanding a northward return flow at depth, the Yellow Sea Warm Current (YSWC) can reach its strongest, about 5 cm/s (Yuan and Su, 1984), and produces a warm tongue of water that follows a path along the deepest axis in the eastern SYS and northern NYS basins (Zheng and Klemas, 1982). The YSWC even penetrates into Bohai Sea and plays a very important role in forming the sand ridges in the east Bohai Sea and dispersing the fine sediments into the west side of the Gulf (Liu et al., 1998).

T-S profiles from published hydrographic data (Fig. 4) indicate that the whole NYS was well mixed under the strong northwesterly winds (Fig. 5a,b). A cold, fresh surface water

flows eastward out of the Bohai Sea into the NYS and SYS along the north coast of Shandong Peninsula, and a warmer, more saline subsurface counter-current flows westwards (Fig. 6)(Guan, 2000). Wintertime suspended sediment concentrations are highest in nearshore regions, with values exceeding 50 mg/l (Fig. 7a).

The summertime hydrography of the NYS is characterized by a pronounced cold-pool in the deeper basin overlain by ~25 m of highly stratified warmer water (Figs. 5c, 5d, 8a) (Martin et al., 1993); upwelling along the northern Shandong shelf (Fig.8b) (Zhao, 1996). However, the stratification breaks down on boundary areas of the NYS, together with the circular current flow westward in the northern side, and eastward in the southern side (Fig. 8c) (Zhao, 1996). A sustained cold surface water around eastern tip of the Shandong Peninsula suggesting possible upwelling induced by strong tidal current past a peninsula (Fig. 7e.f)(Xia and Guo, 1983). The more stratified summertime conditions and calmer weather result in the much lower suspended sediment in NYS coastal waters, generally 5-10 mg/l (Fig. 7b, c, d) (Li and Ding, 1996, Martin et al., 1993). Recent (1995-1997) NOAA-AVHRR satellite images show that large SPM in the coastal water of YS and ECS move offshore from November to March, whereas from May to September transport is to onshore (Sun et al., 2000). The 3-D sediment transport models of the Bohai Sea (Jiang et al., 2000) and Yellow Sea (Yanagi and Inoue, 1995), however, indicates that although there is some eastward and southward transport of sediment in the winter and early spring, most Yellow River-derived sediment remains in the Bohai Sea.

### **2.3 The Yellow River**

The most unique feature of the Yellow Sea is the presence of the Yellow River, which discharges into the Gulf of Bohai, but as recently as 1855 discharged south of the

Shandong Peninsula along the Jiangsu coast. Although the river drains the very arid northern China, its very large sediment load reflects the supply of easily erodable late Pleistocene loess along the middle reaches of the river, as well as impacts of historically poor farming techniques. Over the past 1500 years or so the river has discharged about  $10^9$  t/y of sediment, prior to which its load may have been an order of magnitude lower (Milliman et al., 1987; Saito and Yang, 1995, Saito et al., 2001); recently, however, the annual load has dropped considerably in response to improved land conservation, dam construction, and increased water withdrawal due to decreased precipitation (Yang et al., 1998; Galler, 1999).

Because of its historically large sediment load, the natural Yellow River probably meandered frequently, and as a result its course changed both regionally and locally. In the past 9000 years there have been eleven documented shifts in the Yellow River's path, at least twice when the river flowed south of the Shandong Peninsula (Saito et al., 2001). Although the first such episode is poorly documented, the river apparently shifted to the south in response to heavy floods about 9 ka (Yang et al., 2000), and continued discharging at Jiangsu for the next 2 ky (Liu et al., 2002). For nearly 6-ky beginning about 7 ka, the river discharged mostly or entirely into the Bohai Sea, before shifting southward again in 1128 AD. The river then again shifted to the north in 1855, where it has prograded the present Yellow River delta nearly 50 km (Saito et al., 2001).

Since sea level reached (or exceeded) present-day sea level, about 7.5 ka, sediment has accumulated in coastal areas along the Jiangsu coast and on present-day Yellow River delta in the western Bohai. Prior to that, during the post-LGM sea-level transgression (11-7.5 ka), it accumulated on the South and North Yellow shelves, in response to varying

rates of sea-level rise (Liu and Milliman, submitted) and re-initiation of the SW Monsoon, 11 ka. During this 3.5 ky period a prominent subaqueous delta formed off the Jiangsu coast in South Yellow Sea (SYS), presumably the result of the first south-shift of the Yellow River in the early Holocene (9.0-7.0 ka) (Liu et al., 2002). We submit – and attempt to prove in this paper – that the Shandong mud wedge, abutting the eastern and northern edges of the Shandong Peninsula, is also a relict feature, formed in response to increased sediment discharge (from a strengthened SW (summer) monsoon) and a relative still-stand during post-LGM sea-level transgression.

### **3. Methods**

Since the early 1980s, many oceanographic and geological/geophysical cruises have studied the oceanography, morphology, surface sediments, and shallow stratigraphy of the Yellow Sea. Seismic profiles obtained in 1983-1984 as part of a cooperative study between the Institute of Oceanology, Chinese Academy of Sciences (IOCAS), and the Woods Hole Oceanographic Institution (WHOI) helped define the configuration and boundaries of the Shandong clinoform in the South Yellow Sea (Fig. 2). The distribution and configuration of the clinoform in the Bohai and North Yellow seas were defined by geophysical and geological data obtained during two cruises in 1998 and 1999 aboard the RV Gold Star II of IOCAS. During these two cruises we collected approximately 1200 km of high-resolution seismic profiles, 10 gravity cores (four are used in this study), 70 surface sediment samples (Fig. 2), 5 box cores (Fig. 3). All seismic data were obtained with a 450-kJ ORE Geopulse boomer system fired at 0.5 sec intervals; records were filtered between 500 and 3000 Hz.

Well-documented peat deposits that underlie the mud wedge in the North Yellow Sea were sampled in the gravity cores (NYS-5) (Fig.12) and AMS-dated at WHOI's NOSAMS lab. Radiocarbon ages were calculated using 5568 years as the half-life of radiocarbon and are reported in calendar years using the newly updated CALIB4.3 (Stuvier et al. 1998). The marine sample calibration incorporates a time-dependent global ocean reservoir correction of 400 years;

Analysis for  $^{210}\text{Pb}$  activities were conducted on sediments sampled at 2-cm intervals from 5 box cores (Fig. 3) to determine short-term rates of sediment accumulation. Sediments were dried, ground, homogenized, and packed in 50-mm diameter petri dishes. After waiting at least 20 days for secular equilibrium of  $^{226}\text{Ra}$  daughter isotopes, the samples were counted for 1-3 days by gamma spectrometry, planar germanium detector coupled to a multichannel analyzer. Activities were corrected for shelf-absorption using a radioisotope source (Cutshall et al. 1983). Excess  $^{210}\text{Pb}$  activities were calculated by subtracting the supported levels obtained from parent  $^{226}\text{Ra}$  activities.

Grain size of the surface sediments were measured after first wet-sieving the samples through a 63- $\mu\text{m}$  sieve. Sand fractions retained on the sieve were dried and sieved. Mud fractions passing through the sieve were pretreated using the dispersing agent (sodium hexametaphosphate) to inhibit flocculation, and then dispersed and homogenized using ultrasound before passing through the Cilas Laser Particle Size Analyzer (model: 940L). Size parameters were calculated based on the methods of McManus (1988).

Oceanographic data (temperature, salinity, current, and total suspended particulate matter) are mainly from the historical observations conducted in the NYS between 1959

and 1993 (Xia and Guo, 1983; Milliman et al., 1986; Martin et al., 1993; Li and Ding, 1996; Zhao, 1996) (Fig. 4).

## **4. Results**

### **4.3 Shallow Structure**

GeoPulse profiles (Figs. 9-15) show a prominent clinoform, 15 to 40 m in thickness that thins offshore to thicknesses less than 1 m. It abuts the northern slope of the Shandong Peninsula, and wraps around the eastern end of the Peninsula, connecting with the Shandong subaqueous delta (Alexander et al., 1991) that extends into the South Yellow Sea. The clinoform is underlain by a highly reflective surface that locally is acoustically opaque (Figs 9, 11, 12, 13, 15) and that occurs at or near the seafloor in the central parts of the NYS. Core NYS-5 (Fig. 12) penetrated a dark peat at 120 cm, which AMS  $^{14}\text{C}$  dating (11.8 ky cal BP) indicates was deposited during the last sea-level rise. A compact yellow layer, which we interpret to be loess, was recovered at 230 cm in Core S45 (Fig. 14, 17). We assume that this loess is synchronous with loess exposed along the present-day northern coast of the Shandong Peninsula, and which was deposited during the intensified LGM winter monsoon during LGM (Liu and Zhao, 1995). Other cores penetrated stiff clay or silty-sand layers, which we assume were subaerial during or prior to the post-LGM transgression (Liu et al., 2002). Where modern muds have been winnowed by strong erosion (e.g., northern end of profile 99-C, near the deep channel in the Bohai Strait; Figs. 13, 14) these stiff clays are sufficiently near the seafloor to be sampled with a grab. We therefore conclude that this acoustically reflective surface represents a combination of low-stand stiff silts and clays, and post-LGM peats.



Locally, sub-parallel semi-transparent layers are seen to lie beneath the acoustic reflective surface (Figs. 10, 11, 12), truncated by a prominent ravinement surface (profile 99-B in Fig. 11). Some profiles show this ravinement to be filled with acoustically reflective strata, suggesting a low-stand system tract (Fig. 12), while to the east the ravinement surface appears to outcrop at the seafloor (Fig.9). Perhaps the best evidence of the nature and age of low-stand surface, however, is seen in Profile 99-C, where strong currents near the Bohai Strait have removed the acoustically opaque post-LGM reflector and exposed the morphologically uneven ravinement surface (Fig. 13, top). Close inspection of the seismic profiles (e.g., 99-E, Fig. 12; 83-a; Fig. 9) shows several deeper ravinement surfaces, that we assume represent former low stands of sea level.

In the NYS the clinoform is thickest in the east and thins to less than 15 m in the west (Profile 99-C; Fig. 13); it apparently is poorly defined or non-existent in the Bohai Sea (Fig. 14) (Liu et al., 2002). The shape of this clinoform in the west (such as 99-C) shows a typical sigmoidal structure, but most of others show oblique to complex sigmoidal-oblique clinoform. Topset gradients are much less than 1/1000, whereas foreset gradients are about 2/1000 m (Fig. 3). Sediment volume within the entire Shandong clinoform is estimated to be about 300 km<sup>3</sup>, of which about 200 km<sup>3</sup> are in the NYS.

Careful inspection of many of the clinoform profiles shows a rather complex inner structure, perhaps best seen in Profiles 99-A, B, and F (Figs.10, 11, 12). The lower part of the clinoform lying under the topset and foreset beds tends to be acoustically “turbid”, and in Profile 99-F this turbid layer confirms with a reflector that lies about 7-8 m beneath the upper part of the foreset and ~15 m beneath the lower foreset. Once identified, this turbid layer is seen on all other profiles except Profile 99-C, in the far west of the NYS. Judging

from other clinoforms suggests this turbid layer apparently indicates the presence of biogenic gas (Nittrouer et al., 1996; Diaz et al., 1996). Strata overlying the turbid layer, in contrast, are acoustically transparent, locally to the extent that bedding is difficult to delineate. A closer inspection of the profiles indicates that the "nose" described above consists of younger strata (Figs. 11, 12). The significance of this is seen in the ensuing discussion.

#### **4.2 Sediments and Recent Rates of Sediment Accumulation ( $^{210}\text{Pb}$ )**

Surface sediments throughout the NYS are characterized by medium to fine silts, with the finest sediment occurring near the Shandong Peninsula and in the central part of the basin (Fig. 16a); sand generally constitutes less than 5-10% of the sediments. Interrupting this pattern, however, are two tongues of coarser sediment, one along the northeastern NYS and the other along the southwestern NYS, suggesting, as it were, a cyclonic eddy encircling the fine muds in the central basin. In the northern NYS, the coarse silty-sand surface is consistent with the ravinement surface recorded in the seismic profiles (see below). Water content of the surficial sediments tends to follow grain-size distribution but with subtle differences. Highest water content (>40%) is in the central basin fine silts (Fig. 16b), whereas the fine-silts off the peninsula contain significantly less (32-36%). The two tongues of coarser sediment have water contents less than 32% and locally less than 20% (Fig. 16b).

Four gravity cores taken on the NYS clinoform (S44 and S54 on the bottomset; S45 close to the foreset; and S46 in the foreset; Figs. 2, 3) show the general dominance of clay- and silt-size components (Fig. 17). Sand was essentially completely absent from both of the foreset core S46 and bottomset core S54, only few shell fragments present in the

bottom of S45. In contrast, sand is a prominent constituent below about 40 cm in bottomset core S44, reaching >20% in some layers, and shell fragments are prominent at the bottom of the core. Sand also is present below 180 cm in bottomset core S45, and below 230 cm there are typical yellowish, stiff loess-like sandy-silt, suggesting a relict sediment, separated from the overlain layer with a unconformity surface (Fig. 14).

Sedimentation rates based on  $^{210}\text{Pb}$  geochronology from the 5 box cores from the foreset (S45, S46), and bottomset (S44, S54) strata (Fig. 3) show a differentiation based on location (Fig. 18). Core S49 shows the scatter in the plot (Fig. 19); the scatter might reflect either extensive biogenic reworking or physical mixing. In contrast, the two foreset cores (S45, S46) display a very good decay, with the maximum estimates  $^{210}\text{Pb}$  sediment accumulation rates of 2.9 and 3.9 mm/yr, respectively (Fig. 18). The difference might indicate the dynamic top layer deposits formed by the modern across shelf advection and diffusion processes which will be discussed below. Accumulation rates in the bottomset strata are significantly less than in the foreset strata – 0.7 and 0.9 mm/yr for S44 and S54, respectively (Fig. 18).

## **5. Development of the Shandong Clinof orm**

The semi-enclosed North Yellow Sea (NYS) lies along the landward edge of the broad epicontinental East China/Yellow Sea (EC/YS). Being nowhere deeper than about 70 m, it was entirely subaerially exposed during the last glacial maximum (LGM) lowstand of sea level. The post-LGM processes have been strongly controlled by the sea-level fluctuation and climatic changes, the latter of which influenced sediment input. Using an extensive sea-level database, Liu and Milliman (2001, submitted) have concluded that the post-LGM

transgression in the EC/Ys was punctuated by a series of rapid flooding events (12-45 mm/yr), separated by intervening slow rates of transgression (2-6 mm/yr). By about 15 ka, rising sea level had reached about -100 m (relative to present-day sea level), and seawater had begun to enter the central SYS. A rapid rise during melt water pulse 1A (MWP-1A termed by Fairbanks, 1989) occurred between 14.7 -14.1 ka, when sea level jumped from -98 m to -74 m (40 mm/yr). At the end of this flooding event, the sea water had reached the southern edge of the NYS, following which sea level rose slowly (6 mm/yr) from -72 m to -60 m for the next 2 ky. Beginning about 11.7 ka, sea level again jumped from -60 m to -42 m (MWP-1B of Fairbanks), resulting in a rapid westward flooding of the NYS and initial entrance into the Bohai Sea. Sea-level rise then again stagnated (between -42m to -38 m) for about 1.8 ky, during which much of the Shandong clinoform accumulated. In order to supply the 300 km<sup>3</sup> of sediment within the Shandong mud wedge, however, we need a sediment source as well as a slow-down in the rate of sea-level transgression. Recent paleoclimatic data suggest that prior to the intensification of the SW monsoon (about 11 ka; Wang et al., 1999), the Yellow River may have been predominantly dry (Zhao, 1991), perhaps not unlike its present condition in the past several years (Yang et al., 1998). The presence of thick loess deposits along the northern Shandong Peninsula (Liu and Zhao, 1995) and evidence of relict loess in the shallow sub-bottom NYS sediments (see above) lends further evidence of an arid glacial climate and therefore a dry Yellow River. The well-preserved nature of peats and possible relict loess deposits indicate little disturbance by a large fluvial input, and we find no evidence on our seismic profiles of buried or infilled river channels. We thus conclude that prior to the intensification of the summer monsoon about 11 ka the Yellow River was at best a minor sediment source.

Evidence of a dramatic intensification of the southwestern (summer monsoon) has been noted throughout southern Asia (Wang et al., 1999). The initiation of maximum runoff and sediment discharges also have been observed in other climate-controlled river systems, such as Indus (Prins and Postma, 2000 ), Ganges-Brahmaputra (Goodbred and Kuehl, 2000), and Ebro (Diaz et al. 1996) rivers. It was during this period of slow-rising sea-level and increased Yellow River discharge that the first post-LGM Yellow River subaqueous delta formed in the NYS (Liu et al., 2002).

The first phase of clinoform wedge accreted over the relict or transgressive facies along the northern shore of Shandong Peninsula. Because most of the sediments were deposited proximally, the sediments probably were coarser than those seen the present-day topset deposits: the acoustically turbid nature of the lower portion of the clinoform also suggests that more organic material was stored in this rapidly accreting proximal clinoform (Figs. 10-12). It is during this stage (11-9.8 ka) that most of the Shandong clinoform accreted (Liu et al., 2002).

Beginning about 9.8 ka, sea level again rose rapidly, from -36 m to -16m in 800 years (~45 mm/y). During this period of rapid transgression, extreme flooding of the Yellow River at 9.2 ka (Yang et al., 2000) may have diverted the river south of the Shandong Peninsula to the Jiangsu coast (Liu et al., 2002; Liu and Milliman, in prep). The combination of the diverted flow and rapid sea-level rise means that for the next 2 ky the Shandong clinoform received essentially no proximal sedimentation, instead, the river had built another subaqueous delta in the offshore of Jiangsu in the western SYS (Liu et al., 2002). After about 7 ka, the river again diverted northward, but by this time the rapidly transgressing sea level had moved 200 km westward. It was during this distal phase of the

Yellow River that the acoustically transparent facies of the clinoform accumulated (Figs. 9-15).

By dividing the NYS subaqueous clinoform into two distinct phases of accretion – a proximal phase between 11-9.2 ka and a distal phase after 9.2 ka, we can calculate a rough sediment budget. Total sediment volume of the proximal phase is about 200 km<sup>3</sup> or (assuming a specific gravity of 1.2 t/m<sup>3</sup>) 240 × 10<sup>9</sup> t. Assuming accumulation in 1.8 ky gives a sediment deposition of 0.13 × 10<sup>9</sup> t/y. The subsequent distal phase resulted in accumulation of an estimated 100 km<sup>3</sup> or 120 × 10<sup>9</sup> t of sediment in 9000 years, giving an accumulation rate of 0.013 × 10<sup>9</sup> t/y, which is an order of magnitude less than during the proximal phase. While the proximal phase sediment accumulation rate from the Yellow River is 7-fold lower than the modern river load (0.9 × 10<sup>9</sup> t/y; Galler, 1999), it appears to correspond closely with estimated pre-agriculture loads (e.g., Milliman et al., 1987; Saito et al., 2001). The much lower rate of sediment accumulation within the clinoform during the distal phase (13 × 10<sup>6</sup> t/y) reflects the 200-km distance between the modern delta and the clinoform, as well as the fact that for more than 800 years the river discharged south onto the Jiangsu coast. However, this value is still higher than the 6 × 10<sup>6</sup> t/y that Martin et al. (1993) estimated to be presently escaping from the Bohai. In addition, of course, the small local streams and coastal erosion also may have contributed sediment to the clinoform.

While we hypothesize that much of the Shandong clinoform is a relict feature, formed during post-LGM slackened sea-level transgression and after re-initiation of the summer monsoon, modern processes almost certainly have modified and supplied sediment to the system. Mineralogical analyses show that surficial sediments from the topset and foreset

strata (Liu et al., 1987; Qin et al., 1989) differ rather strongly from modern Yellow River sediments, suggesting that other sediment sources may contribute to the modern sediments (distal phase) overlying the relict clinoform (proximal phase) (Liu et al., 2002). We also note that the bottom part of the foreset slope (that portion we have called the “nose”) progrades not only to the north (Figs. 12, 13), but also to the east (Figs. 10, 11), indicating that the clinoform accretes eastward as well as offshore. Based on the distinct grain-size distribution in the NYS (Fig. 16), Cheng and Gao (2000) suggest that sediments along the northern coast of Shandong Peninsula are transported towards the east and northeast (Fig. 16, 20), while along the northern edge of the NYS sediment is transported westward, in agreement with the regional circulation pattern (Fig. 8b,c; Fig. 20). The finer size of sediments in the central basin suggest a net deposition, something that is also shown by the greater thickness of sediments shown in our seismic profiles, e.g. 98a (Fig. 14). This basin-wide cyclonic gyre system is considered to play a great role in trapping the fine sediments in the central NYS and SYS basins (Hu, 1984; Shen et al., 1996).

Seaward growth of the clinoform occurs primarily by overlap of along-shore and across shore mud transport, creating a superimposed clinoform deposit. Along-shore and seaward surface flow in the upper layer also transport suspended sediment along and across shelf (Figs. 8, 20). The strong upwelling and counter current in the deep layer of the boundary areas in the east Shandong Peninsula (Fig. 7e, f) and NYS (Figs. 6, 8) could allow landward supply of sediment to mud wedge, together with the high TSS concentration in the near-shore bottom water (Fig. 7a-d). The well-stratified cold stagnant water mass in the central NYS basin could prevent too much sediment being transported offshore in the north (Fig. 8a).

## Conclusions

(1) The seismic reflection profiles in the North Yellow Sea (NYS) reveal a wedge-shaped depositional sequence that wraps around the eastern end of the Shandong Peninsula, extending into the South Yellow Sea (SYS).

(2) This Yellow River subaqueous clinoform (up to 40 m thick) contains an estimated approximately  $300 \text{ km}^3$  of sediment. Radiocarbon dating, shallow seismic profiles, and regional sea-level history suggest two-thirds of the mud wedge formed when the rate of post-glacial sea-level rise slackened and the summer monsoon intensified, about 11-9.2 ka; Mean sediment accumulation rate during this 1.8 ky interval was  $0.13 \times 10^9 \text{ t/y}$ . Between 9.2 and 7 ka, the Yellow River discharged into the SYS, and any sediment received by the NYS clinoform was by erosion of the rapidly retreating Yellow River delta and clinoform; accumulation rates during the past 9 ky interval has been  $0.013 \times 10^9 \text{ t/y}$ , an order of magnitude smaller than during the first period.

(3) Modern sedimentation accumulation rates are highest in the forest (3 mm/year) and lowest in the topset and bottomset regions (< 1 mm/year). Fine sediments (clayey-silt) distributed on the surface of the nearshore and distal bottomset regions, the silt distributed in the middle part of the wedge (foreset). Sediments fine seaward and eastward with the alongshore and across shore transport. The very fine clayey-silt ( $>7.5 \phi$ ) in the central NYS corresponds to the stable and weak depositional environment.



(4) The regional and local sediments from the small river discharges and coastal loess erosion have also been directly input, and influenced the sedimentary processes and geochemical composition (Fig. 20).

(5) The basin-wide circulation and counterclockwise gyre in the NYS move water mass eastward along the Shandong Peninsula together with the higher TSS concentration. The corresponding counter-current and landward upwelling help keep the sediments trapped around the Shandong Peninsula (Fig. 20).

## **Acknowledgements**

Many thanks to the crews of RV Goldstar II and our Chinese and American colleagues for their help in obtaining and precessing data. We thank L.D. Wright, Y. Saito, S. Kuehl and J. Perry for their many helpful comments on an earlier version of this paper. Financial support for this program from National Science Foundation of China and US, and the Office of Naval Research. We thank Peggy Schexnayder for her encouragement with this study. This is contribution no.# from Virginia Institute of Marine Science, College of William & Mary.

## References:

- Alexander, C.R., DeMaster, D.J., and Nittrouer, C.A., 1991. Sediment accumulation in a modern epicontinental-shelf setting: The Yellow Sea. *Marine Geology*, 98, 51-72.
- Bornhold. B.D., Yang Z.S., Keller, G.H., Prior, D.B., Wiseman, W.J., Wang, Q., Wright, L.D., Xu, W.D., and Zhuang Z.Y., 1986. Sedimentary framework of the modern Huanghe (Yellow River) Delta. *Geo-Marine Letter*, 6, 77-83.
- Chen, Z.Y., Song, B.P. Wang, Z.H. Cai, Y.L. 2000. Late Quaternary evolution of the subaqueous Yangtze Delta, China: sedimentation, stratigraphy, palynology, and deformation. *Marine Geology* 162, 243-441.
- Cheng, P., Gao, S., 2000. Net sediment transport patterns over the northwestern Yellow Sea, based on grain-size trend analysis. *Oceanologia et Limnologia Sinica* 31 (6), 604-615.
- Cutshall, N.H., Larsen, I.L., Olsen, C.R., 1983. Direct analysis of  $^{210}\text{Pb}$  in sediment samples: Shelf-absorption correction. *Nucl. Instrum. Methods* 206, 309-312.
- Diaz, J.I., Palanques, A., Nelson C.H., Guillen, J., 1996. Morpho-structure and sedimentary of the Holocene Ebro prodelta mud belt (northwestern Mediterranean Sea). *Continental Shelf Research* 16 (4), 435-456.
- Fairbanks, R.G., 1989. A 17,000-year glacio-eustatic sea level record: influence of glacial melting rates on the Younger Dryas event and deep ocean circulation. *Nature* 342, 637-642.
- Galler, J.J., 1999. Medium and long-term changes in fluvial discharge to the sea: The Yellow River case study. Master of Science Thesis, College of William & Mary, pp.78.

- Goodbred, S.L., and Kuehl, S.A., 2000. The significance of large sediment supply, active tectonism, and eustasy on margin sequence development: Late Quaternary stratigraphy and evolution of the Ganges-Brahmaputra delta. *Sedimentary Geology*, 133, 227-248.
- Guan, B.X., 2000. Inversion thermocline in coastal region north and east of Shandong Peninsula in winter and its relation to deep-bottom counter current. *J. Oceanography of Huanghai & Bohai Seas*. 18 (3), 66-71.
- Hu, D.X., 1984, Upwelling and sedimentation dynamics, *Chin. J. Oceanol. Limnol.* 2(1), 12-19.
- Jiang, W.S., Pohlmann, T., Sundermann, J., Feng, S.Z., 2000. A modeling study of SPM transport in the Bohai Sea. *J. of Marine Systems*. 24, 175-200.
- Kuehl, S.A., DeMaster, D.J., Nittrouer, C.A., 1986. Nature of sediment accumulation on the Amazon continental shelf. *Cont. Shelf Res.* 6, 209-225.
- Kuehl, S.A., Levy, B.M., Moore, W.S., Allison, M.A., 1997. Subaqueous delta of the Ganges-Brahmaputra river system. *Mar. Geol.* 144, 81-96.
- Lee, H.J., Jung, K.T., Foreman, M.G., Chung, J.Y., 2000. A three-dimensional mixed finite-difference Galerkin function model for the oceanic circulation in the Yellow Sea and East China Sea. *Cont. Shelf Res.* 20, 863-895.
- Li, F., Ding, Z.X., 1996. Vertical distribution patterns of suspended matter and near bottom turbid water layer in the South Yellow Sea. *Studia Marine Sinica*. 37, 33-42.
- Liu, J.P., Zhao, S.L., 1995. Origin of the buried loess in the Bohai Sea bottom and the exposed loess along the coastal zone. *Oceanologia et Limnologia Sinica* 26, 363-368.
- Liu, J.P., Milliman, J.D., 2001. Post-Glacial Sea-level Transgression in the East China and Yellow Seas: Significance of Periodic Rapid Flooding Events. *Science* (in review).

- Liu, J.P., Milliman, J.D., Gao, S., 2002. The Shandong mud wedge and post-glacial sediment accumulation in the Yellow Sea. *Geo-Marine Letter* (in press).
- Liu, M.H., Wu, S.Y., and Wang, Y.J., 1987. Late Quaternary Sediments of the Yellow Sea. China Ocean Press, Beijing, pp.433.
- Liu, Z.X., Xia, D.X., Berne, S., Wang, K.Y., Marsset, T., Tang, Y.X., Bourillet, J.F., 1998. Total deposition systems of China's continental shelf, with special reference to the eastern Bohai Sea. *Mar. Geol.* 145, 225-253.
- Martin, J.M., Zhang, J., Shi, M.C. and Zhou, Q. 1993. Actual flux of the Huanghe (Yellow River) sediment to the western Pacific Ocean. *Netherlands Journal of Sea Research* 31, 243-254.
- McManus, J.. 1988. grain-size determination and interpretation. In Tucker M. (ed) *Techniques in Sedimentology*. Blackwell, Oxford, 63-85.
- Milliman, J.D., Meade, R.H., 1983. World-wide delivery of river sediment to the oceans. *Journal of Geology* 91, 1-21.
- Milliman, J.D., Li, F., Zhao, Y.Y., Zheng, T.M., Limeburner R., 1986. Suspended matter regime in the Yellow Sea. *Prog. Oceanog.* 17, 215-227.
- Milliman, J.D., Qin Y.S., Ren M.E., Saito Y., 1987. Man's influence on the erosion and transport of sediment by Asian rivers: the Yellow River (Huanghe) example. *J. Geology.* 95, 751-762.
- Milliman, J.D., and Syvitski J.P.M., 1992. Geomorphic/Tectonic Control of Sediment Discharge to the Ocean: The Importance of Small Mountainous Rivers., *Journal of Geology*, Vol. 100, p525-544.

- Morgan, J.P., 1970. Deltaic Sedimentation: Modern and Ancient. SEPM Special Publication No. 15, Tulsa, OK, pp. 278.
- Nittrouer, C.A., Kuehl, S.A., DeMaster, D.J., Kowsmann, R.O., 1986, The deltaic nature of Amazon shelf sedimentation: Geol. Soc. Am. Bull., 97: 444-458.
- Nittrouer, C.A., Kuehl, S.A., Figueiredo, A.G., Allison, M.A., Sommerfield, C.K., Rine, J.M., Faria, L.E.C., Silveira, O.M., 1996. The geological record preserved by Amazon shelf sedimentation. Cont. Shelf Res. 16. 817-841.
- Prins, M.A., Postma, G., 2000. Effects of climate, sea level, and tectonics unraveled for last deglaciation turbidite records of the Arabian Sea. Geology 28, 375-378.
- Qian, N., and Dai, D.Z., 1980. The problems of river sedimentation and present status of its research in China: Chinese Hydraul. Eng., Proc. Int. Symp. River Sedimentation. 1, 1-39.
- Qin Y.S., Zhao, Y.Y., Chen L.R., Zhao, S.L., 1989. *Geology of the Yellow Sea*. China Ocean Press, Beijing, p. 289.
- Saito, Y. and Yang, Z.S., 1995. Historical change of the Huanghe (Yellow River) and its impact on the sediment budget of the East China Sea. Global Fluxes of Carbon and Its Related Substances in the Coastal Sea-Ocean-Atmosphere System, Editors: S. Tsunogai, K. Iseki, I. Koike and T. Oba, M&J International, Yokohama, pp. 7-12.
- Saito, Y., Katayama, H., Ikehara, K., Kato, Y., Matsumoto, E., Oguri, K., Oda M., Yumoto, M., 1998. Transgressive and highstand systems tracts and post-glacial transgression, the East China Sea. Sedimentary Geology. 122, 217-232.
- Saito, Y. Yang, Z.S., Hori, K., 2001. The Huanghe (Yellow River) and Changjiang (Yangtze River) deltas: a review on their characteristics, evolution and sediment discharge during the Holocene. Geomorphology 41, 219-231.

- Shen, S.X., Li, A.C., Yuan, W., 1996. Low energy environmental of the central South Yellow Sea. *Oceanologia et Limnologia Sinica*. 27(5), 518-523.
- Stuiver, M., Reimer, P.J., Bard, E., Beck, J.W., Burr, G.S., Hughen, K.A., Kromer, B., McCormac, F.G., v. d. Plicht, J., Spurk, M., 1998. INTCAL98 Radiocarbon age calibration 24,000 - 0 cal BP. *Radiocarbon*. 40, 1041-1083.
- Sun, X.G., Fang, M., Huang, W., 2000. Spatial and temporal variations in suspended particulate matter transport on the Yellow and East China Sea shelf. *Oceanologia et Limnologia Sinica*. 31(6), 581-587.
- Wang, L., Sarnthein, M., Erlenkeuser, H., Grimalt, J., Grootes, P., Heilig, S., Ivanova, E., Kienast, M., Pelejero, C., Pflaumann, U., 1999. East Asian monsoon climate during the Late Pleistocene : high-resolution sediment records from the South China Sea. *Marine Geology* 156, 245-248.
- Wright, L.D., Coleman, J.M., 1973. Variation in morphology of major deltas as functions of ocean wave and river discharge regime. *Bull. AAPG*. 57, 370-398.
- Wright, L.D., Wiseman, W.J., Bornhold, B.D., Prior D.B., Suhayda, J.N., Keller, G.H., Yang Z.S., Fan Y.B., 1988. Marine dispersal and deposition of Yellow River silts by gravity-driven underflows. *Nature*. 332, 629-632.
- Wright, L.D., Wiseman, W.J., Yang, Z.S., Bornhold, B.D., Keller, G.H., Prior, D.B., Suhayda, J.N., 1990. Processes of marine dispersal and deposition of suspended silts off the modern mouth of the Huanghe (Yellow River). *Cont. Shelf Res.* 10, 1-40.
- Wright, L.D., Friedrichs, C.T., Kim, S.C., Scully, M.E., 2001. Effects of ambient currents and waves on gravity-driven sediment transport on continental shelves, *Marine Geology* 175(1-4), 25-45.

- Xia, Z.W., Guo, B.H., 1983. Cold water and upwelling around the tips of Shandong Peninsula and Liaodong Peninsula. *J. of Oceanography of Huanghai & Bohai Seas.* 1, 13-19.
- Yanagi, T. and Inoue, K., 1995. A numerical experiment on the sedimentation processes in the Yellow Sea and the East China Sea. *J. Oceanography*, 51, 537-552.
- Yang, D.Y., Yu, G., Xie, Y.B., Zhan, D.J., Li, Z.J., 2000. Sedimentary records of large Holocene floods from the middle reaches of the Yellow River, China. *Geomorphology* 33, 73-88
- Yang, Z.S., Milliman, J.D., Galler, J., Liu, J.P., Sun, X.G., 1998. Yellow River's Water and Sediment Discharge Decreasing Steadily. *EOS*, 79 (48): 589-592.
- Yuan, Y., Su, J., 1984. Numerical modelling of the circulation in the East China Sea. In : *Ocean Hydrodynamics of Japan and East China Sea*, Elsevier Oceanography Series, 39. Ichiiye, T., ed. Elsevier, New York, pp.167-186.
- Zhao, B.R. 1996. A study of the circulations of the northern Yellow Sea cold water mass -- Effects of tidal mixing on them. *Oceanologia et Limnologia Sinica.* 27(4), 429-435.
- Zhao, S.L., 1991. China shelf sea desertization and its derived deposits during the last stage of Late Pleistocene. *Oceanologia et Limnologia Sinica*, 22 (3), 285-293.
- Zheng, Q.A., Klemas V., 1982. Determination of Winter Temperature Patterns, Fronts, and Surface Currents in the Yellow Sea and East China Sea from Satellite Imagery. *Remote Sensing of Environment*, 12, 201-218.



**Figure 1.** Location and bathymetric map of the Bohai Sea (BS), North Yellow Sea (NYS), South Yellow Sea (SYS), and East China Sea (ECS). The Yellow Sea Warm Current (YSWC) and the Yellow Sea Coastal Cold Current (YSCCC). Shaded area represents location of the Shandong clinoform. Water depth in m.

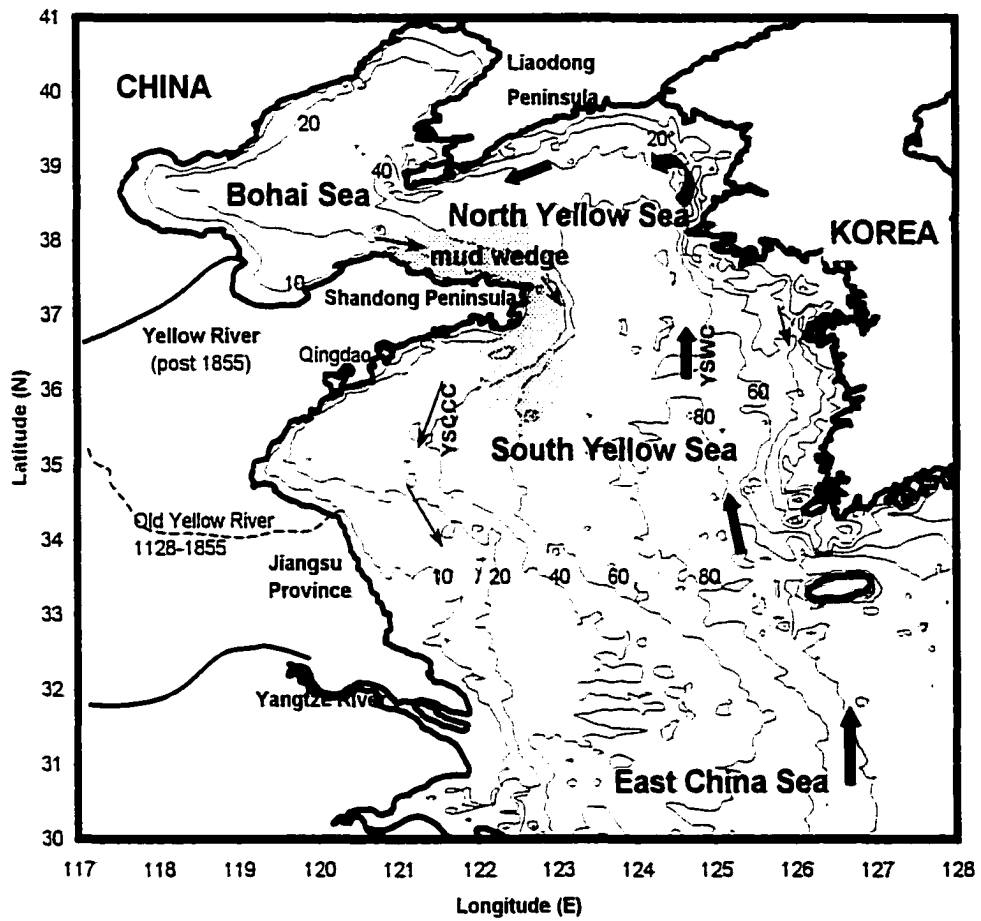
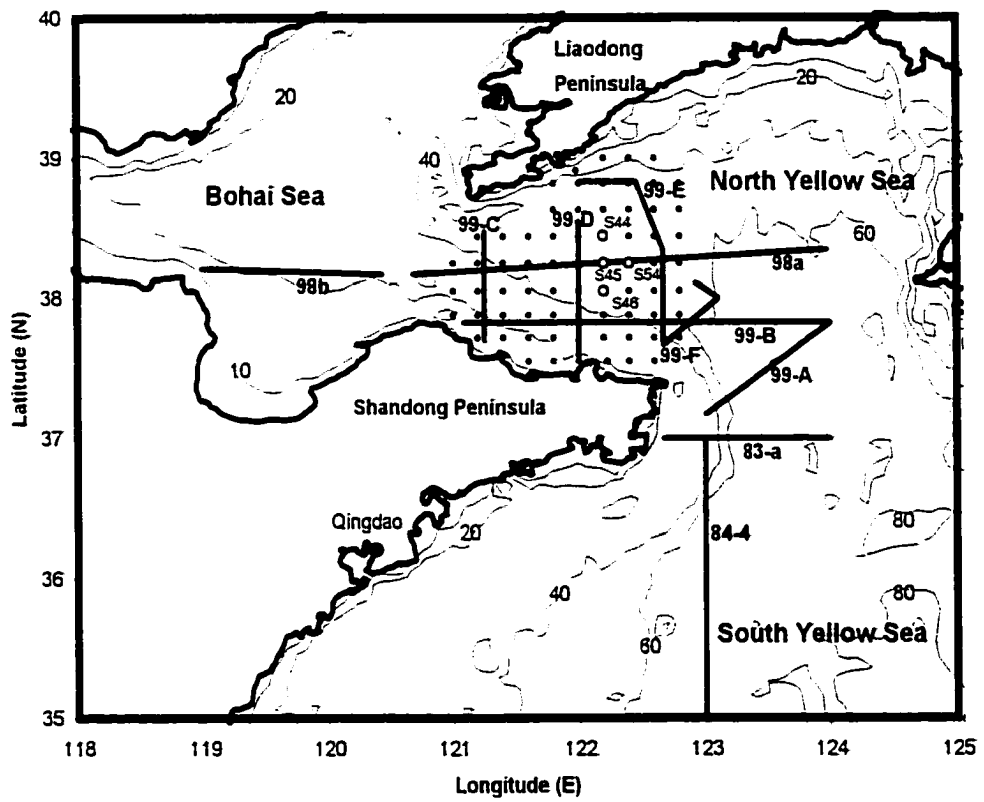


Figure 1.

**Figure 2.** Seismic profile lines (|), surface-sediment sample locations (●), and gravity cores (o) in the North Yellow Sea.



**Figure 2.**

**Figure 3.** 3-dimension seafloor morphology of the North Yellow Sea shows a series of subtle terraces around Shandong Peninsula. It also shows the location of our seismic profiles (black lines) and box cores (square boxes) with relation to the clinoform.

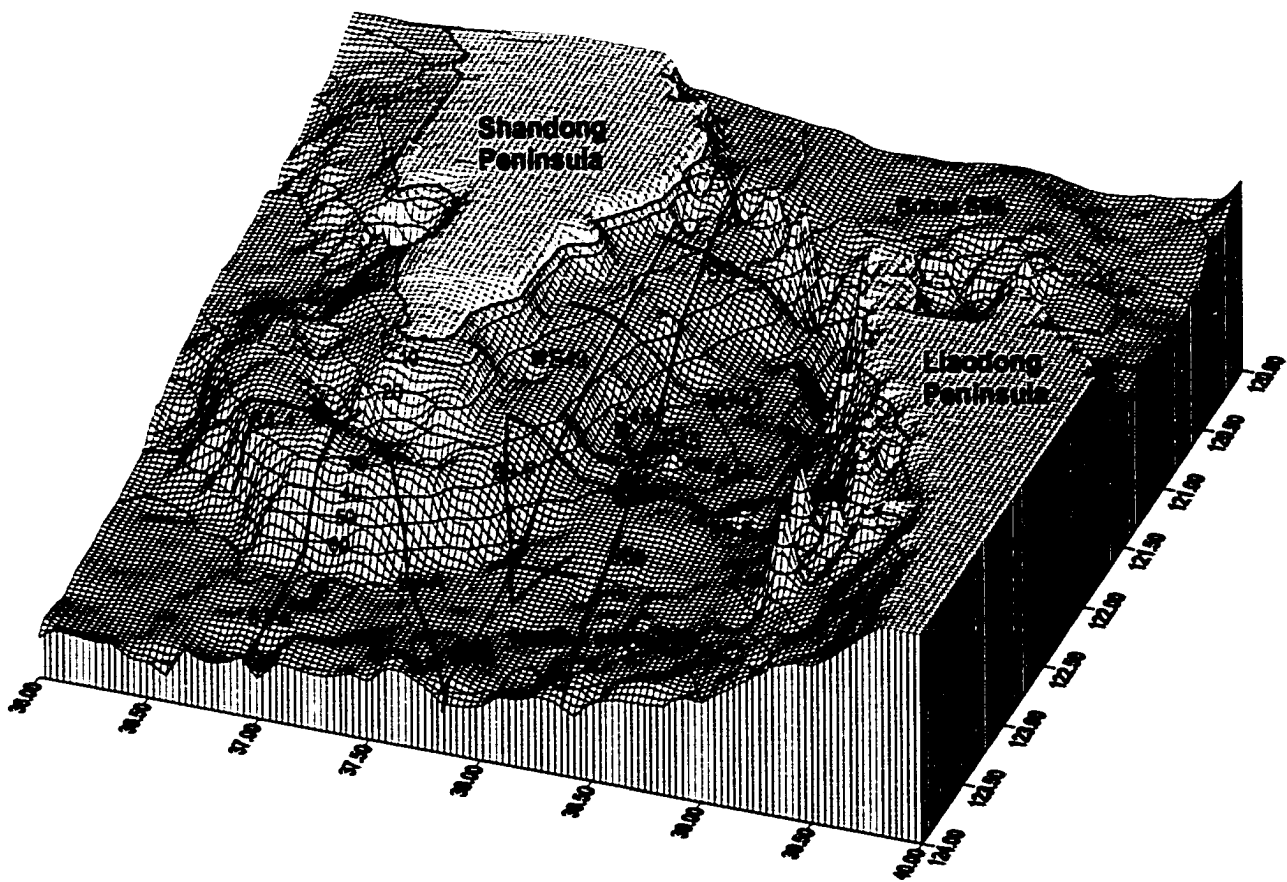
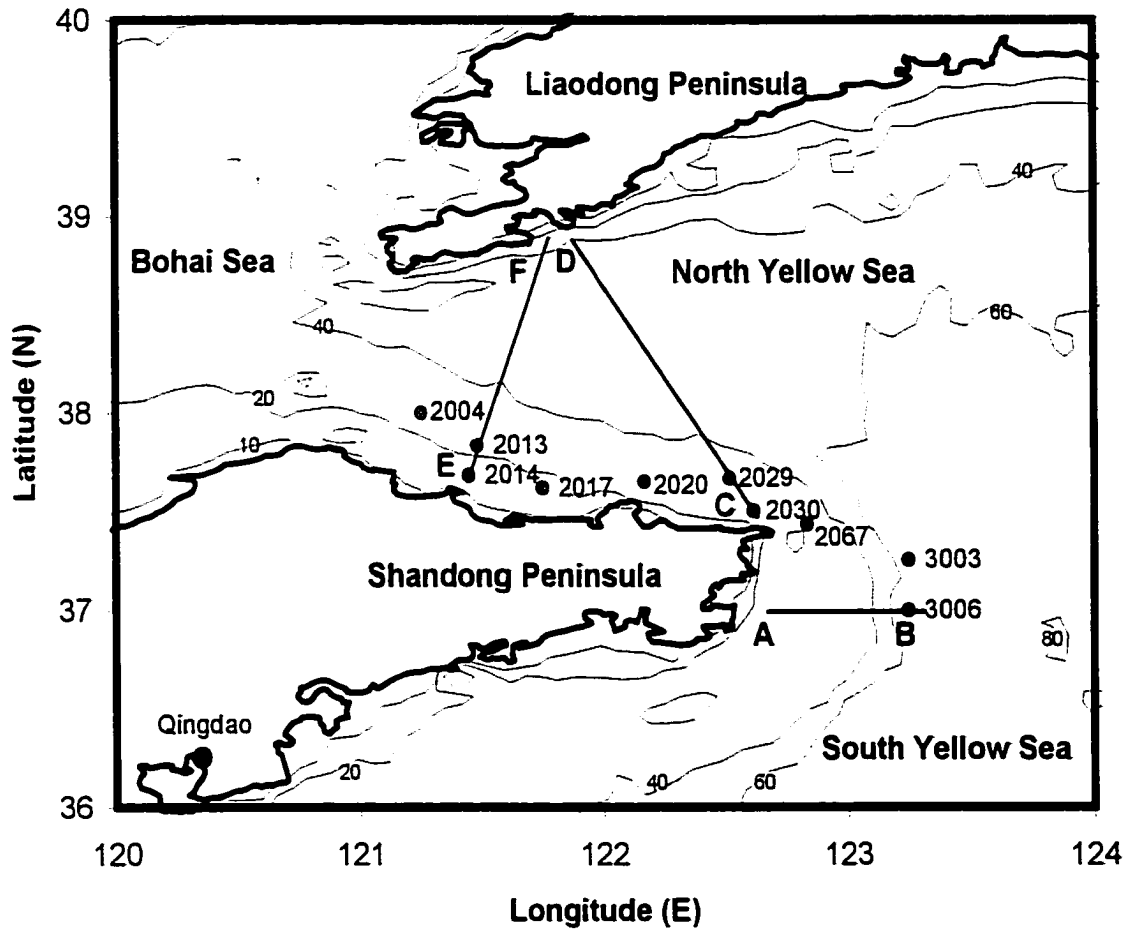


Figure 3

**Figure 4.** Oceanographic observation stations in the North Yellow Sea (●) (Guan, 2000); Transect surveys between A-B (eastern tip of Shandong Peninsula) (Xia and Guo, 1983; Li and Ding, 1996), C-D (cross the NYS from Shandong to Liaodong Peninsula) (Martin et al., 1993; Zhao, 1996), and E-F (across the Bohai strait from Shandong to Liaodong Peninsula) (Martin et al., 1993).



**Figure 4**



**Figure 5.** Vertical profiles of temperature and salinity (1989-1991) of the transect C-D (Fig. 4), which cross the whole NYS. reveal the well mixed winter conditions (a, b), and stratified summer conditions (c, d) with a cold and saltier water in the central bottom (Martin et al., 1993).

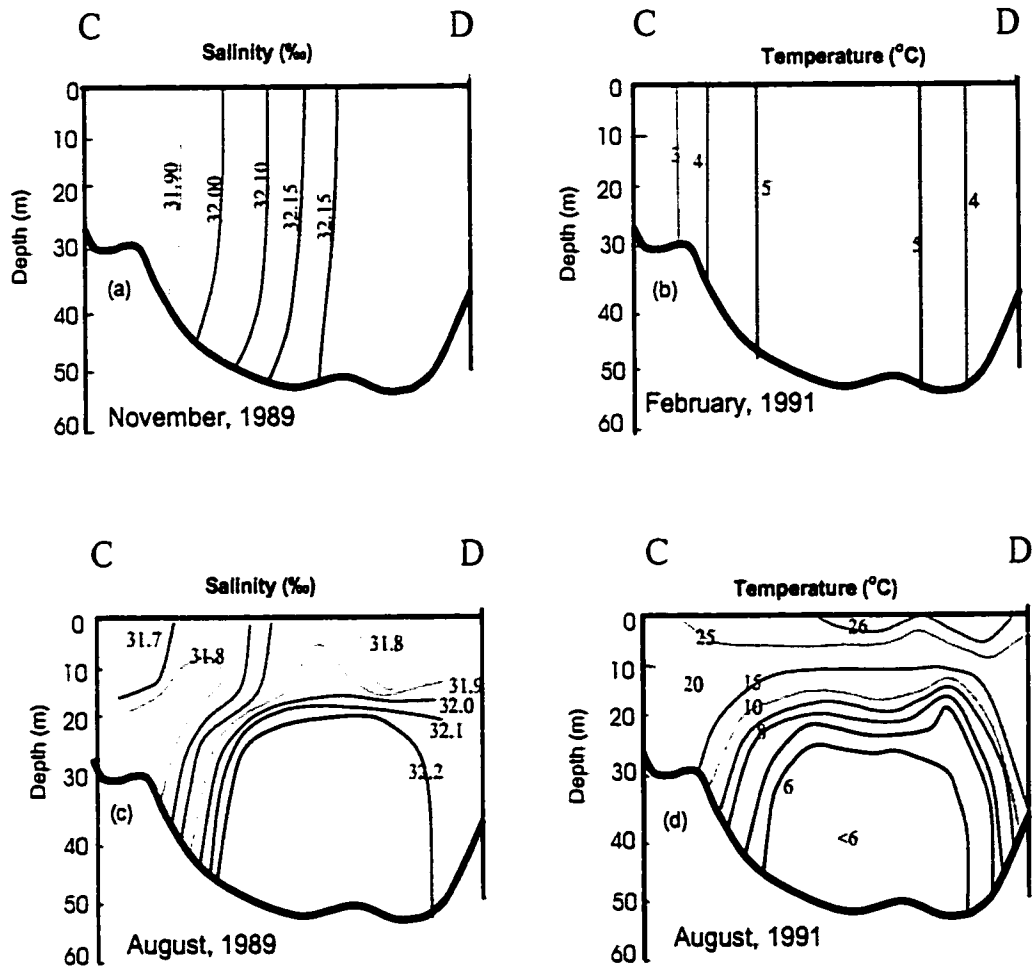


**Figure 5.**

**Figure 6.** Vertical profiles of temperature and salinity (January 1959) oceanographic stations reveal the eastward and south surface transport around the Shandong Peninsula, and the counter current in the deep layer (Guan, 2000). Stations shown in Fig. 4.

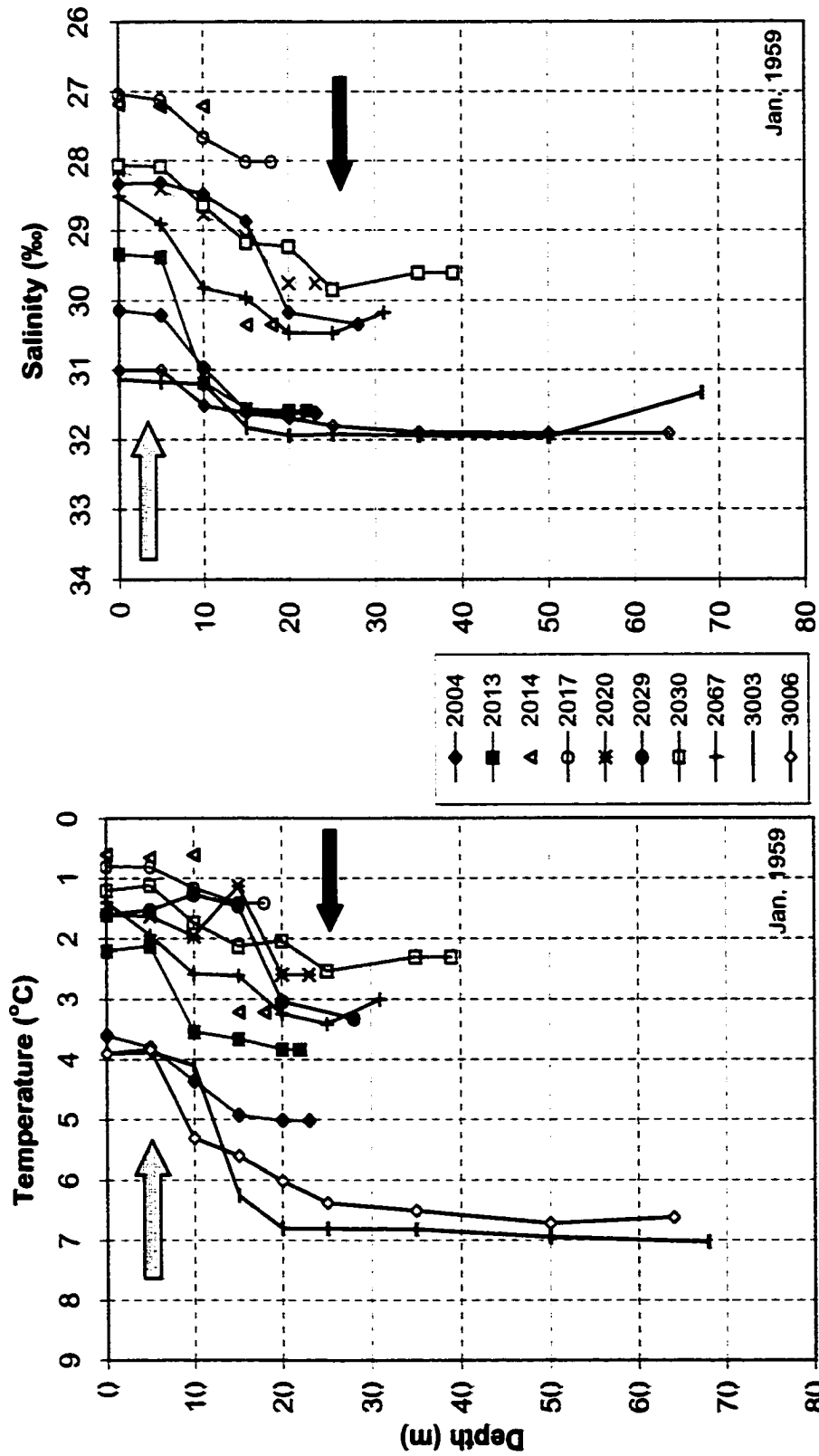


Figure 6.

**Figure 7.** Vertical profiles of TSS distribution along the transect A-B (Li and Ding, 1996) and E-F (Martin et al., 1993) reveal the higher TSS nearshore bottom in winter (a) and lower value in Summer (b-d). T-S distribution in A-B transect also suggest the upwelling occurred in the eastern tip of the Shandong Peninsula (Xia and Guo, 1983). Transect shown in Fig. 4.

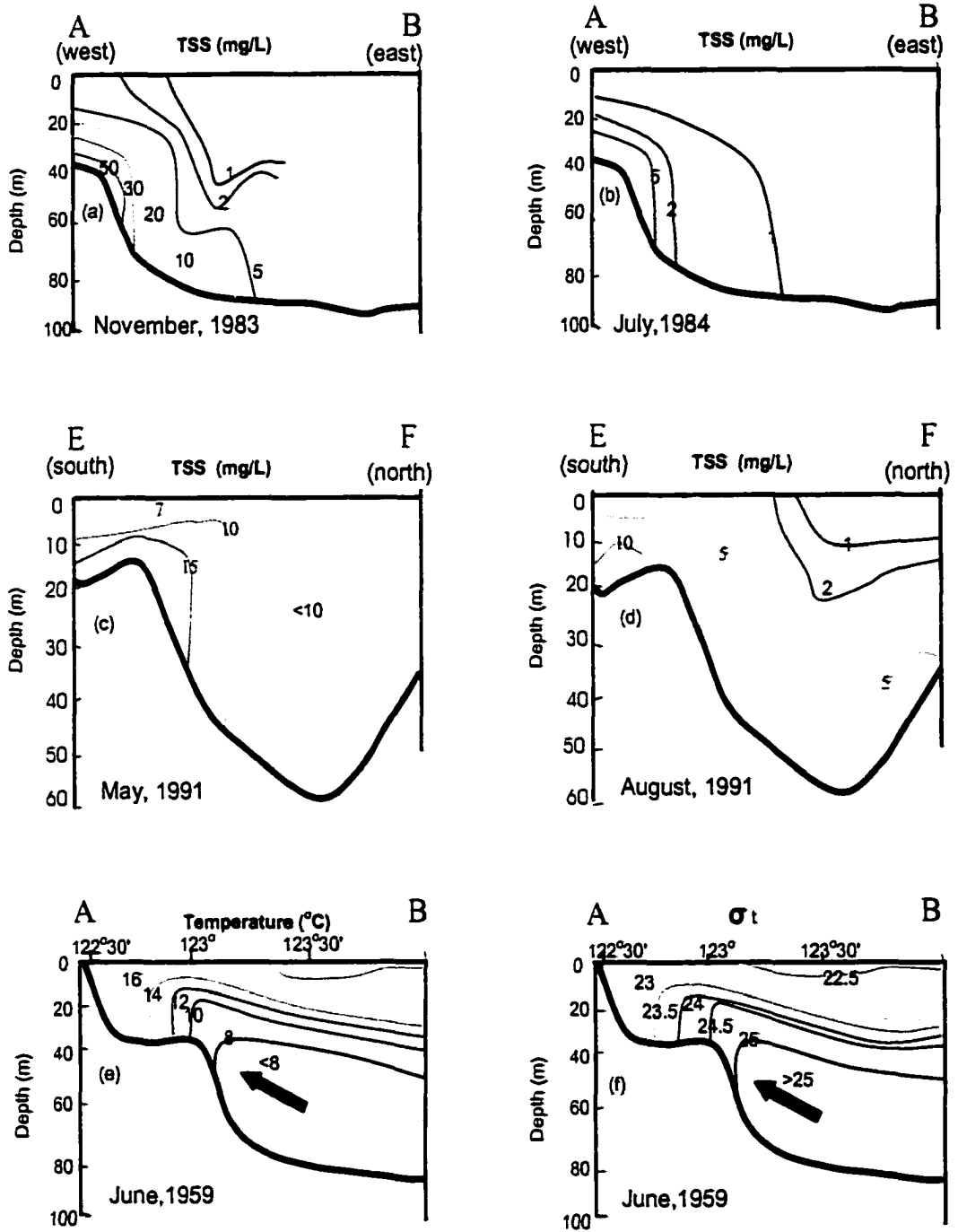
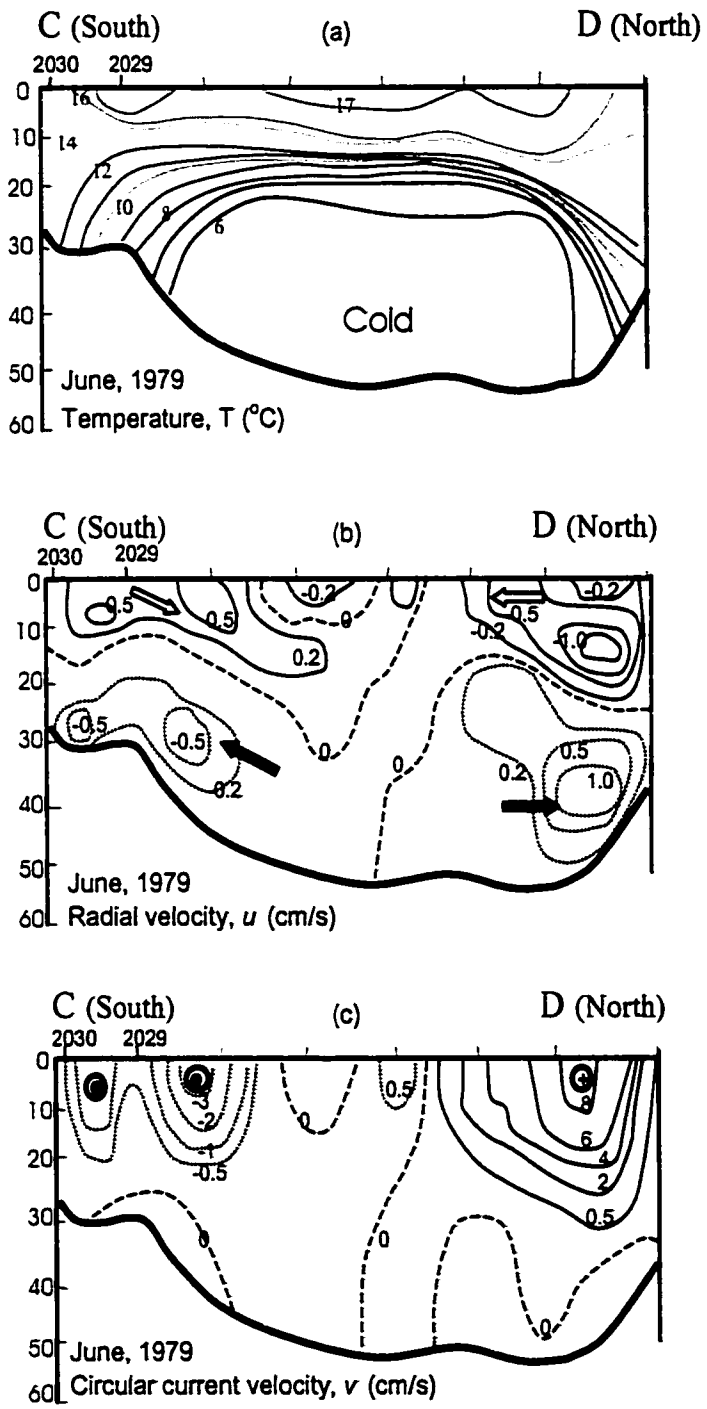


Figure 7.

**Figure 8.** Profiles of temperature and current velocity (June 1979) in the transect C-D from the east tip of Shandong Peninsula northwards Liaodong Peninsula (Zhao, 1996). (a) stratified summer conditions; (b) surface seaward transport and bottom landward upwelling. (c) westward surface flow in the north NYS, and eastward surface flow in the south NYS;



**Figure 8.**



**Figure 9.** GeoPulse records from profiles 99-A and 83-a in the east tip of the Shandong Peninsula showing clinoform in the west, and transgressive, ravinement surface in the east. Profile locations shown in Fig. 2, 3.

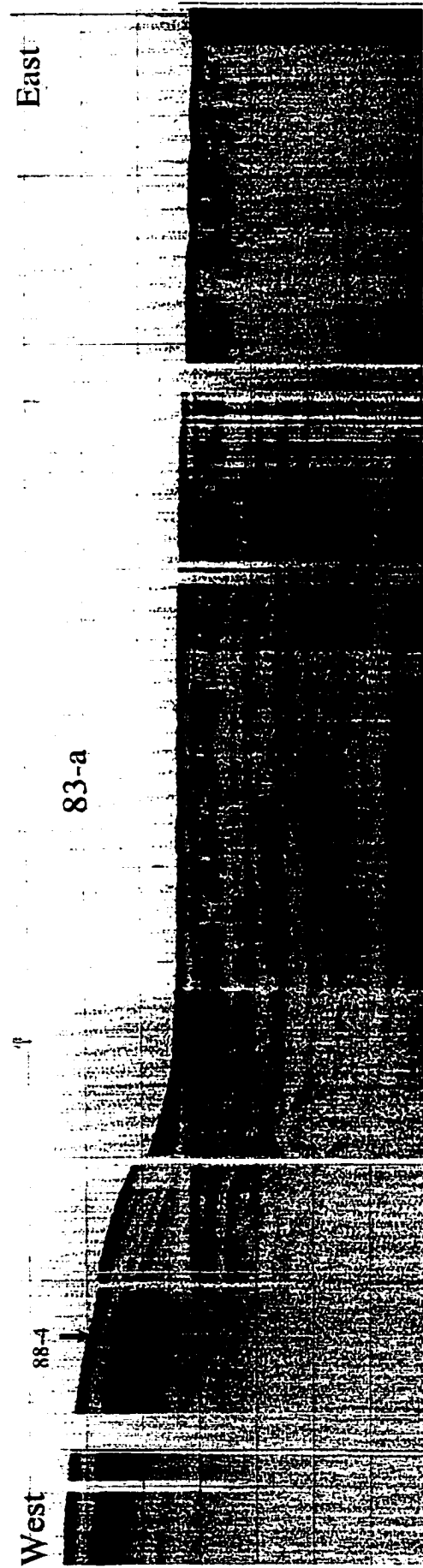
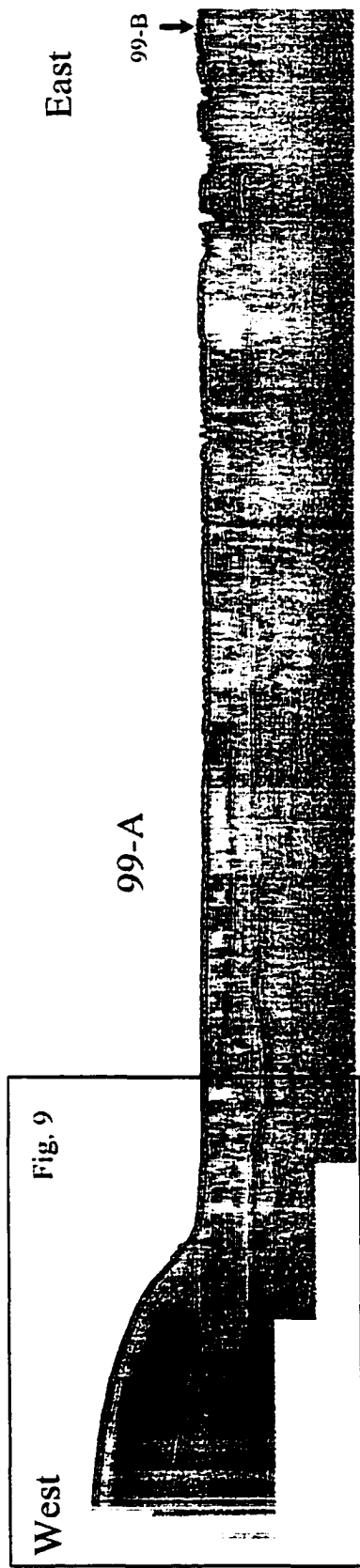


Figure 9.

**Figure 10.** High-resolution GeoPulse records of the westernmost part of the seismic profile 99-A. show a clinoform structure with the oblique features in the west. The early phase bottomset can be seen to be buried by the later foreset deposits. Location of profile is shown in Fig. 2. 3.

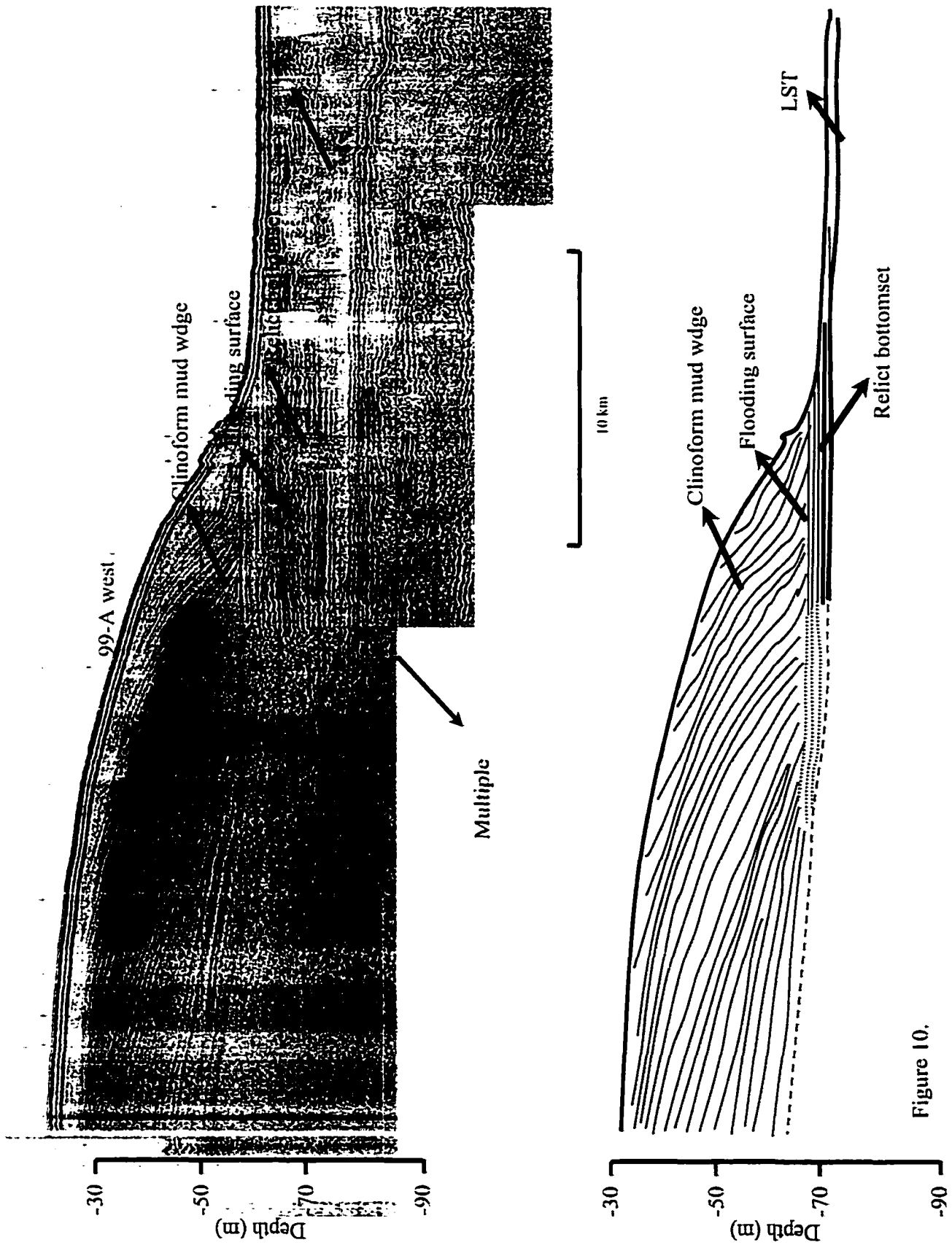


Figure 10.

**Figure 11.** GeoPulse record of profile 99-B from the eastern NYS the western NYS in along the shoreshore of north Shandong Peninsula, which shows the seaward progradation of the mud wedge. An enlargement of the clinoform's toe and easternmost part is shown below. Location of profile is shown in Fig. 2. 3.

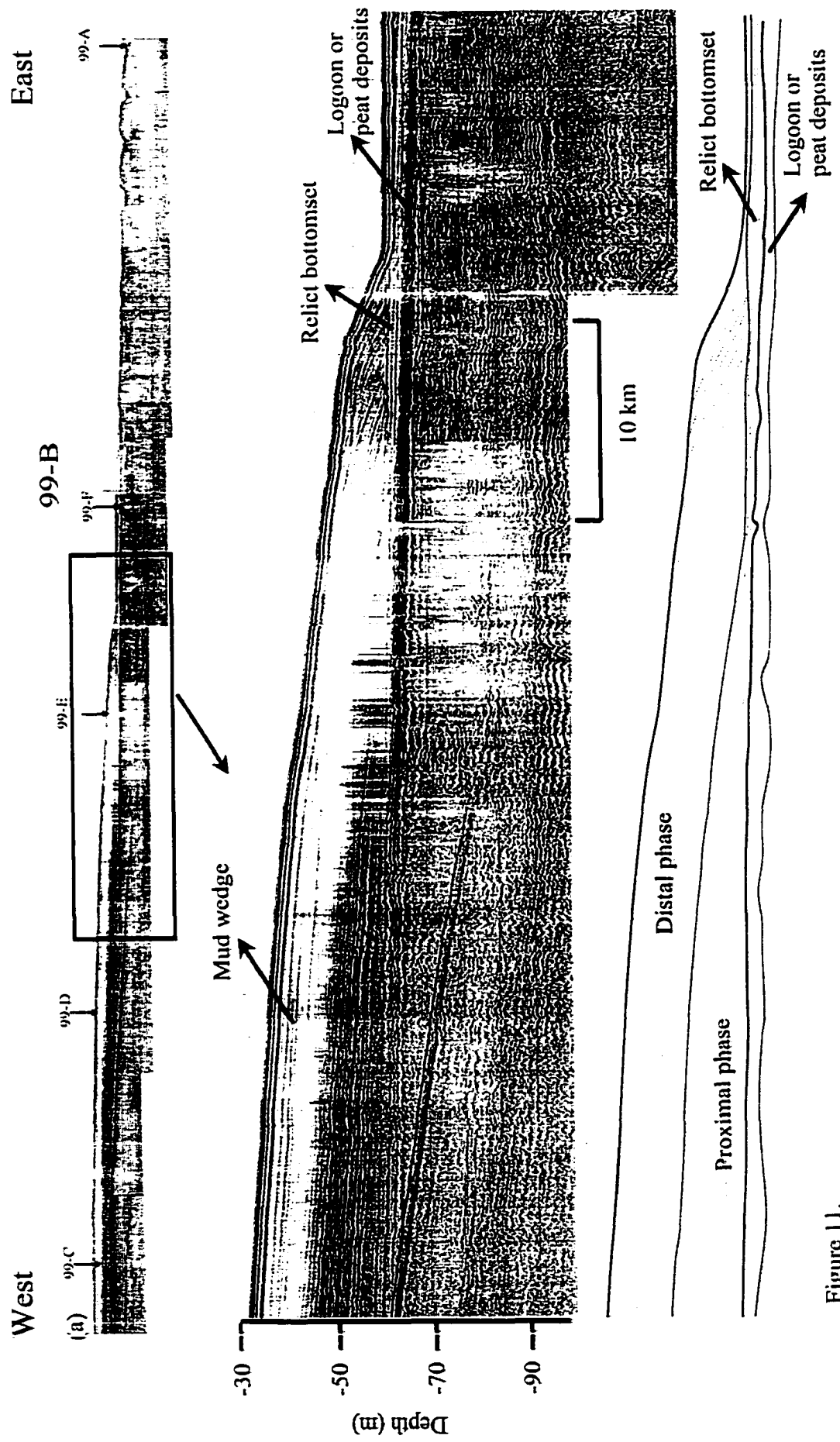


Figure 11.

**Figure 12.** GeoPulse profiles 99-E and 99-F. The gravity core of NYS-5 recovered a peat sample that apparently underlies the soft and transparent mud deposits; this peat layer might represent the strong reflective surface seen in these profiles. Biogenic methane gas is evident in the record on the landward, and limits penetration of the acoustic signal. Location of profiles is shown in Fig. 2, 3.

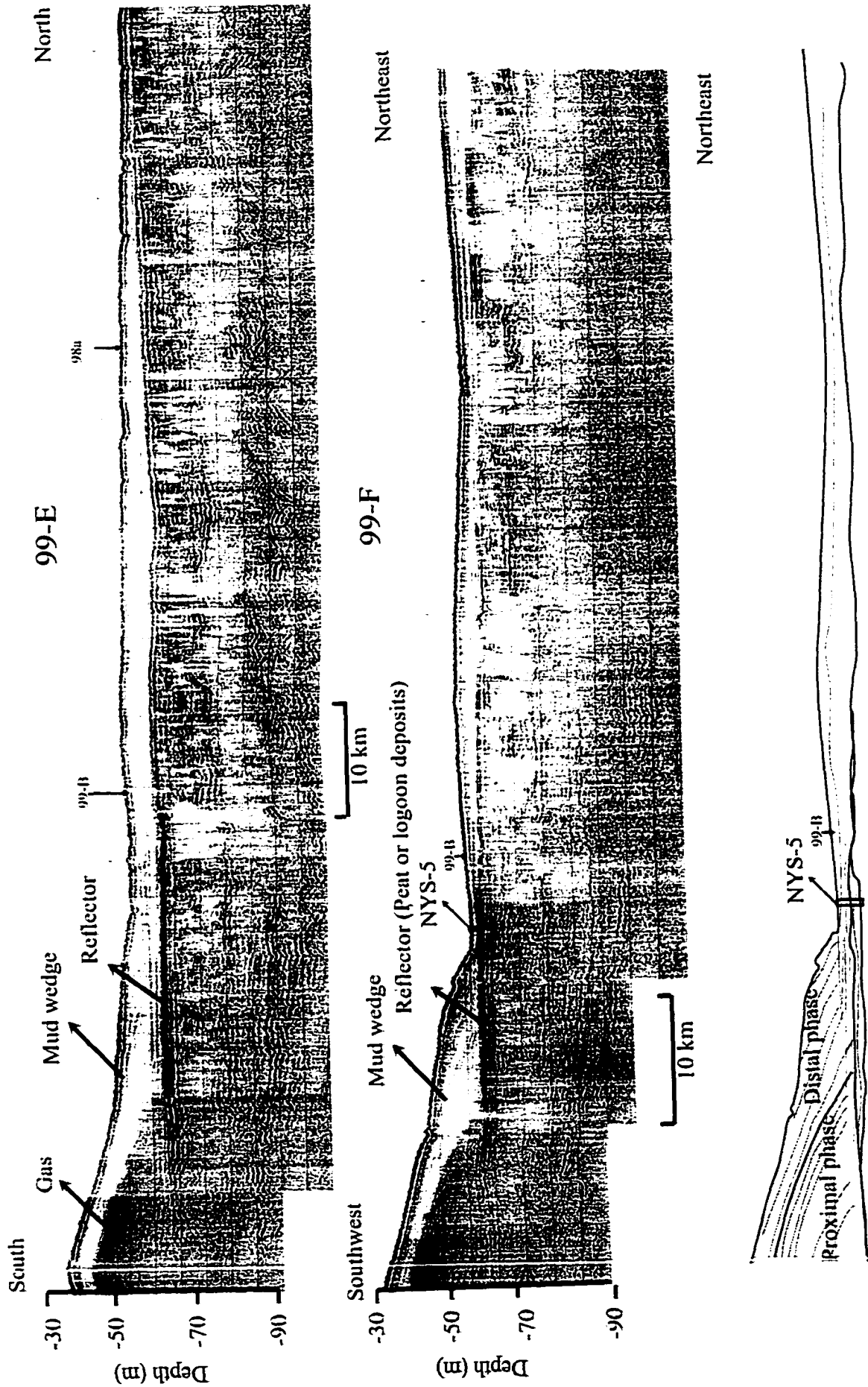


Figure 12



**Figure 13.** GeoPulse record of profile of 99-C in the west NYS and 99-D across the central NYS from south to north. 99-C does not display the transparent character seen in other profiles, which indicate a coarser size-fraction. Location of profiles is shown in Fig. 2. 3.

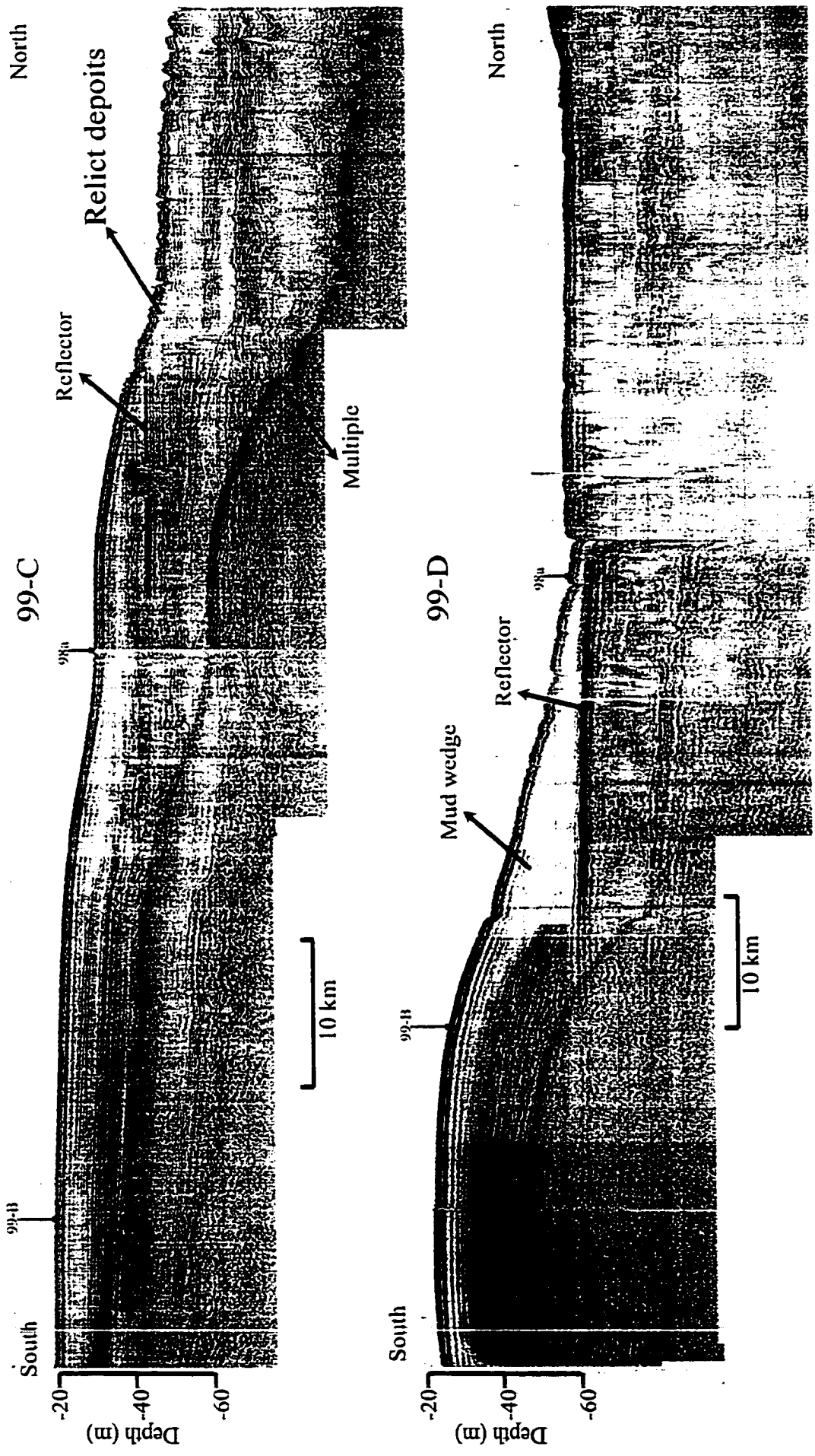


Figure 13

**Figure 14.** Gravity core of S45 reveals the apparent eolian loess deposits lying beneath “modern” muds (also see Fig. 17). This loess may reflect the lowstand LGM depositional environment. Profile 98b indicates less than 10 m Holocene sediments in the eastern part of the NYS and the Bohai Sea. Location of core is shown in Fig. 2.

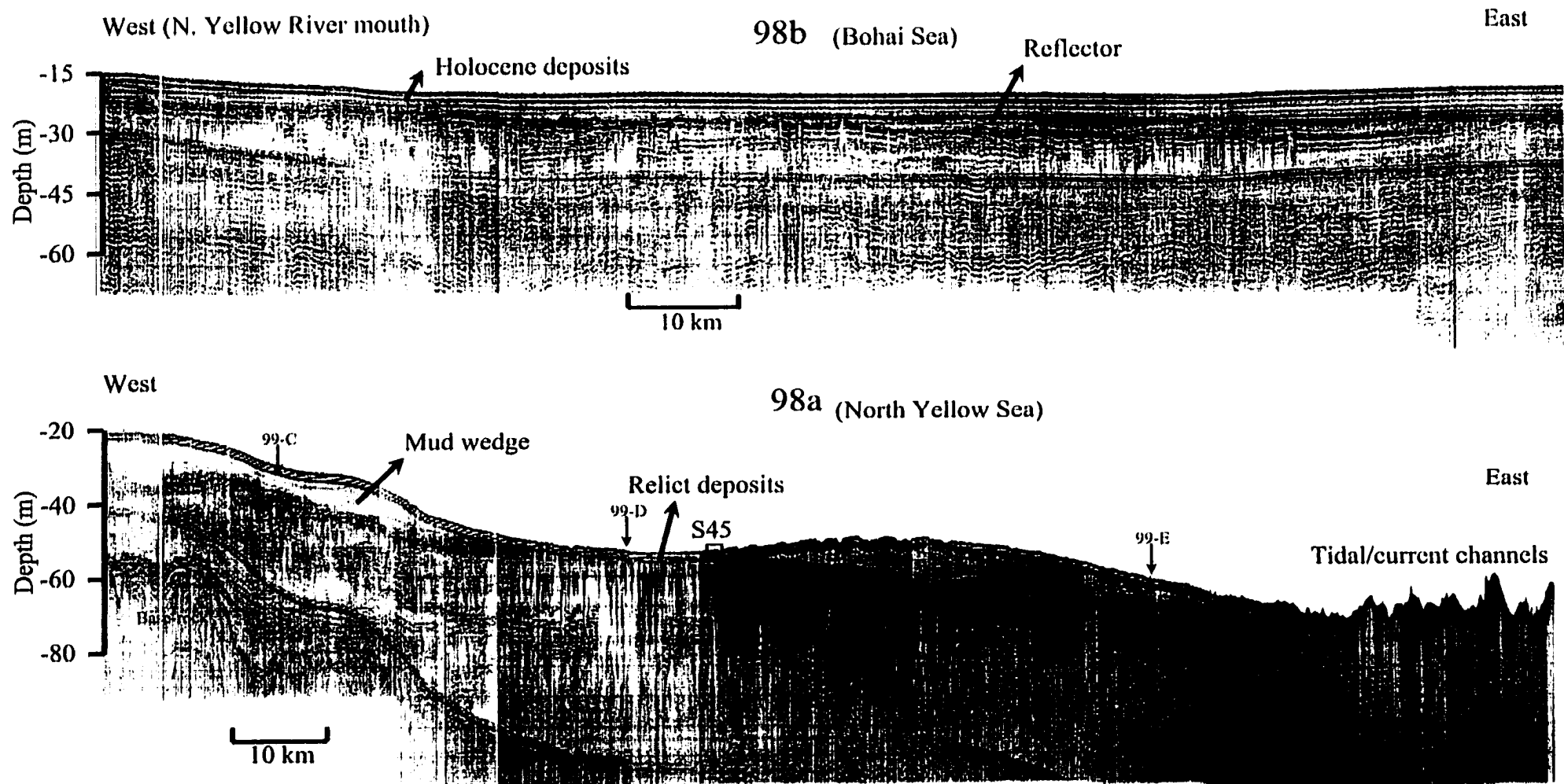


Figure 14

**Figure 15.** GeoPulse profile 84-4, extending south from the tip of Shandong Peninsula into the central South Yellow Sea, reveals the gas-charged southward-trending clinoform. Location of profile is shown in Fig. 2. 3.

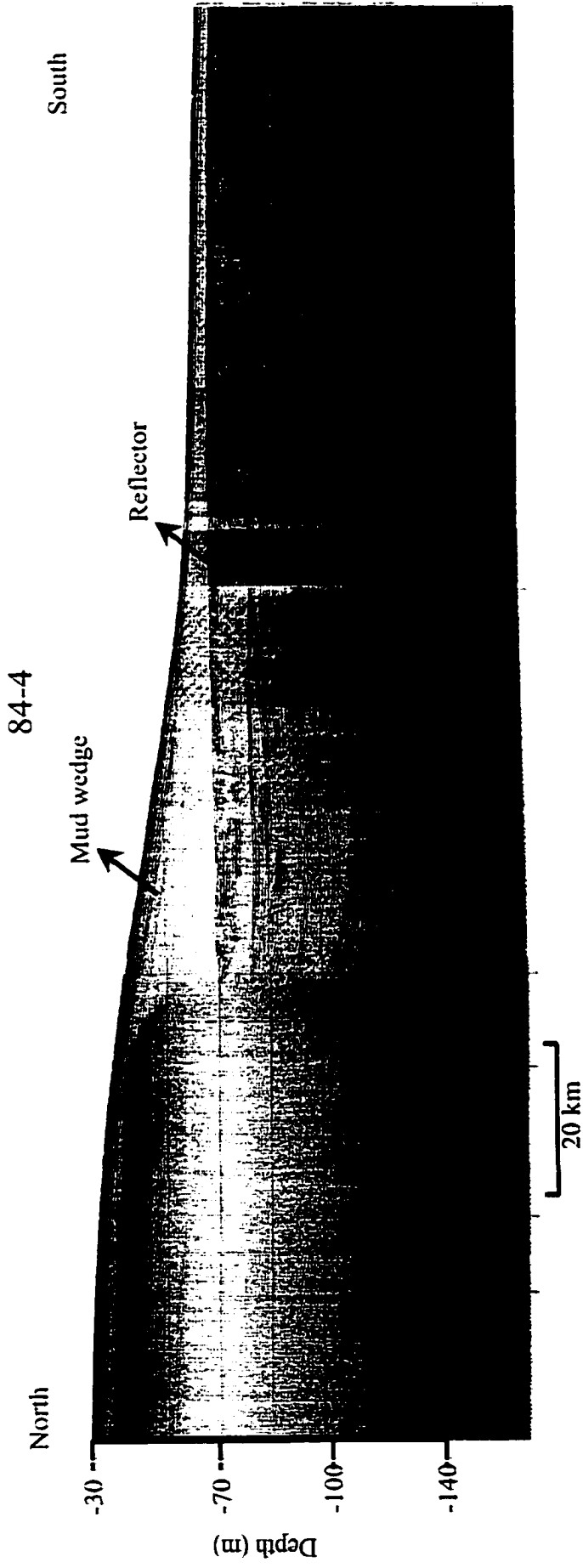


Figure 15

**Figure 16.** Distribution of grain-size and water content in the surface samples. Net sediment transport patterns can be obtained based on grain-size trend analysis (Cheng and Gao, 2000). Sample locations shown in Fig. 2

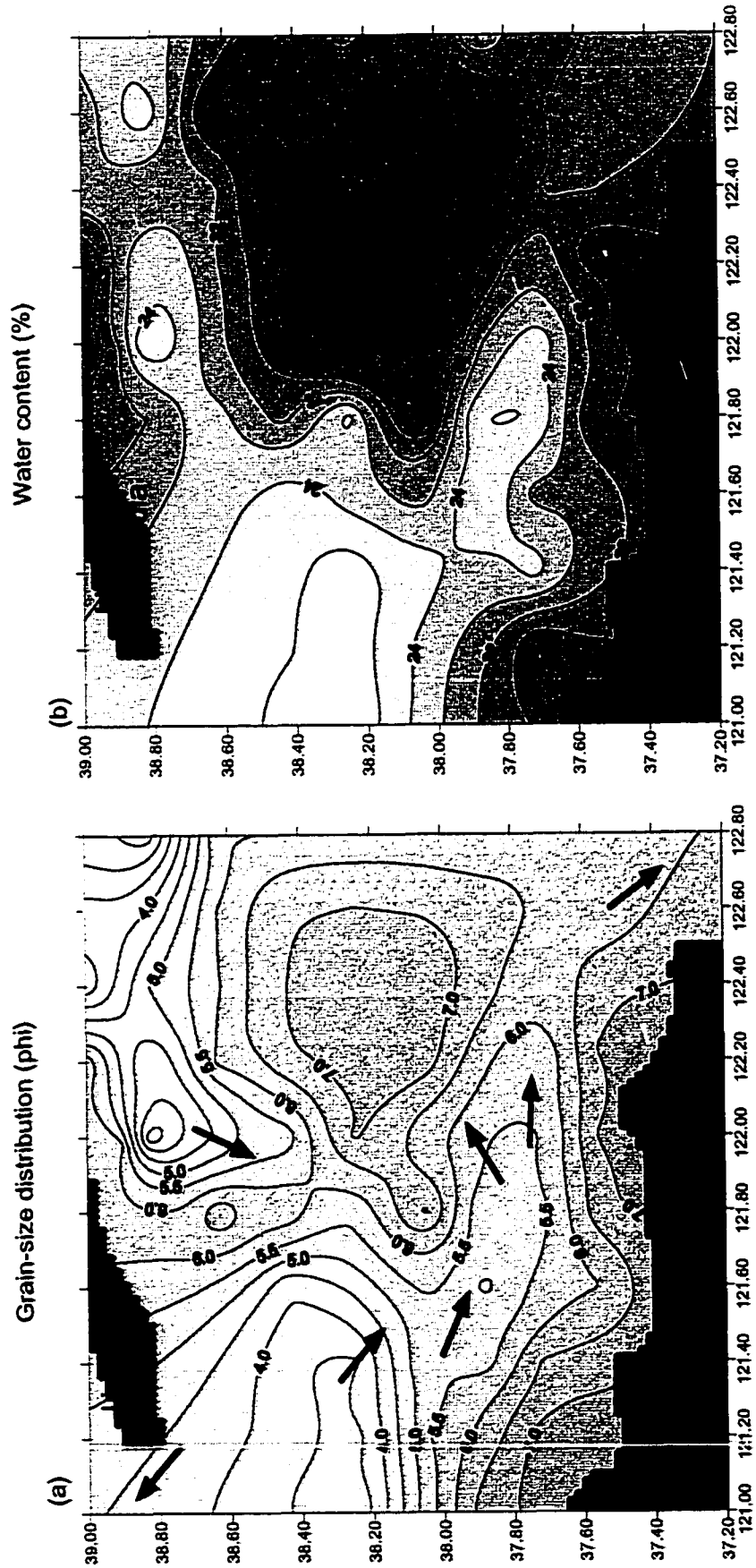


Figure 16



**Figure 17.** Stratigraphic transect through the foreset to bottomset. Thin mud (clayey-silt) was found in the offshore of central NYS, the thick mud is nearshore. The bottom of S44 and S45 shows a sandy-silt layer that represents the pre-transgressive or transgressive deposits that forms the acoustical unconformity. Core locations shown in Fig. 2.

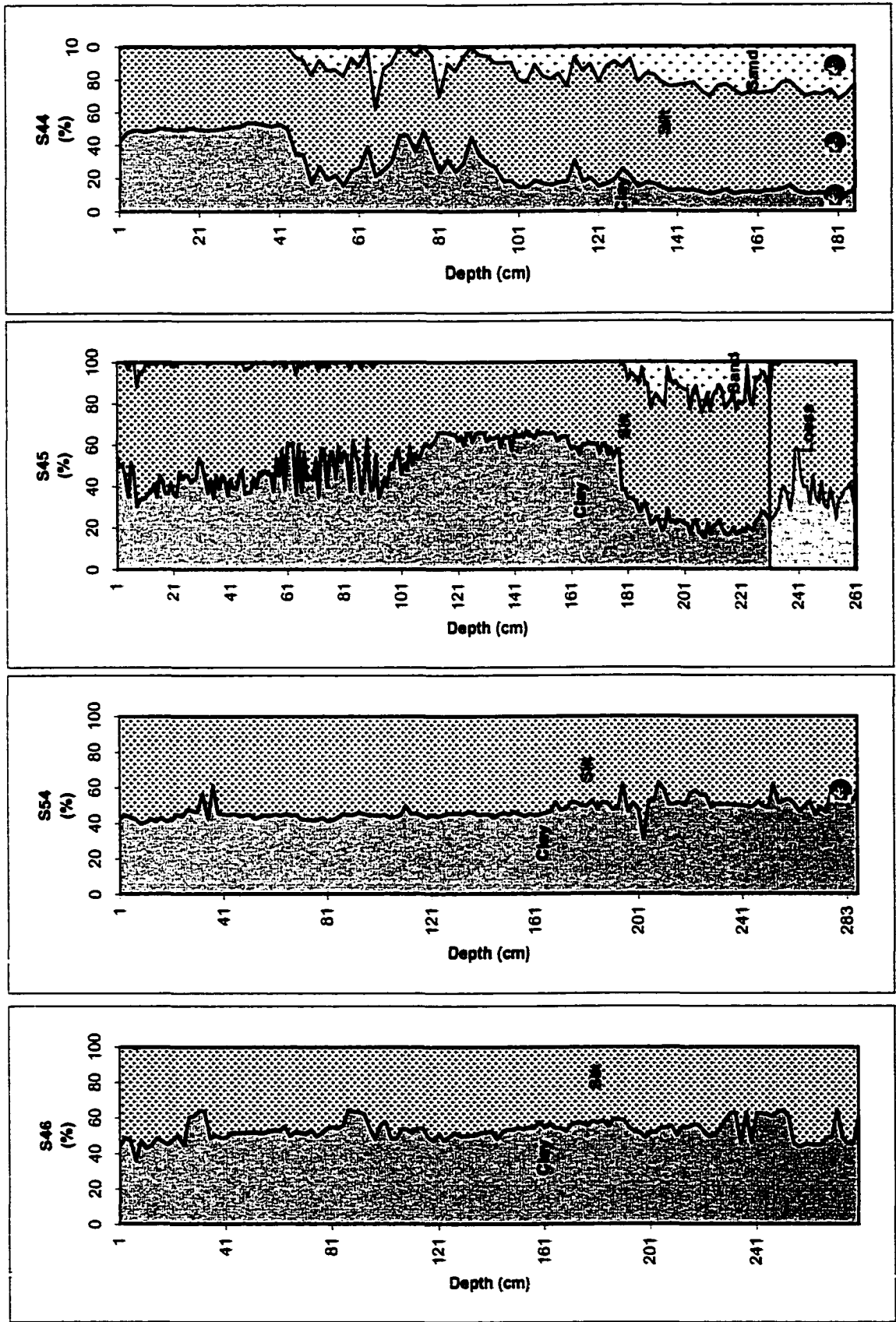


Figure 17.

**Figure 18.** Activity profile for unsupported (excess)  $^{210}\text{Pb}$  of S44, S45, S46, S54 and their linear regression plots with their estimated sedimentation rates. Core locations shown in Fig. 3.

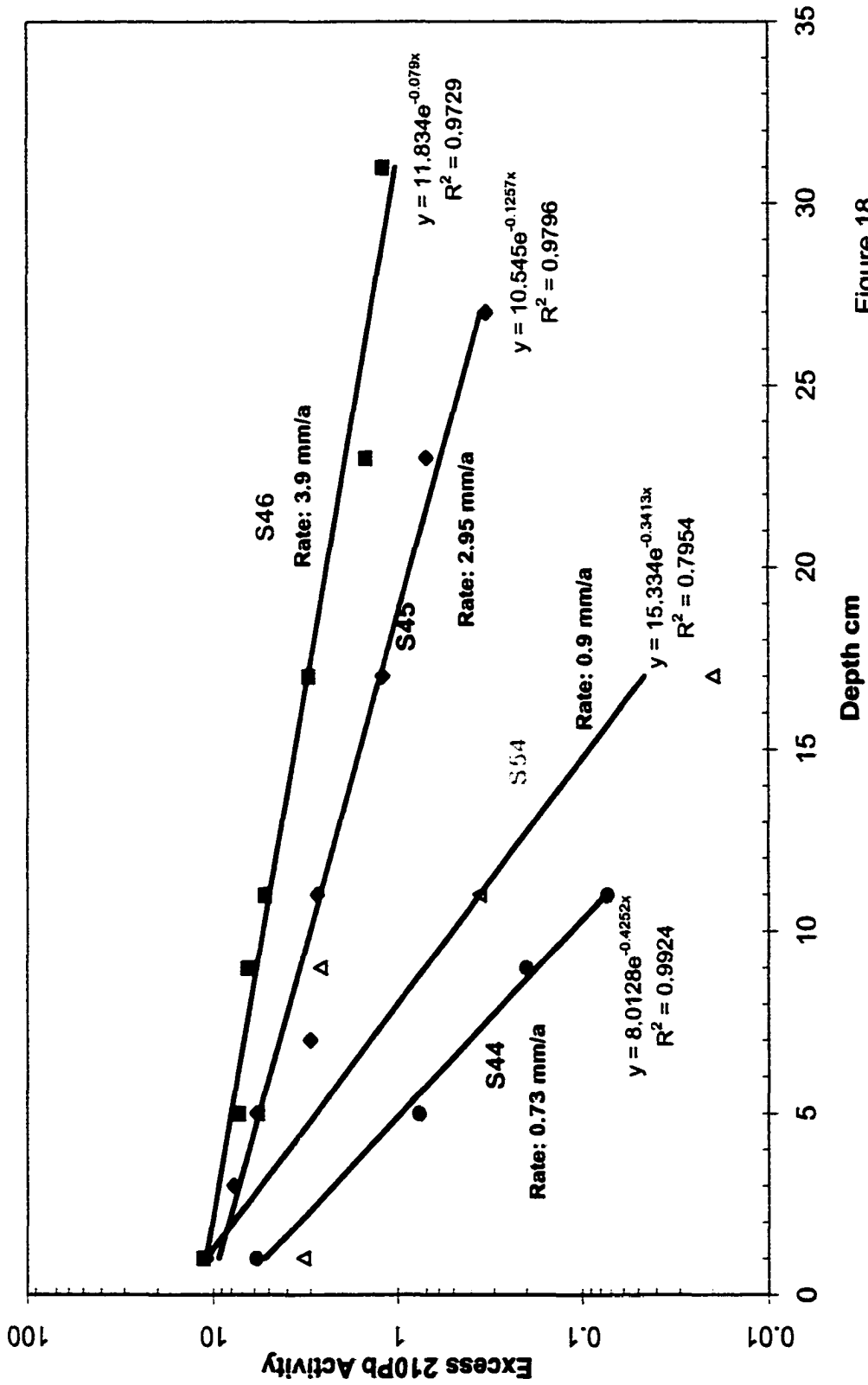


Figure 18

**Figure 19.** Activity profile for total  $^{210}\text{Pb}$  of S49 on the topset. Core locations shown in Fig. 3.

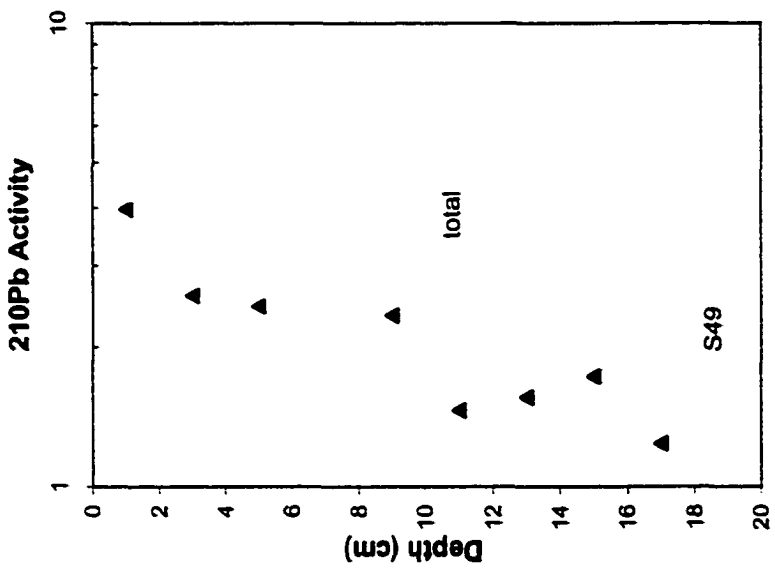


Figure 19

**Figure 20.** Sedimentary processes affecting the morphology of the Yellow River subaqueous delta in the North Yellow Sea - the progradation of the clinoform mud wedge wraps around north and south of the Shandong Peninsula.

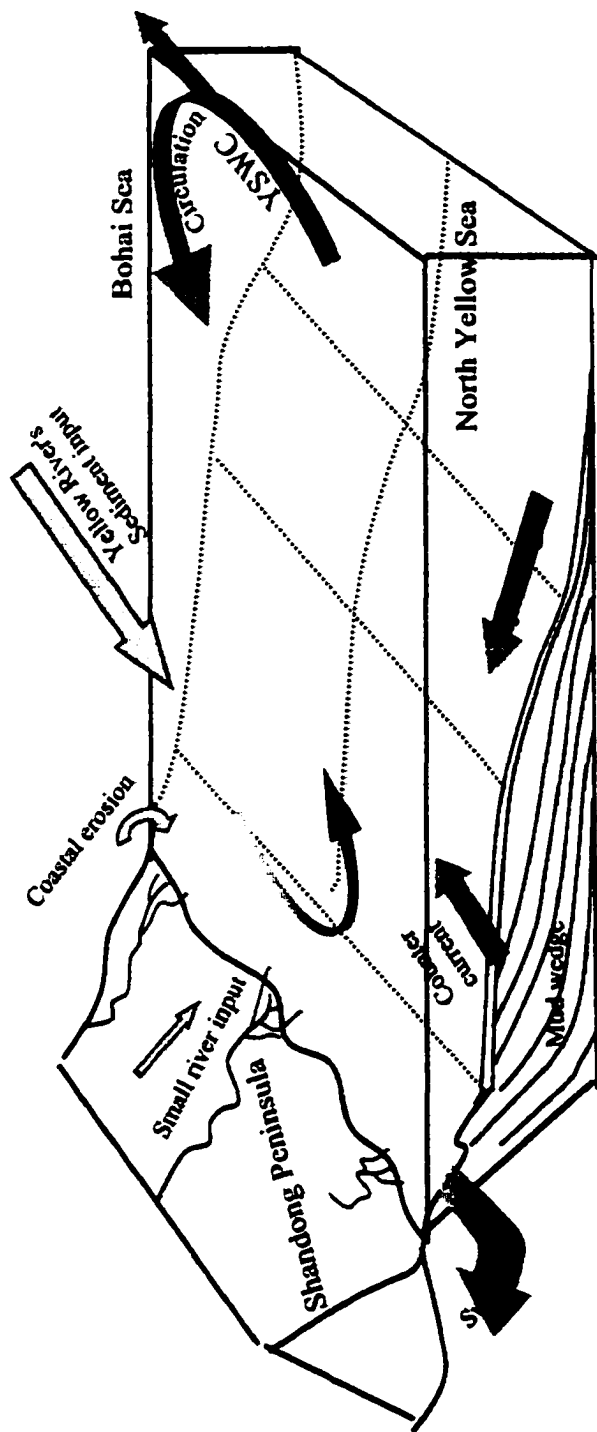


Figure 20



## **Chapter Five Conclusions:**

### **Late Quaternary sequence stratigraphy model in the epicontinental shelf**

#### **– The Yellow Sea**

##### **The post-glacial sea-level history and climatic changes**

Because of its shallow depths (nowhere deeper than 80-90 m, and generally shallower than 60 m) the Yellow Sea was entirely exposed subaerially during the last glacial maximum (LGM). Moreover, due to its generally shallow gradient (often <1:1000) and sediment input from two of the world's largest rivers, the Yangtze and Yellow rivers (Milliman and Meade, 1983), the Yellow Sea has been likely to preserve post-LGM events as sea-level transgressed and climate changed.

Perhaps the most compelling result of the present research has been our ability to delineate - with an unprecedented degree of accuracy – the timing of the post-LGM sea-level transgression in the EC/YS (Chapter 3, Liu and Milliman, submitted). In contrast to previous sea-level curves, the new curve shows that post-LGM sea level rose through a series of rapid flooding events (12-45 mm/y), separated by a series of slow rises (2-6 mm/y) (Fig.1). Said another way, during the 15 ky-interval between the LGM low-stand of sea level (22 ka) and the mid-Holocene high-stand (7 ka), sea-level in southern Asia and Australasia rose approximately 130 m, of which 85 m (65% of the total rise) occurred in just over 3 ky (20% of the time). Sea level during these rapid rise intervals may have back-stepped by as much as 40-50 m/y, whereas during the long periods of stable or slowly rising sea level, shoreline regression may have been only a few m/y.

By about 15 ka, rising sea level had reached about -100 m (relative to present-day sea level), and seawater began to enter the central SYS. A rapid rise during melt water pulse 1A (MWP-1A termed by Fairbanks, 1989) occurred between 14.7 -14.1 ka, when sea level jumped from -98 m to -74 m (40 mm/yr). At the end of this flooding event, the sea water had reached the southern edge of the NYS, after which sea level rose again slowly (6 mm/yr) from -72 m to -60 m for the next 2 ky. Beginning about 11.7 ka, sea level again jumped, from -60 m to -42 m (MWP-1B of Fairbanks), resulting in a rapid westward flooding of the NYS and initial entrance into the Bohai Sea. Sea-level rise then again stagnated (between -42m to -36 m) for about 1.8 ky. Starting about 9.8 ka, the sea-level advanced again from -36m to -16 m at 9.0 ka, in the end most of BS, YS, and ECS had been submerged. Then another slowdown occurred between 9.0-8.0 ka when sea-level rose from -16m to -10m. The last major transgression happened between 8.1 and 7.0 ka, and resulted in Holocene highstand of at least +2 to 4 m along most of Chinese coastline. The post-glacial episodic transgressive processes across the whole Yellow Sea and the derived of landmass configuration changes are shown in Fig. 2.

Superimposed on the impact of post-LGM sea-level rise was the cumulative effect of climate change, particularly on precipitation patterns in northern China and its resulting effect on discharge from the Yellow River. At present northern China has one of the lowest rates of precipitation in Asia. The only reason that the Yellow River has a relatively large freshwater discharge (mean rate of 1200 cm/s) is because it drains a very large area (750,000 km<sup>2</sup>); runoff (discharge divided by drainage basin area), however, is very low - ~50 mm/y, putting it in the classification of an "arid river" (Milliman and Farnsworth, in prep.). During the last glaciation, it is speculated that precipitation (and

therefore river discharge) in the Yellow River watershed was even less, as evidenced by the wide-spread occurrence of loess deposits under the intensified winter monsoon, of which loess formed during LGM is up to nearly 10 m in central China (An and Porter, 1997), and up to 5 m in the Bohai and North Yellow Sea regions (Liu and Zhao, 1995).

Paleoceanographic studies in the South Yellow Sea indicate that increased upwelling during the LGM reflects a strong winter monsoon circulation that dominated Eastern Asia, the summer monsoon began to pick up and reached its first maximum about 11 ka (Wang et al., 1999, ODP leg184 report), after Younger Dryas and subsequent rapid sea-level rise of MWP-1B (Fig. 1). With the intensification of the summer monsoon, precipitation also increased, increasing the discharge of other South Asian rivers such as the Indus (Prins and Postma, 2000) and Ganges-Brahmaputra (Goodbred and Kuehl, 2000). It was during this period of slow-rising sea level and increased Yellow River discharge that the first post-LGM Yellow River subaqueous delta formed in the NYS (Liu et al., 2002).

## **Evolution of the Yellow River and its deltaic depocenters on the shelf**

### **(1) Post-LGM to early-Holocene**

High-resolution seismic profiles and sea-level history didn't indicate any distinct paleo-river channels and related fluvial deposits on the shelf of Yellow Sea during sea-level lowstand of LGM. Instead, there developed the eolian loess deposits in the BS, NYS and adjacent areas (Liu and Zhao, 1995; Chapter 4) (Fig. 2a). Later, the environments in the SYS and NYS had been changed and dominated by swamps and lagoon environment before the Younger Dryas cold event, corresponds to the climatic warming and sea-level at MWP-1A (Fig. 2b). The well-preserved nature of peats and possible relict loess deposits

indicate little disturbance by a large fluvial input, and we find no evidence of buried or infilled river channel. We thus conclude that prior to the intensification of the summer monsoon about 11 ka the Yellow River was at best a minor sediment source; more likely there were periods when the river may not have flowed at all.

### **(2) Early Holocene and initiation of the Yellow River subaqueous delta**

The first Yellow River's subaqueous delta was found to form in the North Yellow Sea only when the rate of post-glacial sea-level rise slackened between -42 and -36m when the summer monsoon intensified at about 11 ka. At that time, the Yellow River was able to flow out across BS region and directly empty into the NYS (Fig. 2d, e). Total sediment of  $240 \times 10^9$  t was deposited in the NYS from the Yellow River, with a sediment accumulation rate of  $0.13 \times 10^9$  t/year (Chapter 4). However, the delta continually accepted sediment distally with a rate of  $13 \times 10^6$  t/year since 9.2 ka to the present.

### **(3) First south-shift of the river into SYS**

At about 9.2 ka. in the middle of the rapid sea-level rise event of MWP-1C, the extreme flooding event recorded in the middle reach south-shifted the river into the South Yellow Sea, offshore of Jiangsu, and built another subaqueous delta in the west of SYS in the next 2 k-yr. under the decreased sea-level rise (-16 m ~ -10m) (Chapter 2) (Fig. 2f, g). The river had deposited around  $240 \times 10^9$  t sediment in the offshore of Jiansu's subaqueous delta with an accumulation rate of  $0.16 \times 10^9$  t/year.

### **(4) North-shift back to Bohai Sea in the middle Holocene**

After 7 ka, another huge flooding event occurred at 6.95 ka might contribute to the Yellow River's north-shift back to the Bohai Sea and had accumulated at least 9 coastal deltas in the west of BS until 1.0 ka, (Fig. 2h). During this 6 k-yr, the river accumulated  $600 \times 10^9$  t sediment, with an average accumulation rate of  $0.1 \times 10^9$  t/year (Chapter 2).

#### **(5) Last south/north-shift of the Yellow River**

Beginning 1128 AD, the river south-shifted back to Jiangsu again, and left another coastal delta with a rate of  $0.43 \times 10^9$  t/year. The recent shift occurred in 1855 AD, and resulted a modern deltaic system built with a much higher accumulation rate of  $0.9 \times 10^9$  t/year, which is attributed to the human cultivation and deforestation (Chapter 2).

#### **Sequence stratigraphy model on the Yellow Sea epicontinental shelf**

The Yellow River has played a prominent role for the sedimentation on the NYS and SYS continental shelves. After reconstructing the evolution of the Yellow River and its sedimentation on the shelf (Fig. 2), we are able to test the sequence stratigraphy on an epicontinental shelf- the Yellow Sea.

Clearly, the flat and broad features of the Yellow Sea provide large accommodation during the last sea-level cycles. There are at least 1000 km horizontal distance from the paleo-coast (east of the ECS) during lowstand to the present sea-level (west of the BS). During the post-glacial transgressive processes, there are at least four elements characterized the development of depositional sequences: 1) sediment supply; 2) sea-level history; 3) accommodation space; and 4) oceanic processes. Among them, the sea-level changes has been considered as a primary control as we discussed in chapter 2-4, however, the importance of sediment supply and its flux variation may play more important role in

controlling the sediment distribution and magnitude. In the East Asia, without the impact of the prominent ice-sheets, changes of the fluvial pattern and sediment discharges have been mainly depending on the climatic forcing, together with the sea-level fluctuations (Chapter 4).

Because of the large scale of the post-glacial sea-level changes, and low-gradient of the wide shelf (huge accommodation), the Yellow Sea shelf can be defined as a transgressive epicontinental shelf (Fig. 3). In contrast with modern sequence stratigraphy models tested in the Gulf of Mexico (Boyd, 1989), sequences on an epicontinental shelf show strong landward horizontal changes, instead of the vertical changes. The regressive or lowstand system tract was partially covered by the transgressive system tract. The first major deltaic deposits was developed together with the decreased sea-level after MWP-1B event, and the intensified summer monsoon and river discharge at about 11 ka. The second subaqueous delta was built between 9-7 ka which during another slackened sea-level. The modern subaqueous and subaerial deltas formed during the sea-level highstand after the last jump of MWP-1D (Fig. 3). All system tracts are currently re-shaped under the modern oceanographic processes.

## Reference

- An, Z.S. and Porter, S.C., 1997. Millennial-scale climatic oscillations during the last interglaciation in the central China. *Geology*, 25, 603-606.
- Boyd, R., Suter, J., and Penland, S., 1989. Relation of sequence stratigraphy to modern sedimentary environments. *Geology* 17(10), 926-929
- Fairbanks, R.G. (1989) A 17,000-year glacio-eustatic sea level record: influence of glacial melting rates on the Younger Dryas event and deep ocean circulation. *Nature*, 342, 637-642.
- Goodbred, S.L., and Kuehl, S.A., 2000. The significance of large sediment supply, active tectonism, and eustasy on margin sequence development: Late Quaternary stratigraphy and evolution of the Ganges-Brahmaputra delta. *Sedimentary Geology*, 133, 227-248.
- Liu, J.P., and S.L. Zhao. 1995. Origin of the buried loess in the Bohai Sea bottom and the exposed loess along the coastal zone. *Oceanologia et Limnologia Sinica*, Vol: 26, No.4. 363-368.
- Liu, J.P., Milliman, J.D., 2001. Post-Glacial Sea-level Transgression in the East China and Yellow Seas: Significance of Periodic Rapid Flooding Events. *Science* (in review).
- Milliman, J.D., and Meade, R.H., 1983. World-wide delivery of river sediment to the oceans. *Journal of Geology*, Vol. 91, No.1, p1-21.
- Milliman, J.D. and Farnsworth, K.L., 2001, River Runoff, Erosion and Delivery to the Coastal Ocean: A Global Analysis. Oxford University Press. In press.
- ODP Leg 184 Preliminary Report, 1999. South China Sea.
- [http://www-odp.tamu.edu/publications/prelim/184\\_pre/184fig07.html](http://www-odp.tamu.edu/publications/prelim/184_pre/184fig07.html)

Prins, M.A., Postma, G., 2000. Effects of climate, sea level, and tectonics unraveled for last deglaciation turbidite records of the Arabian Sea. *Geology* 28, 375-378.

Wang, L., Samthein, M., Erlenkeuser, H., Grimalt, J., Grootes, P., Heilig, S., Ivanova, E., Kienast, M., Pelejero, C., Pflaumann, U., 1999. East Asian monsoon climate during the Late Pleistocene : high-resolution sediment records from the South China Sea. *Marine Geology* 156, 245-248.



**Figure 1.** Proposed eustatic sea-level curve based on the East Chin Sea and Yellow Sea data (Liu and Milliman, 2001). The Asian summer monsoon was intensified after rapid sea-level rise of MWP-1B (Wang, et al., 1999, ODP Leg184 Report, 1999)

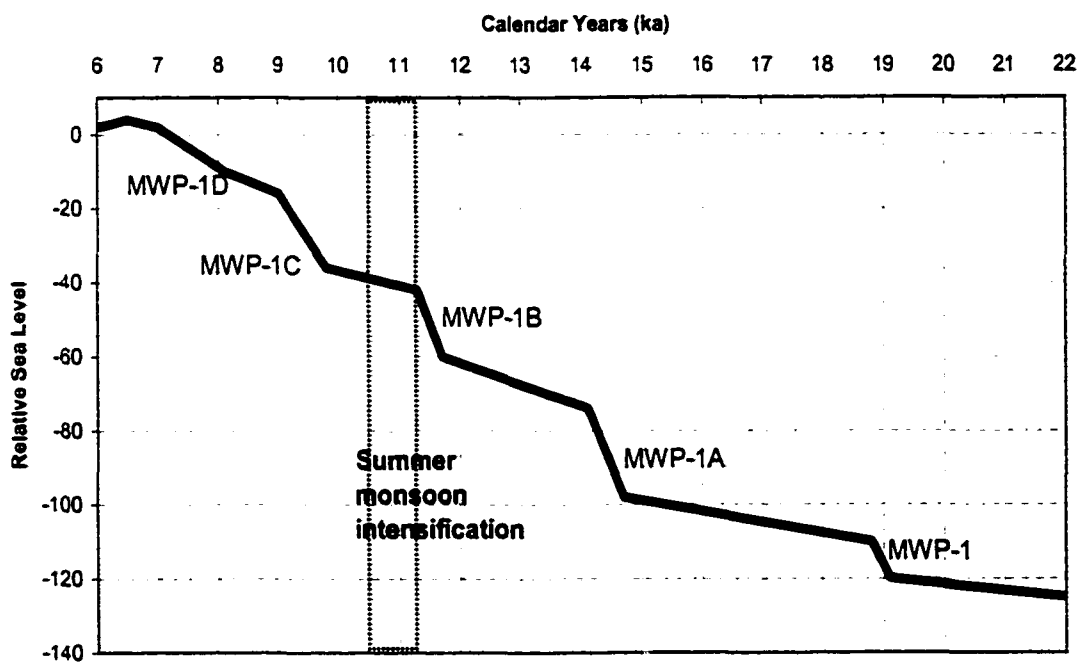


Figure 1.

**Figure 2.** Post-glacial the sea level in the Yellow Sea and the historical evolution of the Yellow River and its subaqueous deltaic deposits

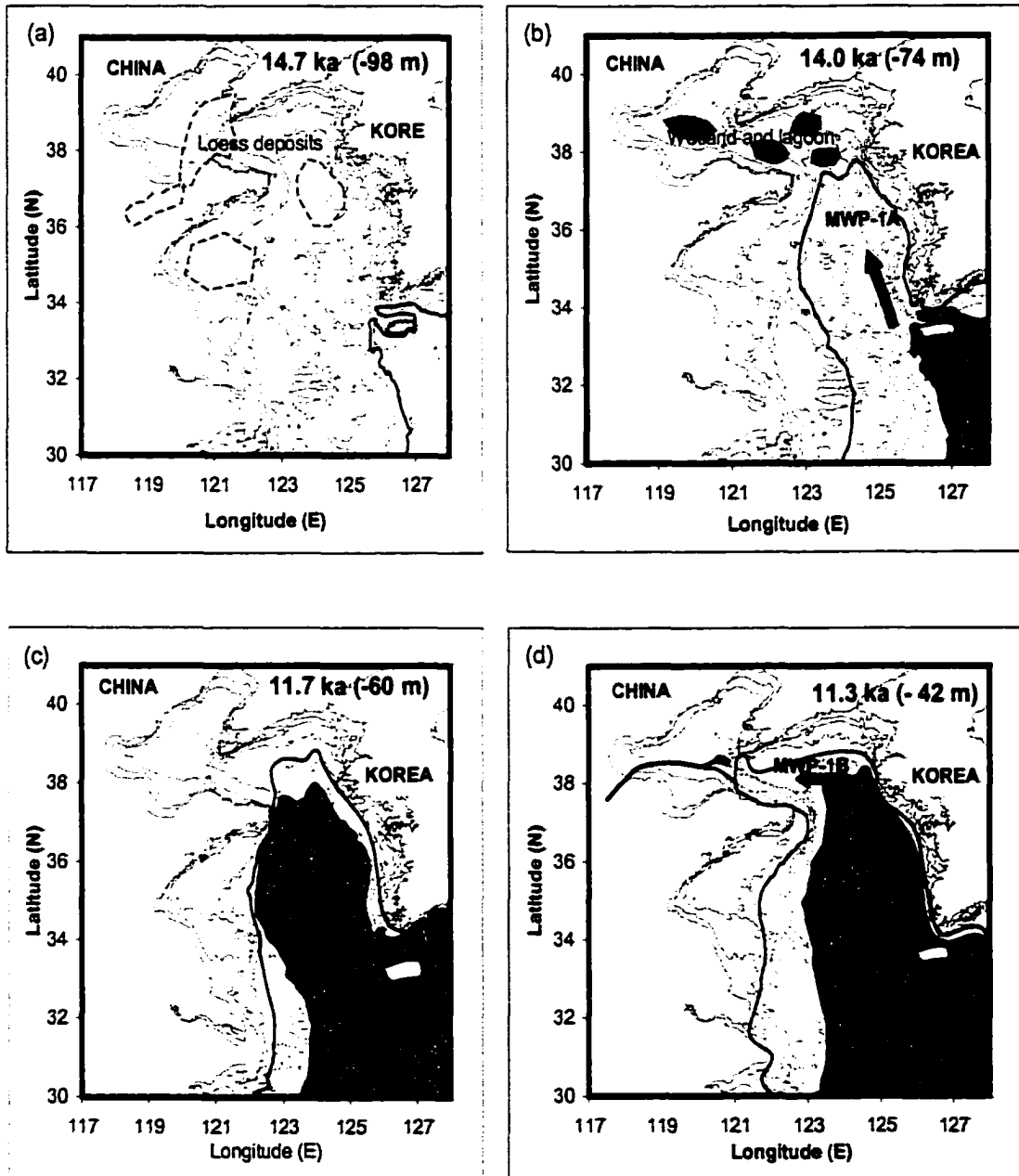


Figure 2.

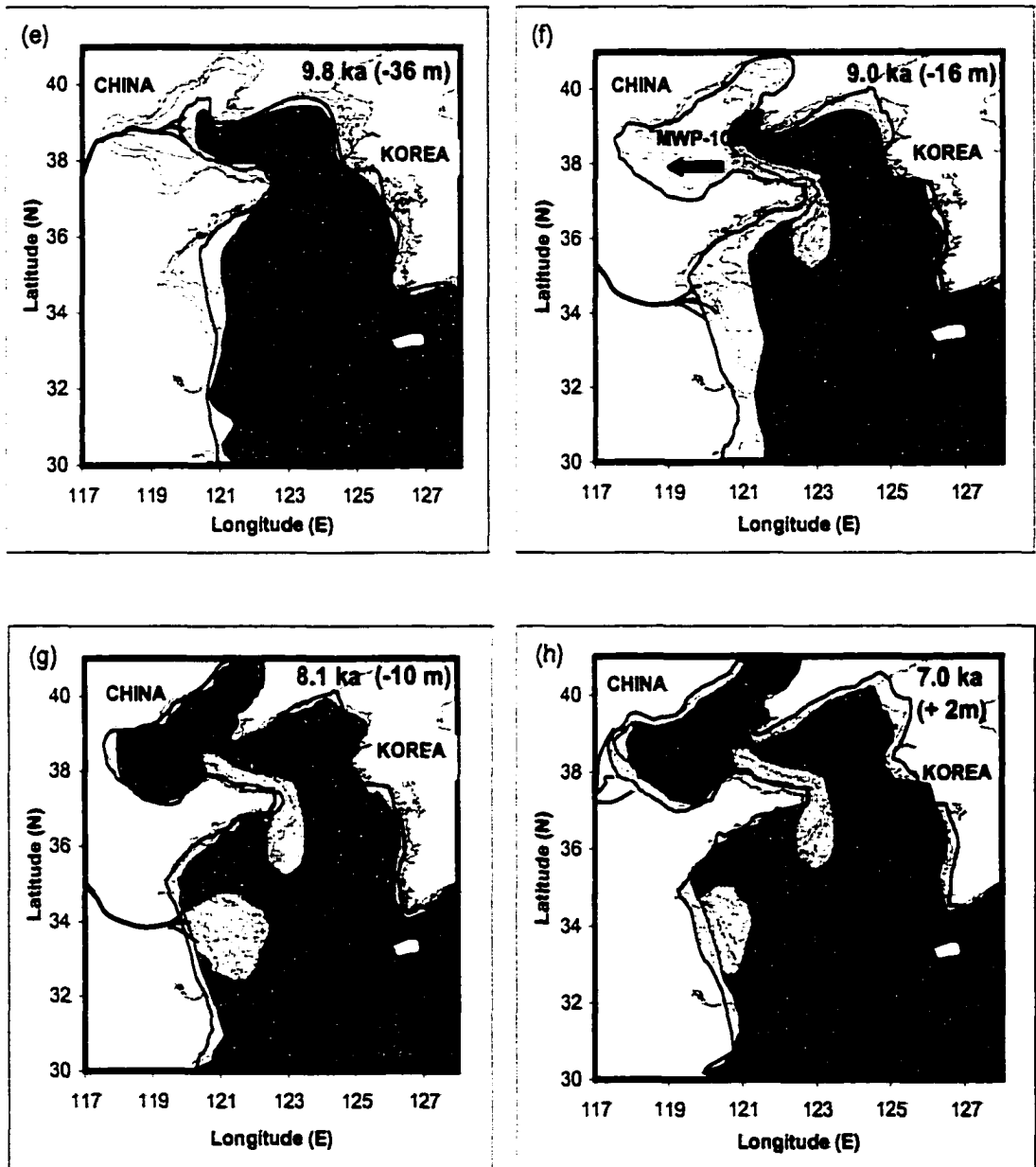
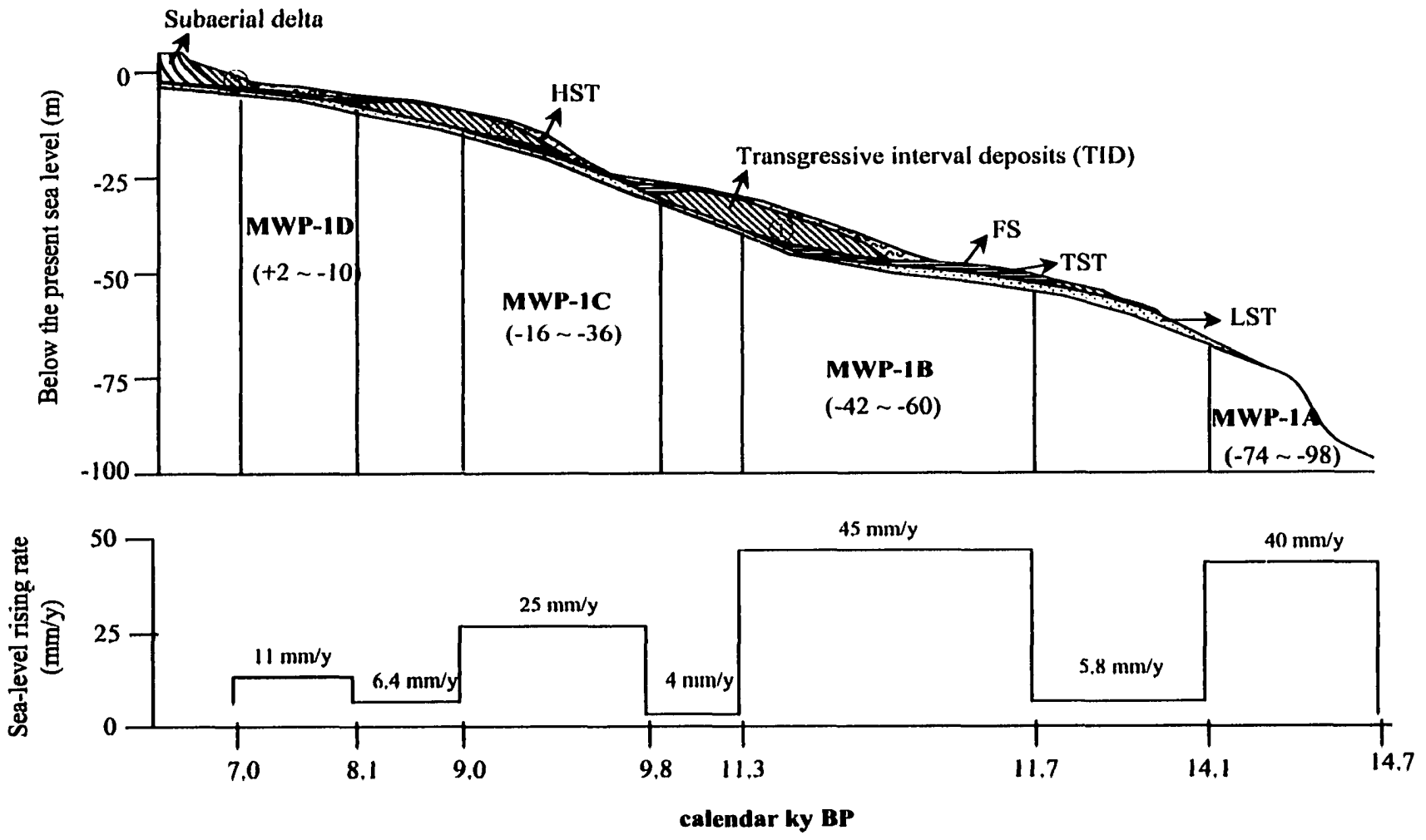


Figure 2.(Cont.)

**Figure 3.** Idealized depositional sequences on an epicontinental shelf, which corresponds to the episodic post-glacial sea-level changes in the Yellow Sea.

- (1) the first subaqueous delta formed in the NYS;
- (2) the subaqueous delta in the SYS, offshore of Jiangsu;
- (3) modern subaqueous subaerial delta in the west Bohai sea.

All of three deltaic systems seem to be formed during the decreased sea-level rise periods.



## APPENDICES





**SUPPLEMENTARY INFORMATION:** Sea-level data form East China Sea and Yellow Sea continental shelves.

Area	Cores	BPSL (m)	Sample dated	Sed. Facies	<sup>14</sup> C dating	δ <sup>13</sup> C‰	Conventional age	References	Calendar Years	1σ range	probability distribution
ECS	CM97	-26.51	<i>Bornioopsis ariakensis</i> Habe	Estuary-Shallow Marine	8400±50	-7.5	8680±50	Hori et al., 2001	9056	9112 - 8998	0.451
ECS	CM97	-37.72	Molluscan shell fragments	Brackish	9740±50	-9.0	10000±50	Hori et al., 2001	10824	10849-10617	0.710
									11033	11034-10967	0.181
									10995	11034-10967	0.181
ECS	JS98	-40.35	<i>Corbicula</i> sp.	Brackish	9510±90	-8.5	9780±90	Hori et al., 2001	10471	10639-10311	0.891
									10568	10639-10311	0.891
									10348	10639-10311	0.891
ECS	JS98	-41.26	<i>Corbicula</i> sp.	Brackish	9780±80	-9.0	10040±80	Hori et al., 2001	10834	10864-10623	0.596
									11062	11110-10956	0.404
									10984	11110-10956	0.404
ECS	JS98	-48.36	<i>Euspira</i> sp.	Brackish	10250±100	-9.2	10510±100	Hori et al., 2001	11462	11576 -11317	0.486
									11630	11732-11580	0.272
									11416	11576 -11317	0.486
ECS	HQ98	1.21	<i>Bornioopsis</i> sp.	Inter-Subtidal flat	4120±50	-7.6	4410±50	Hori et al., 2001	4540	4635-4482	1.000
ECS	HQ98	0.41	<i>Bornioopsis</i> sp.	Inter-Subtidal flat	5230±30	-9.0	5490±30	Hori et al., 2001	5883	5904-5854	1.000
ECS	HQ98	-0.24	<i>Bornioopsis</i> sp.	Inter-Subtidal	5580±60	-7.1	5870±60	Hori et al., 2001	6279	6333-6213	1.000

ECS	HQ98	-42.41	<i>Corbicula sp.</i>	flat	10250±80	-10.3	10490±80	Hori et al., 2001	11497	11552-11313	0.507
									11617	11707-11584	0.237
									11387	11552-11313	0.507
ECS	HQ98	-49.59	<i>Corbicula sp.</i>	Brackish	10250±70	-9.2	10510±70	Hori et al., 2001	11462	11559-11321	0.498
									11630	11725-11583	0.283
									11416	11559-11321	0.498
ECS	HQ98	-51.00	<i>Corbicula sp.</i>	Brackish	10150±70	-8.4	10420±70	Hori et al., 2001	11343	11508-11289	0.495
ECS	HQ98	-52.04	<i>Euspira sp.</i>	Brackish	10240±40	-10.2	10480±40	Hori et al., 2001	11511	11546-11312	0.574
									11610	11691-11587	0.223
									11378	11546-11312	0.574
ECS	KS-3	-136.00	<i>Polamocorbula amurensis</i>	Brackish	19,800±190	0.020	210±190	Suk et al, 1990	23360	23801-22920	1.000
ECS	KS-5	-98.00	<i>Modiolus diffusus</i>	0-10 SM intertidal	11,210±120	0.01	1,620±120	Suk et al, 1990	13139	13193-12933	0.867
ECS	KS-5	-103.00	<i>Pitar sulfureum</i>	flat	12,690±120	0.013	1,100±120	Suk et al, 1990	14606	14714-14341	0.504
									15233	15427-14967	0.496
									14448	14714-14341	0.504
ECS	KS-7	-80.00	<i>Anisicorbula venusta</i>	0-20 SM	10,370±150	0.010	1,780±150	Suk et al, 1990	12012	12358-11900	0.654
									12097	12358-11900	0.654
									11971	12358-11900	0.654
ECS	Z3	-64.00	<i>Macra chinensis</i>	0-10m, SM	10,000±600	0.010	1,410±600	Emery et al., 1971	11338	12348-10764	0.921

ECS	D4	-112.00	<i>Ostrea gigas</i>	Brackish	15,200±850	0.015,610±850	Emery et al., 1971	18067	19083-17050	1.000
ECS	dh3	-120.00	<i>Paphia amabilis</i>	SM	15,740±750	0.016,150±750	Liu Xiqing, 1987	18688	19593-17783	1.000
ECS	§141/C	-53.50	Shell fragments	Marine	9480±340	0.09,890±340	Shen, 1985; Yang, 1983;	10631	10884-10259	0.742
ECS	7056	-141.70	Shell fragments	Marine	17600±800	0.018010±800	Shen, 1985	20829	21804-19854	1.000
ECS	7087	-98.50	Shell fragments	Marine	13200±750	0.013610±750	Shen, 1985	15761	16531-14940	0.787
ECS	7287/L	-100.30	<i>Ostrea gigas</i>	Brackish	14,440±750	0.014,850±750	Shen, 1985;	17192	17811-16274	1.000
ECS	D	-53.60	Shell fragments	Marine	9,170±340	0.09,580±340	Yang, 1983	10294	10653-9839	0.926
ECS	E	-61.00	Shell fragments	Marine	8,640±800	0.09,050±800	Yang, 1983	9673	10636-8694	0.997
								9779	10636-8694	0.997
								9644	10636-8694	0.997
ECS	Yang	-83.00	not specified	Marine	10,400±300	0.010,810±300	Yang, et al., 1998	12121	12645-11647	0.961
								12238	12645-11647	0.961
								12285	12645-11647	0.961
ECS	Han3	-64.00	<i>Macra chinensis</i>	0-10m, SM	10,000±600	0.010,410±600	Han et al., 1987	11338	12348-10746	0.921
ECS	F28	-12.10	Organic mud	Brackish	7,820±270	-6.08,140±270	Li, et al., 2000	8593	8894-8357	1.000
ECS	F5	-16.50	Organic mud	Brackish	7,950±255	-6.08,260±255	Li, et al., 2000	8785	8961-8442	1.000
ECS	F23	-11.30	Organic mud	Brackish	7,400±400	-6.07,720±400	Li, et al., 2000	8167	8776-7776	1.000
SYS	CC-02	-79.20	Foraminifera(mixed)	shallow marine		-2.89,840±200	Kim and Kucera, 2000	10599	10830-10313	0.985
SYS	CC-02	-80.25	<i>Ammonia Beccarii</i>	shallow marine		-3.511,340±80	Kim and Kennett, 1998	12903	13003-12820	0.856
SYS	CC-04	-83.70	Foraminifera(mixed)	shallow marine		-3.010,670±80	Kim and Kucera, 2000	11826	12143-11636	0.923

										11912	12143-11636	0.923	
										11740	12143-11636	0.923	
SYS	CC-04	-84.10	Foraminifera(mixed)	shallow marine						Kim and Kucera, 2000	10307	10366-10225	0.509
				shallow marine									
SYS	CC-04	-84.40	Foraminifera	shallow marine						Kim and Kucera, 2000	12802	12861-12716	0.436
											12733	12861-12716	0.436
											12652	12681-12616	0.208
SYS	CC-04	-84.60	Shell fragments	shallow marine						Kim and Kucera, 2000	13106	13156-12964	1.000
											13113	13156-12964	1.000
											13021	13156-12964	1.000
SYS	CC-04	-85.10	Shell fragments	Brackish						Kim and Kucera, 2000	14217	14363-14087	0.619
											14251	14363-14087	0.619
											14155	14363-14087	0.619
SYS	DH4-1	-2.30	Gastropod shell	Brackish						Kim and Kennett, 1998	4563	4694-4482	1.000
SYS	DH4-1	-2.80	Oyster shell	Brackish						Kim and Kennett, 1998	7252	7374-7153	1.000
SYS	YSDP103	-80.00	Foraminifera	intertidal	11,780±120					Jin and Chough, 1998	13689	13707-13460	0.778
											13796	13839-13749	0.222
											13535	13707-13460	0.778
SYS	YSDP103	-78.00	Foraminifera	shallow marine	12,080±1850					Li, et al., 1997, Park, et al. 2000	14045	16524-11890	0.978
											13927	16524-11890	0.978
											13856	16524-11890	0.978

SYS	YSDP105	-53.00	Biogenic Sample	Marine	9,900±1810	-0.2	10,300±1810	Chang et al., 1996	11163	13448-9024	1.000
SYS	YSDP105	-74.45	Carbon Particle	Intertidal	12,410±800	-0.2	12,810±800	Liu, et al., 1997	14299	15629-13774	0.915
SYS	84-B-03	-132.3	<i>Megacardita koreana</i>	Inter-Subtidal	15,030±150	0.0	15,440±150	Yoo and Park, 1997	17871	18180-17561	1.000
SYS	M2	-121.14	Shell fragments	Marine	16,330±250	0.0	16,740±250	Park, et al., 2000	19367	19776-18958	1.000
SYS	QC1	-33.23	not specified	Marine	7,760±445	-5.08	110±445	Zheng, 1991	8573	9007-8095	0.993
SYS	QC2	-64.07	not specified	shallow marine	9,910±100	-6.3	10,210±100	Zheng, 1991	11132	11333-11030	0.645
SYS	QC2	-66.08	not specified	Salty marsh	10,340±110	-5.0	10,690±110	Zheng, 1991	11925	12179-11638	0.860
									11816	12179-11638	0.860
									11749	12179-11638	0.860
SYS	I180-11	-73.00	Shell mud	Marine	10,440±320	-1.0	10,840±320	Liu, et al., 1987.	12164	12656-11659	0.943
									12219	12656-11659	0.943
									12308	12656-11659	0.943
SYS	I180-11	-74.30	Shell mud	Marine	11,560±270	-1.0	11,960±270	Liu, et al., 1987.	13442	13607-13157	0.809
SYS	I180-11	-74.30	Shell and <i>Ammonia Beccarii</i>	Brackish	12,090±270	-1.0	12,490±270	Liu, et al., 1987.	13893	14345-13469	1.000
									14062	14345-13469	1.000
									13879	14345-13469	1.000
SYS	I180-13	-71.00	Silty mud	Marine	11,040±1400	-1.0	11,440±1400	Liu, et al., 1987.	12977	14364-10792	0.964
SYS	I180-14	-73.90	Silty Mud	shallow marine	12,260±700	-1.0	12,660±700	Liu, et al., 1987.	14119	15376-13748	0.886

SYS g7	0.50Shell		Marine	809±94	-2.61211±94	Geng, et al, 1987.	737841-668	1.000
SYS g8	-0.50Shell		Marine	1,420±170	-2.61,822±170	Geng, et al, 1987.	13471555-1202	1.000
SYS g11	0.00Shelly sand		Marine	1,485±75	-2.61,887±75	Geng, et al, 1987.	14151508-1351	1.000
SYS g12	0.00Shell		Marine	2,532±75	-2.62,934±75	Geng, et al, 1987.	20062785-2608	1.000
SYS g20	1.50Shell		Marine	5,060±90	-2.65,462±90	Geng, et al, 1987.	58625916-5726	1.000
SYS g21	3.00Shell		Marine	5,205±75	-2.65,607±75	Geng, et al, 1987.	59786081-5913	1.000
SYS HJ-03	0.07Crassostrea		Brackish	1,925±58	-1.22,325±58	Kim, Y.H. et al, 1999	19301996-1868	1.000
SYS HJ-23	-2.08Osireadae unid. Sp		Brackish	1,515±86	-1.21,915±86	Kim, Y.H. et al, 1999	14711545-1358	1.000
SYS HJ-31	-2.37Crassostrea gigas		Brackish	1,128±58	-1.21,528±58	Kim, Y.H. et al, 1999	10661145-1012	1.000
NYS H80-17	-75.00Shell mud		shallow marine	10,600±200	-1.011,000±200	Liu, et al, 1987.	1247212688-12265	0.629
							1262312688-12265	0.629
							1239212688-12265	0.629
NYS H80-18	-72.00Osirea rivularis		Brackish	10,380±100	-1.010,780±100	Liu, et al, 1987.	1209712340-11906	0.776
							1201212340-11906	0.776
							1197112340-11906	0.776
NYS H80-18	-72.00Osirea gigas		Brackish	10,390±100	-1.010,790±100	Liu, et al, 1987.	1210512347-11908	0.775
							1200112347-11908	0.775
							1197912347-11908	0.775

NYS	H77-31	-77.00	<i>Molitis sp.</i>	Estuary - Intertidal flat	10,980±150	-1.011,380±150		Jiu, et al, 1987.	1292313046-12822	0.782
NYS	H19	1.50	Shell buried by lagoon-swamp	Brackish	4,345±85	-2.64,747±85		Geng, et al, 1987.	49715083-4854	0.940
BS	HK20	-13.00		Marine	7,920±655	-2.68,322±655		Han et al, 1987.	88589603-8133	1.000
BS	H3	-18.13	Shell fragments	Marine	7,340±50	-3.47,690±50		Zhuang, 1999	81508187-8056	1.000
BS	H3	-19.13	Shell fragments	Brackish	8,570±50	-9.48,830±50		Zhuang, 1999	91899249-9080	0.502
									91409249-9080	0.502
									94229478-9287	0.494
BS	CD05	-33.65	Marine Organic mud	shallow marine	8,350±150	-2.08,750±150		Wang Minglian, 2000	92409453-9015	1.000
									93729453-9015	1.000
									90939453-9015	1.000
BS	C05	-36.20	Lagoon mud	Brackish	8,650±100	-2.09,050±100		Wang Minglian, 2000	96739824-9579	0.733
									97799824-9579	0.733
									96449824-9579	0.733
BS	H9602	-17.14	Shell fragments	Marine	8,440±60	-7.88,720±60		Saito et al, 2000	90779131-9023	0.367
BS	H9602	-17.41	<i>Corbicula leana</i> Prime	estuary	8,280±40	-9.68,540±40		Saito et al, 2000	89819050-8914	1.000
BS	H9602	-17.53	<i>Littoraria coccinea</i>	Brackish	8,280±60	-8.78,550±60		Saito et al, 2000	89869056-8909	0.945
BS	H2	-0.50	Oyster Chenier	Brackish	520±85	-2.6922±85		Geng, et al, 1987.	519601-474	1.000
BS	H4	-0.50	Oyster Chenier	Brackish	770±75	-2.61172±75		Geng, et al, 1987.	702781-650	1.000



BS	g13	2.00	Oyster Chenier	Brackish	2,888±80	-2,63,390±80	Geng, et al, 1987.	32583347-3158	1,000
BS	g14	2.00	Oyster Chenier	Brackish	3,495±115	-2,63,897±115	Geng, et al, 1987.	38584006-3696	1,000
BS	Xiyoul	0.50	Shell Chenier	Brackish	3,815±130	-2,64,217±130	Geng, et al.; Han et al, 1987;	43074477-4126	1,000
BS	CJZ	2.00	Shell	Marine	5,680±110	-2,66,082±110	Geng, et al.; Han et al, 1987;	64906627-6392	1,000
BS	Xiyoul2	-1.50	Shell	Marine	5,800±120	-2,66,202±120	Geng, et al.; Han et al, 1987;	66426763-6488	1,000
BS	g26	2.00	Shell	Marine	6,100±80	-2,66,502±80	Geng, et al, 1987.	69907094-6894	0.962

Area	Cores	BPSL (m)	14-C (a BP)	Sample dated	Sed. Facies	References	Cal. Yrs	1σ range	probability distribution
ECS	5137B	-62.10	12,140±750	Peat	Terristrial	Shen, 1985; Yang, 1983	14112	15419 - 13450	1,000
ECS	K	-102.50	15000±750	Peat	Terristrial	Yang, 1983	17940	18846 - 17034	1,000
ECS	1YC1	-47.00	11,510±570	Mud	Terristrial	Qin, et al, 1987	13459	14286 - 12866	1,000
ECS	1YC2	-43.20	11520±690	Peat	Terristrial	Qin, et al, 1987	13463	14353 - 12802	0.894
ECS	1YC2	-59.40	10,250±130	Peat	Terristrial	Qin, et al, 1987	12052	12233-11689	0.977
							12055	12233-11689	0.977
							11955	12233-11689	0.977
ECS	Ch1	-43.90	12,990±400	Mud	Terristrial	Qin, et al, 1987	15619	16173-15135	0.797
ECS	Ch1	-60.10	10,700±125	Peat	Terristrial	Qin, et al, 1987	12839	12936-12626	0.906
ECS	Ch1	-72.40	18,740±650	Mud	Terristrial	Qin, et al, 1987	22244	23064-21424	1,000
ECS	Ch2	-27.60	10,700±270	Mud	Terristrial	Qin, et al, 1987	12839	13018-12312	0.965
ECS	Ch3	-62.30	10,475±300	Mud	Terristrial	Qin, et al, 1987	12372	12861-11939	0.982



SYS	YSDP103	-82.87	13,990±1290	Carbon Particle	Terristrial/tidal	Li, et al., 1997	16778	18377-15228	0.966
SYS	YSDP104	-57.75	13,970±1580	Carbon Particle	Terristrial/tidal	Li, et al., 1997	16755	18496-14986	0.907
SYS	YSDP105	-84.30	18,070±1090	Carbon Particle	Terristrial	Liu, et al., 1997	21473	22761-20184	1.000
SYS	Q2169	-74.63	18,280±970	not specified	Terristrial	Lan and Shen, 2000	21715	223874-20555	1.000
SYS	Q2C	-68.97	11,100±260	not specified	Terristrial	Yang, et al., 1996	13132	13399-12895	1.000
SYS	Q2C4	-13.15	10,080±95	not specified	Terristrial	Zheng, 1991	11633	11754-11540	0.492
							11612	11754-11540	0.492
							11575	11754-11540	0.492
SYS	H408	-67.60	14,100±810	Mud	Terristrial	Yang, et al., 1996	16905	17927-15881	1.000
SYS	H2-II	-81.70	14,380±400		Terristrial	Meng, et al., 1998	17227	17743-16710	1.000
SYS	H106	-76.95	19,035±694	not specified	Terristrial	Qin, et al., 1989	22583	23444-21722	1.000
SYS	H136	-53.14	12,000±570	HARD CLAY	Terristrial	Qin, et al., 1989	14065	14441-13416	0.699
SYS	H136	-53.15	11,400±570	not specified	Terristrial	Qin, et al., 1989	13411	14135-12800	0.968
SYS	H136	-55.00	14,400±720	not specified	Terristrial	Qin, et al., 1989	17250	18136-16364	1.000
SYS	H148	-31.20	17,310±540	not specified	Terristrial	Qin, et al., 1989	20598	21294-19903	1.000
SYS	Y9	-13.50	10,800±140	Peat	Terristrial	Qin, et al., 1989	12889	13009-12789	0.740
SYS	J1	-13.00	11,000±1000	lake bog	Terristrial	Han, 1987	12999	14070-11388	0.995
SYS	J2	-21.15	11,000±1000	Peat	Terristrial	Geng, et al., 1987	12999	14070-11388	0.995
SYS	ZQ2005	-1.006	9,55±100	Lagoon mud	Terristrial	Mu, 1984	7757	7848-7681	0.952
							7773	7848-7681	0.952
							7786	7848-7681	0.952
SYS	SW07	-3.497	0,32±98	Woods	Terristrial	Kim, Y.H. et al. 1999	7842	7940-7778	0.905
							7903	7940-7778	0.905
							7913	7940-7778	0.905

SYS	P1	1.00	4,157±67	Peat	Terristrial	Kim, Y.H. et al. 1999	4671	4741-4612	0.655
SYS	P2	0.30	5,470±100	Peat	Terristrial	Kim, Y.H. et al. 1999	6284	6350-6175	0.855
SYS	D1	-3.63	7,270±270	Peat	Terristrial	Kim, Y.H. et al. 1999	8090	8349-7839	1.000
							8107	8349-7839	1.000
							8035	8349-7839	1.000
SYS	D2	-2.96	6,910±450	Peat	Terristrial	Kim, Y.H. et al. 1999	7719	8185-7320	1.000
							7709	8185-7320	1.000
							7698	8185-7320	1.000
NYS	H177-8	-56.85	12,050±200	Peat	Terristrial	Geng, et al, 1987	14083	14340-13801	0.812
NYS	H177-8	-59.85	12,400±200	Peat	Terristrial	Geng, et al, 1987	14336	15030-14110	1.000
NYS	H180-18	-72.00	18,500±600	Clayey-silt	Terristrial	Liu, et al, 1987.	21968	22738-21198	1.000
NYS	H180-23	-56.70	11,690±300	Peat	Terristrial	Liu, et al, 1987.	13680	14070-13338	0.981
							13797	14070-13338	0.981
							13544	14070-13338	0.981
NYS	H180-23	-57.00	14,130±140	Silty mud	Terristrial	Liu, et al, 1987.	16939	17220-16658	1.000
NYS	H180-23	-57.80	14,400±150	Shell mud	Terristrial	Liu, et al, 1987.	17250	17545-16955	1.000
NYS	g31	0.50	1,450±135	Peat	Terristrial	Geng, et al, 1987.	1316	1518-1263	1.000
NYS	g42	1.50	6,050±150	Peat	Terristrial	Geng, et al, 1987.	6889	7029-6728	0.846
							6816	7029-6728	0.846
							6811	7029-6728	0.846
NYS	g49	-22.00	9,295±170	Swamp mud	Terristrial	Geng, et al, 1987.	10437	10645-10242	0.923
							10496	10645-10242	0.923
							10432	10645-10242	0.923
BS	BC-1	-40.00	13,490±150	mud	Terristrial	Qin, et al, 1984	16203	16498-15906	1.000
BS	BC-1	-40.00	15,145±610	mud	Terristrial	Qin, et al, 1984	18107	18415-17799	1.000
BS	g62	-49.40	11,570±140	Lamprotula	Terristrial	Geng, et al, 1987.	13480	13811-13404	1.000

BS	#46	-15,608,620±140	Peat	Terristrial	Geng, et al, 1987.	95489781-9484	0.916
BS	#47	-25,009,080±345	Peat	Terristrial	Geng, et al, 1987.	1022210594-9706	0.974
BS	#48	-30,009,165±155	Peat	Terristrial	Geng, et al, 1987.	1035610555-10189	1.000
						1035110555-10189	1.000
						1024310555-10189	1.000
BS	#15	-16,008,830±130	Peat	Terristrial	Han et al, 1987.	98939967-9714	0.652
						98979967-9714	0.652
						99099967-9714	0.652
BS	#15	-16,709,405±120	Peat	Terristrial	Han et al, 1987.	1021610288-10139	0.500
BS	#3	-21,138,340±120	Salt peat	Terristrial	Zhuang, 1999	94019486-9251	0.905
BS	#12	-30,009,165±100	Organic mud	Terristrial	Geng, et al., 1982.	1035110419-10224	0.960
						1035610419-10224	0.960
						1024310419-10224	0.960
BS	#D05	-40,8515,300±200	Trishoptia pallens Jacobi	Terristrial	Wang Mingtian, 2000	1828518639-17932	1.000
BS	#19602	-19,3311,980±70	Logoon mud	Terristrial	Saito et al, 2000	1428414387-14101	0.623
BS	#30	2,50840±65	Peat	Terristrial	Geng, et al, 1987.	734792-680	0.892
BS	#39	7,005,030±120	Peat	Terristrial	Geng, et al, 1987.	57465896-5660	1.000
						58325896-5660	1.000
						58375896-5660	1.000
BS	#44	-9,457,780±170	Peat	Terristrial	Geng, et al, 1987.	85868775-8395	0.927
						85728775-8395	0.927
						85438775-8395	0.927
SYS	#45	-14,008,460±300	Peat	Terristrial	Geng, et al, 1987.	94889777-9055	0.939
BS	#50	-21,709,645±120	Peat	Terristrial	Geng, et al, 1987.	1111310960-10761	0.594
BS	#51	-27,0010,095±110	Swamp mud	Terristrial	Geng, et al, 1987.	1164011766-11541	0.466

							11685	11766-11541	0.466
							11584	11766-11541	0.466
BS	NPH	-12.90	8,590±190	Peat	Terristrial	Qin, et al., 1984	9544	9897-9423	0.973
NYS	NYS-3	-50.70	10,700±55	Peat	Terristrial	this study	12839	12904-12786	0.575
NYS	NYS-5	59.00	10,200±60	Peat	Terristrial	this study	11804	11980-11691	0.792
							11930	11980-11691	0.792
							11768	11980-11691	0.792
BS	CG71	-15.85	10,300±200	Peat	Terristrial	Li, et al., 1995.	12246	12380-11690	0.825
							12273	12380-11690	0.825
							12110	12380-11690	0.825
BS	CG256	-18.85	8,645±130	Peat	Terristrial	Li, et al., 1995.	9552	9786-9523	0.863
BS	ZK218	-18.90	8,870±105	Peat	Terristrial	Cheng, et al., 1987	10022	10167-9881	0.845
							10109	10167-9881	0.845
							9918	10167-9881	0.845
BS	ZK224	-25.90	11,600±400	Peat	Terristrial	Cheng, et al., 1987	13492	14071-13152	1.000
BS	ZK228	-17.60	8,835±100	Peat	Terristrial	Cheng, et al., 1987	9893	9967-9750	0.613
							9895	9967-9750	0.613
							9910	9967-9750	0.613
SYS	g32	2.00	2,440±105	Peat	Terristrial	Geng, et al, 1987.	2466	2508-2356	0.546
SYS	g38	4.00	5,000±100	Peat	Terristrial	Geng, et al, 1987.	5728	5766-5647	0.595
ECS	HQ98	-36.84	9080±120	Plant	Terrestrial	Hori et al., 2001	10216	10288-10139	0.500
ECS	CM97	-58.58	10820±50	Snail shell	Terrestrial	Hori et al., 2001	13142	13172-13004	1.000

**References:**

Chang, J.H., Lee, C.W., Kim, S.P., Park, Y.S., Shin, W.C., Kim, W.S., Kim, J.K., Bong, P.Y., Lee, H.Y., Choi S., J., Park, Y.A., Park, S.C., and Yoon, H.W. 1996. Yellow Sea drilling program for studies on Quaternary geology (analyses of YSDP 102, YSDP-103, YSDP-104, YSDP-105 cores). Korea Institute of Geology, Mining and Material Research report, 32-34.

- Emery K.O., Niino H., and Sullivan B., 1971, Post-Pleistocene levels of the East China Sea. In: *The late Cenozoic glacial ages*, K.K. Turekian, editor, Yale University Press. p. 381-390.
- Geng X., Wang, Y., and Fu, M. 1987. Holocene sea level oscillations around Shandong Peninsula, In: Qin, Y., and Zhao S., (Eds), *Late Quaternary Sea-level Changes*. Beijing: China Ocean Press. p81-96.
- Han, Y.S., and Meng G.L., 1987. On the Sea-level Changes along the Eastern Coast of China during the past 12,000 years. In: Qin, Y., and Zhao S., (Eds), *Late Quaternary Sea-level Changes*. Beijing: China Ocean Press. p119-136.
- Hori, K., Saito, Y., Zhao, Q., Xheng, X.R., Wang, P.X., Sato Y., and Li.C.X. , 2001. Sedimentary facies of the tide-dominated paleo-Changjiang (Yangtze) estuary during the last transgression. *Marine Geology*, 177, 331-351.
- Jin, J.H. and Chough, S.K. 1998, Partitioning of transgressive deposits in the southeastern Yellow Sea: a sequence stratigraphic interpretation. *Marine Geology*, 149, 79-92.
- Kim Jung-Moo and Kennett James P., 1998. Paleoenvironmental changes associated with the Holocene marine transgression, Yellow Sea (Hwanghae). *Marine Micropaleontology* 34: 71-89.
- Kim, Y.H., Lee, H.J., Chun, S.S., Han, S.J., and Chough, S.K. 1999. Holocene transgressive stratigraphy of a macrotidal flat in the southeastern Yellow Sea: Gomso Bay, Korea. *Journal of Sedimentary Research Section B: Stratigraphy and Global Studies*. vol. 69, no. 2, pp. 328-337.
- Kim Jung-Moo and Kucera Michal, 2000, Benthic foraminifer record of environmental changes in the Yellow Sea (Hwanghae) during the last 15,000 years. *Quaternary Science Reviews*, 19: 1067-1085.
- Lan, X.H., and Shen, S.X., 2000. Geochemical characteristics of sediment cores from the central South Yellow Sea. *Marine Geology and Quaternary Geology*, Vol. 20, no.2,33-38.
- Li Congxian and Zhang Guijia, 1995. A sea-running Changjiang River during the last glaciation? *Acta Geographica Sinica*, Vol. 50, No.5 459-463.
- Li Congxian, Chen Qingqiang, Zhang Jiaqiang, Yang Shouye, and Fan Daidu, 2000 Stratigraphy and paleoenvironmental changes in the Yangtze Delta during the Late Quaternary. *Journal of Asian Earth Science*. 18, 453-469.
- Li, Shaoquan, Liu Jian, Wang Shengjie, Yang Zigeng, 1997. Sedimentary Characters in the Eastern South Yellow Sea during the Post-Glacial Transgression, *Marine Geology and Quaternary Geology*, Vol. 17, No.4, 1-12.
- Liu, J., Li, S.Q., Wang S.J., Yang Z.G., and Ge, Z.S., 1997. A rock-magnetic study of the last deglacial to Holocene sedimentary sequence in the YSDP105 core on the northeast shelf of the South Yellow Sea. *Marine Geology and Quaternary Geology*. Vol. 17, No.4: 13-24.
- Liu, J., Li S.Q., Wang, S.J., Yang, Z.G., Ge, Z.S., and Chang, J.H., 1999. Sea-level Changes of the Yellow Sea Warm Current since the last Deglaciation. *Marine Geology and Quaternary Geology*. Vol 19, No.1: 13-24.
- Liu, M.H., Wu, S.Y., and Wang, Y.J., 1987. Late Quaternary Sediments of the Yellow Sea. China Ocean Press, Beijing.
- Liu Xiqing, 1987. Relict sediments in China continental shelf. *Marine Geology & Quaternary Geology*, Vol. 7, No.1 1-14.
- Meng G.L., Han Y.S., Wang S.Q., Paleoclimatic events and environment evolution of the shelf area in the south Yellow Sea during the past 15ka. *Oceanologia et Limnologia Sinica*, Vol: 29, No.3. 297-305.

- Park, S.C., Lee, H.H., Han, H.S., Lee, G.H., Kim, D.C., and Yoo D.G., 2000. Evolution of late Quaternary mud deposits and recent sediment budget in the southeastern Yellow Sea. *Marine Geology*, 170: 271-288.
- Park, S.C., Yoo, D.G., Lee, C.W., and Lee, E.I., 2000. Last glacial sea-level changes and paleogeography of the Korea (Tsushima) Strait, *Geo-Marine Letters*, 20: 64-71.
- Peng Funan, Sui Liangren, Liang Juting and Shen Huati, 1984. Data on lowest sea level of the East China Sea in late Pleistocene. *Scientia Sinica (B)* No.865-876.
- Qin Y.S., Zhao, Y.Y., Chen L.R., Zhao, S.L., 1989. *Geology of the Yellow Sea*. China Ocean Press, Beijing.
- Qin Y.S., Zhao, Y.Y., Chen L.R., Zhao, S.L., 1987. *Geology of the East China Sea*. China Science Press, Beijing.
- Qin Y.S., Zhao, Y.Y., Chen L.R., Zhao, S.L., 1989. *Geology of the Yellow Sea*. China Ocean Press, Beijing.
- Saito, Y., Wei, h., Zhou, Y., Nishimura, A., Sato, Y. and Yokota S., 2000. Delta progradation and chenier formation in the Huanghe(Yellow River), delta China. *Journal of Asian Earth Sciences*, v.18: 489-497.
- Shen Huati, 1985. East China Sea continental shelf relict sediment's dating and origin model. *Acta Oceanologica Sinica*, vol:7,no.1, 67-77.
- Suk, B.C., Nakamura T., Nakai, N., and Taira A., 1990. Radio-carbon age determination by Tandem Accelerator Mass Spectrometry Technique and its application to the Korean sea. *The Korean Journal of Quaternary Research*. Vol. 4, no. 1, 27-40.
- Wang Mingtian, Zhuang Zhenye, Ge Shulan, Jiang Hua, Sunhuaicheng, Ren Shiyan, 2000, Sediment Characteristics of the Shallow Buried Paleo-Channels in the North-central Liaodong Bay and Their Negative Effects on Nautical Engineering. *Journal of Oceanography of Huanghai and Bohai Seas*. Vol. 18, No.2 P18-24.
- Yang Wenda, 1983. The age and dynamical sedimentary features of the self sand out of Yangtze estuary. *Marine Geology 7 Quaternary Geology*. Vol.3, no.2, p41-49.
- Yang, Z.G., and Xu, D.Y., 1996. Quaternary orbital events and nonorbital events in the South Yellow Sea since last Glaciation. *Proceedings of The Korea-China International Seminar on Holocene and Late Pleistocene environments in the Yellow Sea Basin*, Seoul, Korea, 37-51.
- Yang, Z.S., Sun, X.G., and Chen, .R., and Pang, C.G., 1998. Sediment discharge of the Yellow River to the Sea: its past, present, future and Human Impact on it. *Health of the Yellow Sea*, edited by Hong, G.H., Zhang, J., and Park, .B.K, The Earth Love Publication Association, Seoul,
- Yoo, D.G., and Park, S.C. 1997. Late Quaternary lowstand wedges on the shelf margin and trough region of the Korea Strait. *Sediment Geology*, 109: 121-133.
- Zheng, Ci.Y. 1991 *Quaternary Geology in the Yellow Sea*. Science Press, Beijing, China.
- Zhuang, Z.Y., Xu, W.D., Liu, D.S., Zhuang, L.H., Liu, B.Z., Cao, Y.Y., and Wang Q., 1999. Division and environmental evolution of late Quaternary marine beds of S3 hle in the Bohai Sea. *Marine Geology & Quaternary Geology*. Vol.19, no.2, p27-35.
- Zong Chongkai, Jin Changmao, and Wang Xiaobo, 1986. The contact relation between the sea-level changes and stratum on the continental shelf of East China Sea. *China Sea Level Changes*. China Ocean Press. 149-155.



## VITA

### **Jing-Pu Liu**

Born in Shandong, China, 9 January 1970. Graduated from First High School of Zhangqiu, Shandong, in 1988. Earned B.E. in Hydrology and Engineering Geology from Ocean University of Qingdao in 1992. Received M.S. in Marine Geology from Institute of Oceanology, Chinese Academy of Sciences, in 1995. Entered doctoral program at College of William and Mary, School of Marine Science, in 1997.